AD-A089 103 WOODS HOLE OCEANOGRAPHIC INSTITUTION MASS F/G 8/7
THE EVOLUTION OF THE INDIAN OCEAN TRIPLE JUNCTION AND THE FINIT--ETC(U)
SEP 80 C R TAPSCOTT N00014-74-C-0262
UNCLASSIFIED WHOI-80-37 NL

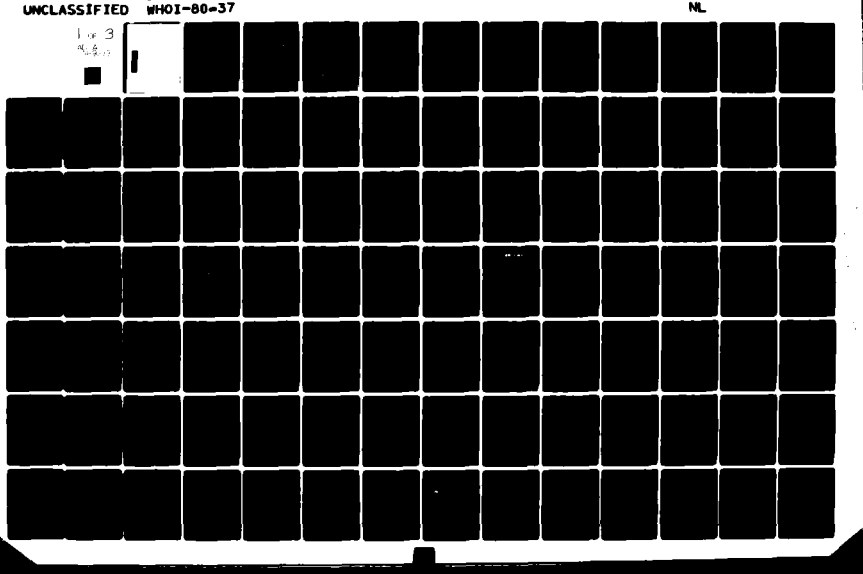

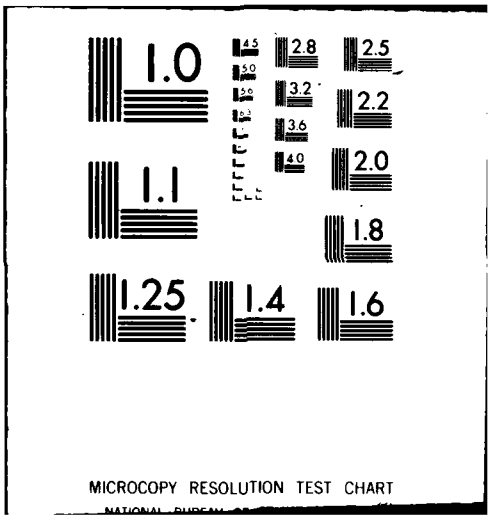
1.0
1.1
1.25
1.4
1.6
1.8
2.0
2.2
2.5
2.8
3.2
3.6
4.0
4.5
5.0
MICROCOPY RESOLUTION TEST CHART

WHOI-80-37

12

THE EVOLUTION OF THE INDIAN OCEAN TRIPLE JUNCTION AND THE FINITE ROTATION PROBLEM

by

Christopher R. Tapscott

WOODS HOLE OCEANOGRAPHIC INSTITUTION
Woods Hole, Massachusetts 02543

September 1980

DOCTORAL DISSERTATION

Prepared for the Office of Naval Research under Contracts N00014-74-C-0262; NR 083-004 and N00014-75-C-0291 (MIT).

Approved for Distribution:

John I. Ewing

John I. Ewing, Chairman
Department of Geology & Geophysics

Charles D. Hollister

Charles D. Hollister
Dean of Graduate Studies

SECURITY CLASSIFICATION OF THIS PAGE (When Date Entered)

REPORT DOCUMENTATION PAGE		READ INSTRUCTIONS BEFORE COMPLETING FORM
1. REPORT NUMBER (14) WHOI-80-37	2. GOVT ACCESSION NO. AD-A089 103	3. RECIPIENT'S CATALOG NUMBER
4. TITLE (and Subtitle) (4) THE EVOLUTION OF THE INDIAN OCEAN TRIPLE JUNCTION AND THE FINITE ROTATION PROBLEM,		5. TYPE OF REPORT & PERIOD COVERED (9) Doctoral thesis, Technical 6. PERFORMING ORG. REPORT NUMBER
7. AUTHOR(s) (10) Christopher Robert Tapscott		8. CONTRACT OR GRANT NUMBER(s) (15) N00014-74-C-0262; N00014-75-C-0291;
9. PERFORMING ORGANIZATION NAME AND ADDRESS Woods Hole Oceanographic Institution Woods Hole, MA 02543		10. PROGRAM ELEMENT, PROJECT, TASK AREA & WORK UNIT NUMBERS NR 083-004
11. CONTROLLING OFFICE NAME AND ADDRESS NORDA National Space Technology Laboratory Bay St. Louis, MS 39529		12. REPORT DATE (11) Sep[redacted]980 13. NUMBER OF PAGES (12) 210
14. MONITORING AGENCY NAME & ADDRESS (if different from Controlling Office)		15. SECURITY CLASS. (of this report) Unclassified 15a. DECLASSIFICATION/DOWNGRADING SCHEDULE

16. DISTRIBUTION STATEMENT (of this Report)

Approved for public release; distribution unlimited.

17. DISTRIBUTION STATEMENT (of the abstract entered in Block 20, if different from Report)

18. SUPPLEMENTARY NOTES

19. KEY WORDS (Continue on reverse side if necessary and identify by block number)

1. Plate tectonics
2. Earth's lithosphere

20. ABSTRACT (Continue on reverse side if necessary and identify by block number)

Refer to page 12 of thesis for abstract.

DD FORM 1 JAN 73 1473 EDITION OF 1 NOV 65 IS OBSOLETE S/N 0102-014-6601 |

SECURITY CLASSIFICATION OF THIS PAGE (When Date Entered)

3x100

THE EVOLUTION OF THE INDIAN OCEAN TRIPLE JUNCTION

and

THE FINITE ROTATION PROBLEM

by

CHRISTOPHER ROBERT TAPSCOTT

A.B., Swarthmore College
(1972)

SUBMITTED IN PARTIAL FULFILLMENT
OF THE REQUIREMENTS FOR THE
DEGREE OF

DOCTOR OF PHILOSOPHY

at the

MASSACHUSETTS INSTITUTE OF TECHNOLOGY
and the
WOODS HOLE OCEANOGRAPHIC INSTITUTION

June, 1979

Signature of Author _____

Joint Program in Oceanography, Massachusetts Institute of Technology/Woods Hole Oceanographic Institution, and the Department of Earth and Planetary Sciences, Massachusetts Institute of Technology, March, 1979

Certified by _____
John G. Sclater

Thesis Supervisor

Accepted by _____

Chairman, Joint Oceanographic Committee in the Earth Sciences, Massachusetts Institute of Technology/Woods Hole Oceanographic Institution

TABLE OF CONTENTS

LIST OF FIGURES

Page No.

Page No.

LIST OF TABLES

BIOGRAPHICAL SKETCH

I was born in New York City on April 2, 1950, and was raised in Westfield, New Jersey. I attended Swarthmore College (Swarthmore, Pennsylvania) from 1968-1972 and was graduated in June, 1972, with a Bachelor of Arts Degree in physics, awarded with high honors. In June, 1972, I began graduate studies in nuclear physics at Princeton University (Princeton, New Jersey). I took a leave of absence from Princeton in June, 1973, to work at the Woods Hole Oceanographic Institution (Woods Hole, Massachusetts) in order to pursue an interest in marine geology and geophysics which I had acquired while a summer fellow at WHOI in 1971, during which time I worked with Dr. James R. Heirtzler.

In the autumn of 1974 I entered the WHOI/MIT Joint Program in Oceanography. Since then my work has concentrated on determining the past configurations of the earth's lithospheric plates and relating these to geologic and paleo-oceanographic events.

My publications and papers in preparation include:

1. Denham, C.R., and C. Tapscott, Experimental geodynamics I: Reversing the geomagnetic field, submitted to J. Irrep. Res..
2. Phillips, J.D., R. Feden, H.S. Fleming, and C. Tapscott, Aeromagnetic studies of the Greenland/Norwegian Sea and the Arctic Ocean, in preparation.
3. Phillips, J.D., and C. Tapscott, The evolution of the Atlantic Ocean north of the Azores, EGS Abstract, EOS Trans. Am.

Geophys. Un., 60, 105, 1979.

4. Sclater, J.G., C. Bowin, R. Hey, H. Hoskins, J. Pierce, J. Phillips, and C. Tapscott, The Bouvet triple junction, J. Geophys. Res., 81, 1857-1869, 1976.
5. Sclater, J.G., R.L. Fisher, P. Patriat, C. Tapscott, and B. Parsons, Eocene to recent development of the Southwest Indian Ridge, a consequence of the evolution of the Indian Ocean triple junction, submitted to Geol. Soc. Amer. Bull..
6. Sclater, J.G., S. Hellinger, and C. Tapscott, Paleobathymetry of the Atlantic Ocean from the Jurassic to the Present, J. Geology, 85, 509-552, 1977.
7. Sclater, J.G., and C. Tapscott, The depth of the Atlantic Ocean through time, Scientific American, in press.
8. Tapscott, C., P. Patriat, R.L. Fisher, J.G. Sclater, H. Hoskins, and B. Parsons, The Indian Ocean triple junction, submitted to J. Geophys. Res..

ACKNOWLEDGMENTS

Since part of this thesis consists of co-authored papers, I first want to acknowledge the contributions my co-authors have made to this research. John Sclater was the principal organizer of legs 5 and 6 of R/V Atlantis II Cruise 93 to the Southwest Indian Ridge and the Indian Ocean triple junction. That expedition resulted in Chapters 2 and 3 of this thesis, and John Sclater's efforts and insight are responsible for much of their content. Bob Fisher contributed much data from the Scripps Institution of Oceanography and gave invaluable aid in interpreting bathymetric information and revising the manuscripts. Phillipe Patriat generously allowed us to use French oceanographic data from the Indian Ocean and contributed significantly to both papers. Hartley Hoskins and Barry Parsons helped collect and interpret the data and critically reviewed the manuscripts. I also thank Steve Hellinger who gave freely of his time and his expertise in the statistics of finite rotations to help me formulate the three plate finite rotation method that forms the basis of Chapter 4.

Many of the scientists, staff, and students at WHOI and MIT have helped make my graduate experience rewarding, but I would particularly like to thank my thesis advisor and friend, John Sclater, who guided me toward the problems of finite rotations and encouraged and supported me through all these years; Jim Heirtzler, whose guidance has been invaluable; and Chuck Denham and all the denizens of DESC Building (human and canine) for

their help, friendship, and well-balanced outlook on work. Furthermore, I thank Jake Peirson, without whom the career of every graduate student in the Joint Program would vanish in a bureaucratic morass.

Above all others to whom I am indebted is my wife, Susan. Without her patience and support, this thesis would never have been completed. I am also grateful to her for typing much of the final draft of this thesis.

THE EVOLUTION OF THE INDIAN OCEAN TRIPLE JUNCTION

and

THE FINITE ROTATION PROBLEM

by

Christopher Robert Tapscott

Submitted to the Woods Hole Oceanographic Institution/ Massachusetts Institute of Technology Joint Program in Oceanography on February 23, 1979, in partial fulfillment of the requirements for the degree of Doctor of Philosophy.

ABSTRACT

A major goal in the study of plate tectonics is the acquisition of a knowledge of the history of relative motion among the rigid plates of the earth's lithosphere. The three papers of this thesis contribute to this effort and demonstrate that studies of the stability and evolution of triple junctions and of the finite rotations of systems of three plates can yield significantly more accurate tectonic histories than can studies of the relative motions between two plates alone. Topographic and magnetic investigation of the Southwest Indian Ridge and reconstruction of the plate system of the Indian Ocean shows that both Africa and Antarctica are rigid plates and their pole of relative rotation has remained fixed near 8°N, 42°W since the Eocene. A detailed survey of the Indian Ocean triple junction reveals that the Indian Ocean plate motions have remained constant since 10 Ma. The stability conditions of the junction show that the general morphology of the Southwest Indian Ridge results from the evolution of the Indian Ocean triple junction. A method is presented for determining the finite rotations best reconstructing the past relative positions of three plates around a triple junction. The method is illustrated by reconstructions of the plates around the Labrador Sea triple junction at the times of anomalies 24 (56 Ma) and 21 (50 Ma). The region of uncertainty of the Greenland-North America finite pole is mapped for each reconstruction, and it demonstrates that consideration of the three plate system yields more well-constrained results than does a treatment of the two plates alone.

Thesis Supervisor: J. G. Sclater
Title: Professor

CHAPTER 1

INTRODUCTION AND OVERVIEW

One of the earliest and most important goals in the study of the new global tectonics has been to determine the relative positions of the earth's lithospheric plates at various times in the past. Initially, such plate reconstructions were for the purpose of demonstrating the plausibility of the continental drift hypothesis (e.g., Wegener, 1912; Du Toit, 1937; Bullard et al., 1965), but they have since come to form much of the basis for research in geology and in the physics of the earth. An accurate and precise knowledge of the history of relative motions among the lithospheric plates is imperative, since for several hundred million years, these motions have been the principal mechanism shaping the face of the planet.

The history of sea-floor spreading, for example, has almost entirely determined the thermal evolution of the oceanic lithosphere and thus the general topography of the ocean basins (see discussion in Parsons and Sclater, 1977). From plate reconstructions one may then discover the three-dimensional shape of the ocean basins as a function of time (Sclater et al., 1977). This, in turn, has heavily influenced paleo-oceanographic conditions and the history of sedimentation (van Andel et al., 1977). Plate reconstructions thus provide both a background against which to view paleo-oceanographic and sedimentological studies and a powerful tool with which to pursue them. Furthermore, the plate motions are the most concrete evidence against which theories of mantle convection and of the driving forces of plates must be tested (Forsyth and Uyeda, 1975; Solomon et al., 1975; Solomon et al., 1977).

The bold outlines of sea-floor spreading are now established over most of the earth, but the scientific considerations above and the related search for economic resources in the ocean basins call for ever more detailed analyses of plate motions. This thesis is a collection of three papers which contribute to this effort. In particular, they focus on the value of studying triple junctions and systems of three or more plates in order to determine both instantaneous and finite relative plate rotations with the greatest possible accuracy and precision. The geometry and evolution of a triple junction are highly dependent on the local relative motions among the three plates, and thus the sea-floor formed near a triple junction is a particularly sensitive recorder of any changes in the relative velocities. Moreover, the relative rotations within a system of three rigid plates are interdependent. This is true for both the instantaneous and finite cases and can provide important additional constraints not available within a two plate system. Therefore, one may more precisely define the relative plate motions.

* * *

The tectonic evolution of the southern oceans (Figure 1) is the least well-known of all the earth's oceanic areas. The region is vast, remote, and relatively poorly surveyed. It is also complex, involving a large number of major plates and having experienced severe changes of spreading poles and even of plate boundaries. An understanding of the southern oceans is vital, however, to a general understanding of the global

FIGURE 1

Chart showing the major tectonic features of the Indian and South Atlantic Oceans. From Norton and Sclater (in press).

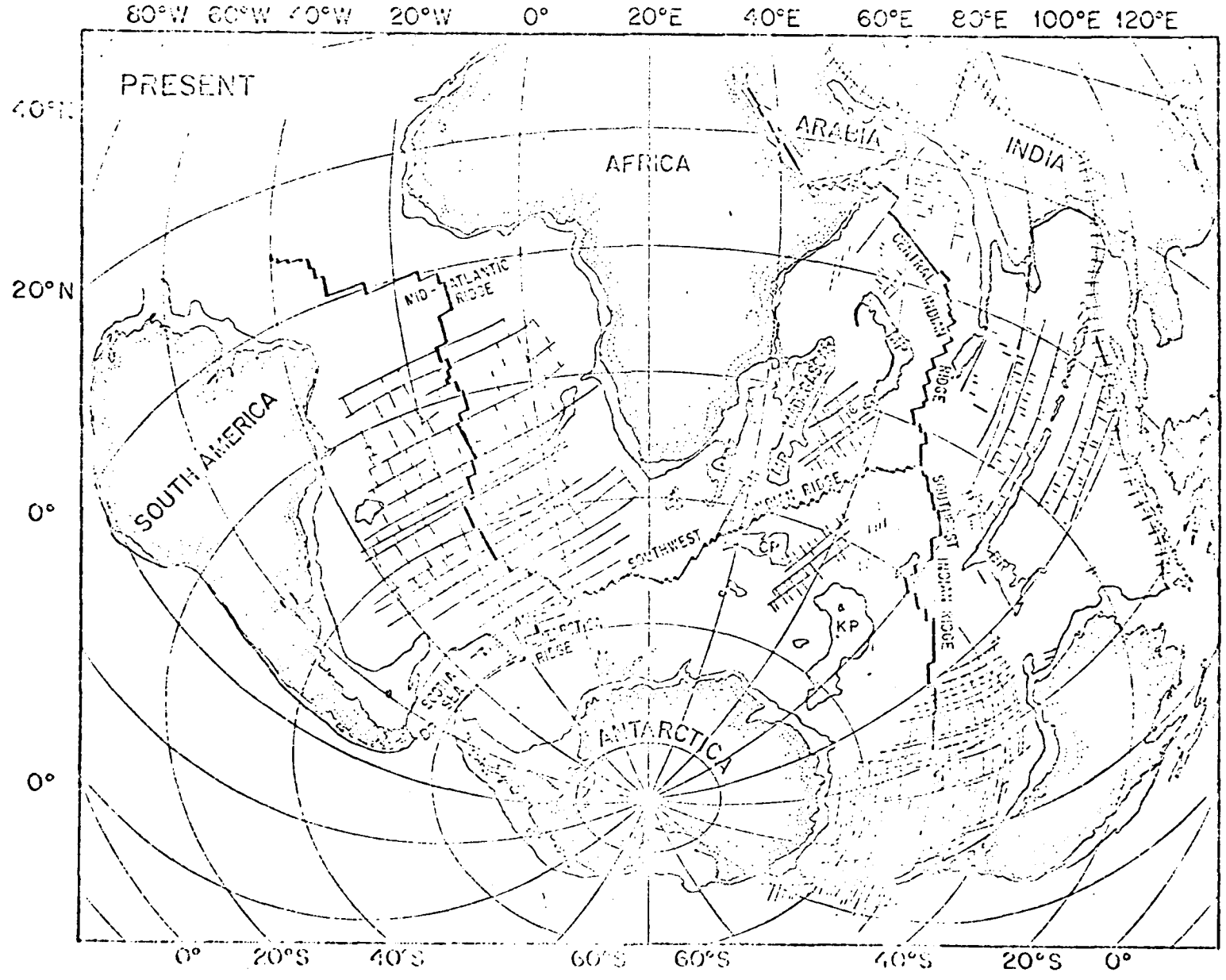
PRESENT
80°W 60°W 40°W 20°W 0° 20°E 40°E 60°E 80°E 100°E 120°E
40°N
20°N
0°
0°
0° 20°S 40°S 60°S 60°S 40°S 20°S 0°
AFRICA
ARABIA
INDIA
SOUTH AMERICA
ANTARCTICA
MID-ATLANTIC RIDGE
CENTRAL INDIAN RIDGE
SOUTHWEST INDIAN RIDGE
SOUTHEAST INDIAN RIDGE
AMSTERDAM-ST PAUL PLATEAU
KP

tectonic history. Knowledge of the relative motions among Africa, India, and Antarctica is necessary in order to directly connect the history of the Atlantic plate system with that of the Pacific, all other paths being broken by subduction zones. Moreover, the regional tectonic evolution has had a dominant effect on paleo-oceanographic conditions as the surrounding continents separated from Antarctica, fostering the formation of a circumpolar oceanic current system. Even at present, regional tectonic conditions influence the movement of water masses, since deep fracture zones across the Southwest Indian Ridge provide pathways by which Antarctic bottom water reaches the western Indian Basin (Warren, 1978).

Chapter 2 of this thesis presents the results of a topographic and magnetic study of the eastern portion of the Southwest Indian Ridge, the boundary between the African and Antarctic plates, an area not heretofore well surveyed. Because of the slow spreading rate of less than 10 mm/yr, magnetic anomalies are poorly resolved, yet our careful survey allows us to determine the pole and rate of relative motion across the ridge. This pole is consistent with data from farther westward (Sclater et al., 1976; Sclater et al., 1978; Bergh and Norton, 1976), indicating that both the African and Antarctic plates are behaving as rigid bodies. Consideration of the three plate system of the Indian Ocean using published sea-floor spreading data and finite rotations for the other plate pairs then shows that the Africa-Antarctica relative rotation has been constant since the Eocene to within a temporal resolution

of about 10 m.y.. Moreover, the dominant morphologic trends along the eastern portion of the Southwest Indian Ridge are a direct result of the evolution of the Indian Ocean triple junction.

* * *

Since McKenzie and Morgan (1969) pointed out the sensitive dependence of the stability and evolution of triple junctions on the motions of the plates around them, several investigators have studied triple junctions in order to better determine the instantaneous relative motions of lithospheric plates (Falconer, 1972; Sclater et al., 1976; Hey, 1977). In addition to the sensitivity mentioned above, these efforts are aided by an important possible redundancy of sea-floor spreading data. If one assumes the plates are locally rigid, then any four of the six quantities describing plate motion about a triple junction (three rates and three directions of relative motion) are sufficient to determine the other two. If one is able to measure all six quantities, then one can test the local rigidity of the plates.

Chapter 3 presents results of a study of the evolution of the Indian Ocean triple junction near 25°S, 70°E. We are able to determine rates and directions on all three plate boundaries and show that the velocity triangle is closed and the plates are locally rigid. The plate velocities in the vicinity of the triple junction are consistent with those elsewhere along the Indo-Atlantic plate boundaries, and we determine the poles of instantaneous relative rotation. A

careful mapping of the evolution of the triple junction shows that these poles have remained constant since 10 Ma.

* * *

Since Bullard et al. (1965) first used a statistical criterion to fit together the continental shelves around the Atlantic Ocean, several methods have been developed to find by similar means the best fit of crustal isochron patterns as defined by sea-floor spreading data (e.g., McKenzie and Sclater, 1971; Pilger, 1978). Recently, Hellinger (1979) has presented a new technique for determining the finite rotation defining the best reconstruction of the past relative positions of two plates. The assumptions about the data implicit in the method are well-suited to a wide class of sea-floor spreading data, and, significantly, the errors in the data contribute rigorously to a statistically defined region of confidence about the optimal rotation tensor.

In Chapter 4, Hellinger's technique is extended to treat the relative finite rotations of a system of three plates about a triple junction. Dealing with a three plate system has a number of advantages over dealing with pairs of plates alone. For example, the additional constraints imposed by simultaneously seeking reconstructions of three plate pairs might overcome difficulties arising from a paucity of data along one or more of the boundaries. Moreover, it is important that any proposed set of finite rotations for a reconstruction be internally consistent. This method insures that this condition is satisfied. If no such satisfactory set can be found, one must

re-examine the assumption of rigid plate behavior.

The method is illustrated by application to the plates around the now extinct Labrador Sea triple junction. Using available magnetic anomaly identifications (Srivastava, 1978; Phillips and Tapscott, in preparation), we reconstruct the relative positions of Greenland, North America, and Rockall Bank at the times of anomalies 21 (50 Ma) and 24 (56 Ma) and determine the relative finite rotations of the plates. These finite rotations yield a better reconstruction than do those of other authors. They are also more well-constrained, since their error ellipses are smaller than those derived by considering only two plates at a time. The three plate method for calculating finite rotations should prove a valuable tool for refining our ideas of the tectonic history of the earth.

* * *

These three studies demonstrate the value of considering the evolution of three plate systems and the stability of triple junctions in determining and refining relative rotations, both instantaneous and finite. These methods will continue to contribute to a more complete and detailed understanding of the history of sea-floor spreading. Perhaps the most interesting immediate result of these papers is the surprising constancy of the rotations between the Indian Ocean plates since 40 Ma, and especially since 10 Ma. More detailed reconstructions of the region should now be possible with relatively little new data. It was originally intended that Chapter 4 would illustrate the three plate finite rotation method with an application to

the Indian Ocean system. However, preliminary investigations revealed that, except for the area near the triple junction, well-located crossings of magnetic anomaly lineations and fracture zones are still too sparse. A meaningful treatment would first require extensive reinterpretation of published data along the Central and Southeast Indian Ridges, and this is a subject for future work.

REFERENCES

Bergh, H.W., and I.O. Norton, Prince Edward Fracture Zone and the evolution of the Mozambique Ridge, J. Geophys. Res., 81, 5221-5239, 1976.

Bullard, E.C., J.E. Everett, and A.G. Smith, The fit of the continents around the Atlantic, Trans. Roy. Soc. London, 258A, 41-51, 1965.

Du Toit, A.L., Our Wandering Continents, 366p., Oliver and Boyd, Edinburgh, 1937.

Falconer, R.K.H., The Indian-Antarctic-Pacific triple junction, Earth Planet. Sci. Lett., 17, 151-158, 1972.

Forsyth, D.W., and S. Uyeda, On the relative importance of driving forces of plate motion, Geophys. J. Roy. Astron. Soc., 43, 163-200, 1975.

Hellinger, S., The statistics of finite rotations in plate tectonics, Ph.D. thesis, Mass. Inst. of Technol., 1979.

Hey, R., Tectonic evolution of the Cocos-Nazca spreading center, Geol. Soc. Amer. Bull., 88, 1404-1420, 1977.

McKenzie, D.P., and J.G. Sclater, The evolution of the Indian Ocean since the Late Cretaceous, Geophys. J. Roy. Astron. Soc., 25, 437-528, 1971.

Norton, I.O., and J.G. Sclater, A model for the evolution of the Indian Ocean and the breakup of Gondwanaland, J. Geophys. Res. (in press).

Parsons, B., and J.G. Sclater, An analysis of the variation of ocean floor bathymetry and heat flow with age, J. Geophys. Res., 82, 803-827, 1977.

Pilger, R.H., Jr., A method for finite plate reconstructions with applications to Pacific-Nazca plate evolution, Geophys. Res. Lett., 5, 469-472, 1978.

Sclater, J.G., C. Bowin, R. Hey, H. Hoskins, J. Peirce, and C. Tapscott, The Bouvet triple junction, J. Geophys. Res., 81, 1857-1869, 1976.

Sclater, J.G., H. Dick, I.O. Norton, and D. Woodroffe, Geophysical and petrological study of the Antarctic plate boundary east and west of Bouvet Island, Earth Planet. Sci. Lett., 37, 393-400, 1978.

Sclater, J.G., S. Hellinger, and C. Tapscott, The paleo-bathymetry of the Atlantic Ocean from the Jurassic to the Present, J. Geology, 85, 509-552, 1977.

Solomon, S.C., N.H. Sleep, and D.M. Jurdy, Mechanical models for absolute plate motions in the Early Tertiary, J. Geophys. Res., 82, 203-212, 1977.

Solomon, S.C., N.H. Sleep, and R.M. Richardson, On the forces driving plate tectonics: Inferences from absolute plate velocities and intraplate stress, Geophys. J. Roy. Astron. Soc., 42, 769-801, 1975.

Van Andel, T.H., J. Thiede, J.G. Sclater, and W.W. Hay, Depositional history of the South Atlantic Ocean during the last 125 million years, J. Geology, 85, 651-698, 1977.

Warren, B.A., Bottom water transport through the Southwest Indian Ridge, Deep Sea Res., 25, 315-321, 1978.

Wegener, A., Die Entstehung der Kontinente, Geol. Rundschau, 3, 276-292, 1912.

CHAPTER 2

EOCENE TO RECENT DEVELOPMENT OF THE SOUTHWEST INDIAN RIDGE

Eocene to Recent Development of the Southwest Indian Ridge, a Consequence of the Evolution of the Indian Ocean Triple Junction*

John G. Sclater — Department of Earth and Planetary Sciences, Massachusetts Institute of Technology, Cambridge, MA

Robert L. Fisher — Scripps Institution of Oceanography, La Jolla, CA

Philippe Patriat — Laboratoire de Géophysique Marine, Institut de Physique du Globe de Paris, Saint-Maur-des Fossés, FRANCE

Christopher Tapscott — Department of Earth and Planetary Sciences, Massachusetts Institute of Technology, Cambridge, MA and Woods Hole Oceanographic Institution, Woods Hole, MA

Barry Parsons — Department of Earth and Planetary Sciences, Massachusetts Institute of Technology, Cambridge, MA

*Submitted to Geological Society of America Bulletin.

ABSTRACT

The Southwestern Indian Ridge, the contact between the African and Antarctic plates, lies between the Bouvet Triple Junction in the South Atlantic and the Indian Ocean Triple Junction about 2100 kms east of Madagascar. From the vicinity of Prince Edward Island at 40°E it trends northeasterly and it is segmented by a suite of deep north-south gashes terminating on the northeast with two spectacular meridional fracture zones, the "Atlantis II" and the "Melville", at 57°30'E and 60°30'E respectively. From there northeast to the Indian Ocean Triple Junction at 25°30'S, 70°00'E the ridge trends N75°E; it is characterized by a triangle of rough topography with the triple junction at the eastern apex. From all available data an instantaneous pole of relative motion for Africa/Antarctica was computed; it lies at 8.4°N, 42.4°W, with a rate of 0.15 degrees/my.

Since the marked change in the direction and rate of spreading in the Madagascar, Crozet, and Central Indian Basins that occurred in the Eocene (44 Ma, Anomaly 19), the poles of relative motion for the African, Indian, and Antarctic plates have changed very little. We fixed the Africa/Antarctica and Africa/India poles and computed that for India/Antarctica. We justified this pole by comparisons of predicted isochrons with observed magnetic lineations and determined the tectonic history of the triple junction.

Since the Eocene (44 Ma, Anomaly 19), this junction has moved as rapidly eastwards with respect to Africa as Antarctica has moved south. The resultant geometry and slow spreading account for the triangle of rough topography produced by the Southwest Indian Ridge east of the Melville Fracture Zone. The triple junction evolved as a stable Ridge-Ridge-Ridge type with the Southeast Indian Ridge remaining approximately constant in length. It was not resolved whether this constancy in length is maintained by frequent ridge jumps or by oblique spreading on the Southwest and Central Indian Ridges near the triple junction.

INTRODUCTION

The topography of the Indian Ocean is dominated by three major active mid-ocean ridge systems. The most northerly of these features starts in the Gulf of Aden, becomes the southeast-trending Carlsberg Ridge southeast of the gulf, and at 1°N and 60°E continues as the en echelon offset, northerly-trending Central Indian Ridge. Near 25°S, at the so-called Indian Ocean Triple Junction, this ridge bifurcates into the Southeast Indian Ridge and Southwest Indian Ridge. The Southeast Indian Ridge, with fast spreading ($\sim$3 cm/yr) and relatively smooth topography, is offset strikingly to the south by two fracture zones close to Amsterdam Island and St. Paul Island (Schlich and Patriat, 1971) before trending southeastward between Australia and Antarctica. The Southwest Indian Ridge, by contrast, spreads more slowly (<1 cm/yr) and it has much rougher topography and many more extremely deep fracture zones. This ridge system is offset markedly to the south in the vicinity of Marion and Prince Edward Islands and it terminates at the Bouvet Triple Junction in the South Atlantic.

The three major active mid-ocean ridges mark the present boundaries of the Indian, African, and Antarctic plates. Each of these active plate boundaries has been studied in detail in areas of considerable extent along its length. For example, McKenzie and Sclater (1971) and Fisher and others

(1971) have elucidated the present tectonic structure of the Carlsberg and Central Indian Ridges, and Weissel and Hayes (1972) have sorted out the history of separation of Australia and Antarctica from initial break-up to the present. The southwest branch has been studied south of Africa by Norton (1976) and Sclater and others (1978) and Bergh and Norton (1976) have examined the northward extension of the Prince Edward Fracture Zone. Apart from the study of Fisher and others (1971) on the Central Indian Ridge, however, none of the detailed work has been concentrated close to the Indian Ocean Triple Junction, and hence little is known about the tectonic history of this feature. Furthermore, until recently the geometry of the Southwest Indian Ridge was poorly known. Poles determined for the Africa/Antarctica plate boundary near Bouvet Island (Sclater and others, 1978) and by closure around the Bouvet Triple Junction (Forsyth, in Sclater and others, 1976) differ strikingly from those determined by closure around the Indian Ocean Triple Junction (McKenzie and Sclater, 1971) and from global closure (Minster and others, 1974). This has led to the tentative suggestion that the African plate might consist of two subplates (Forsyth, 1976; Sclater and others, 1976).

This lack of detailed knowledge of the late Tertiary history of the Indian Ocean contrasts markedly with a surprisingly complete understanding of the late Cretaceous and early Tertiary history. For example, well identified

and clearly lineated anomalies have been identified in the Central Indian Basin by McKenzie and Sclater (1971), in the Wharton Basin by Sclater and Fisher (1974), and in the Mascarene, Madagascar, and Crozet basins by Schlich (1975). These authors have demonstrated that from 80 million years ago (Anomaly 34) to 50 million years ago (Anomaly 21) the spreading centers trended almost east-west. In the early Eocene, India collided with Eurasia (Molnar and Tapponier, 1976), there was an abrupt slowdown in spreading, and between anomalies 21 and 16 (39 million years ago) the direction of spreading changed to northeast-southwest. Finally, the Chagos Fracture Zone terminated as a north-south lineation, the Chagos-Maldives region split off from the Mascarene Plateau and the en echelon Central Indian Ridge was formed (Fisher and others, 1971). However, aside from a study at the southwestern end of the Ninetyeast Ridge by Sclater and others (1976), almost nothing is known about the history of the Central Indian Ridge and Southeast Indian Ridge from then until 9 million years ago (Anomaly 5).

Norton and Sclater (in preparation) have used the fit of the Chagos Bank into Nazareth Bank in the Mascarene Plateau, DSDP Site 238 (Fisher and others, 1974) and a recent reanalysis of the magnetic data south of Australia by Weissel (1977) to reconstruct the positions of the African, Antarctic, and Indian Plates 39 Ma (Anomaly 16). The striking feature of this reconstruction is that the

positions of the finite poles describing the motion of the three plates are little different from the instantaneous poles. These authors have speculated that all of the changes in direction of the three plates took place prior to 39 Ma (Anomaly 16) and that since then their directions of relative motion have changed very little.

In this paper a topographic and a magnetic anomaly chart of the Southwest Indian Ridge east of 53°E and of the Indian Ocean Triple Junction are presented. In the analysis of these data the following problems are addressed:

(a) What is the geometry of the Southwest Indian Ridge?

(b) Is the direction of motion observed on the Africa/Antarctic plate boundary close to the Indian Ocean Triple Junction compatible with that close to Bouvet Island?

(c) What has been the tectonic history of the Southwest Indian Ridge and the triple junction east of 53°?

TOPOGRAPHY

Only since the International Geophysical Year 1957-58 and the International Indian Ocean Expedition 1960-65 has there been any attempt to gather substantial quantities of well-controlled, precise bathymetric data in the Indian

Ocean. Most of the topographic information on the Southwest Indian Ridge east of 40°E has come from recent cruises of the Scripps Institution of Oceanography, the Woods Hole Oceanographic Institution, and the Institut de Physique du Globe de Paris. The first detailed attempts to understand the tectonics and crustal composition were carried out from R/V Argo by Scripps Institution of Oceanography on CIRCE Expedition (1968). This cruise was followed by more detailed work in this area and on the Central Indian Ridge from R/V Melville during S.I.O.'s expedition ANTIPODE 1970-71. The final work reported here was two months of R/V Atlantis II Cruise 93, legs 5 and 6, to the Southwest Indian Ridge and the Indian Ocean Triple Junction in 1976 and two lines of Marion Dufresne Cruise 11 run in the same year. The precisely controlled topographic information gathered on the R/V Melville and R/V Atlantis II cruises marks the main data source; it is complemented by the long, generally northwest-southeast lines run by the Institut de Physique du Globe between Réunion and Crozet, Réunion and Kerguelen, and Kerguelen and Amsterdam (Gallieni prior to 1971 and Marion Dufresne since then). A few other lines, such as from S.I.O. expeditions MONSOON (1960), LUSIAD (1962-63) and DODO (1964), and some isolated lines from reconnaissance of the Lamont-Doherty Geological Observatory or Glomar Challenger (in 1972) also have been

used.

The most spectacular features on this topographic chart of the Southwest Indian Ridge (Figure 1) are the three deep north-south trending gashes, with shallow lips, between 57° and 61°E and the rough v-shaped axial topography between the easterly fracture zone and the Indian Ocean Triple Junction near 25°30'S, 70°00'E. The three fracture zones were recognized and delineated aboard R/V Melville (Engel and Fisher, 1975) and R/V Atlantis II (this paper); the two most prominent, intersecting the ridge crest at 60°30'E and 57°00'E, have been named after these two research vessels, respectively. Two, at least, reach depths of more than 6000 meters; all three provide avenues for the passage of deep Antarctic bottom water from the Crozet Basin north into the Mascarene Basin (Warren, 1978). The gashes extend well to the north and south of the deepest sections which characteristically occur at or near their intersections with the ridge crest. They all offset the ridge crest as it is identified by earthquake epicenters, and they all appear to have some 7 to 9 degrees of north-south extent. The north-south cross-grain of the Southwest Indian Ridge terminates sharply at the Melville Fracture Zone at 61°E (Figure 1). To the east the rough topography appears to form a right triangle with the most acute apex at the triple junction and the shortest side being the Melville Fracture Zone.

FIGURE 1

Topographic chart of the Southwest Indian Ridge between 53°E and the Indian Ocean triple junction.

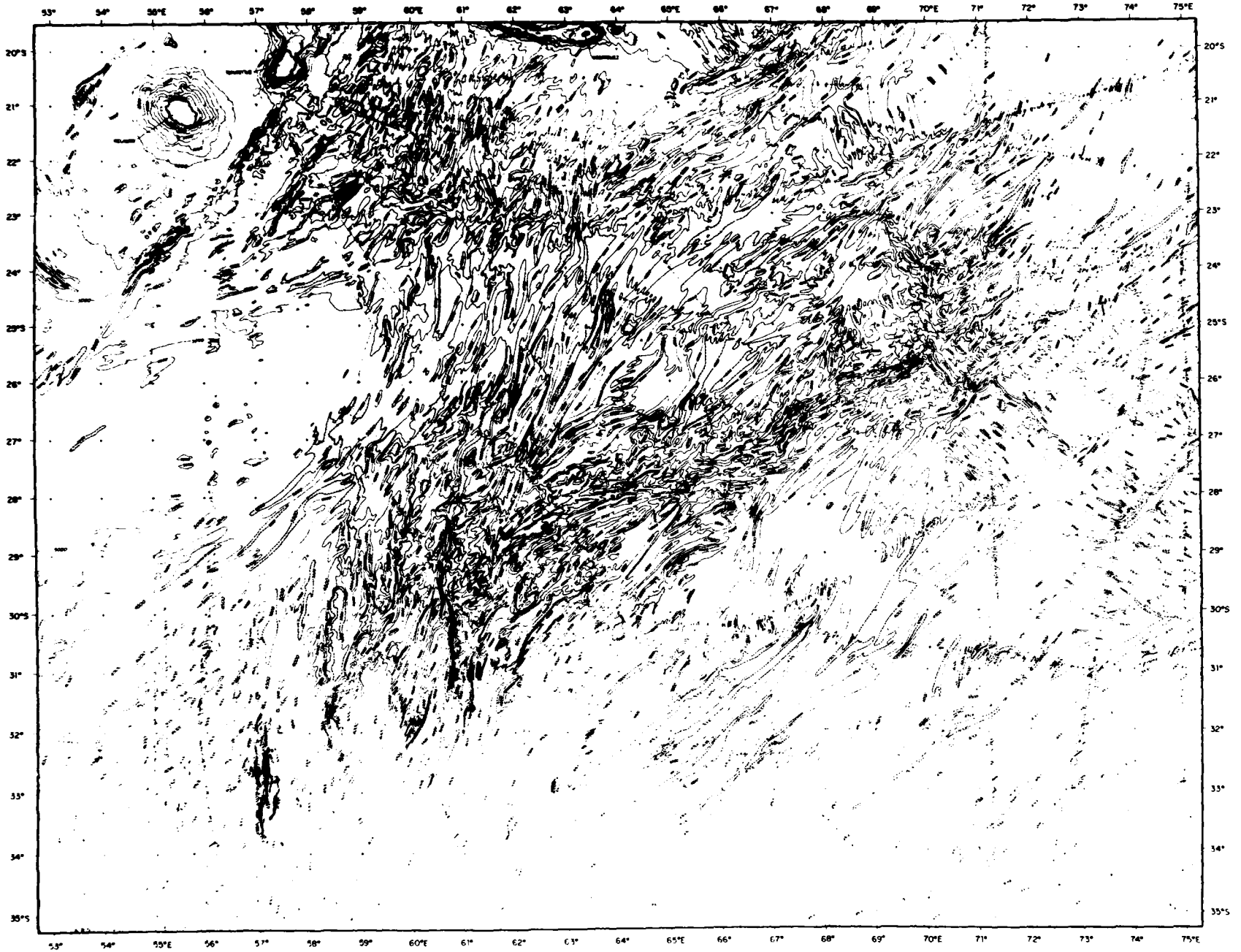
53°
54°
55°E
56°
57°
58°
59°
60°E
61°
62°
63°
64°
65°E
66°
67°
68°
69°
70°E
71°
72°
73°
74°
75°E
20°S
21°
22°
23°
24°
25°S
26°
27°
28°
29°
30°S
31°
32°
33°
34°
35°S

Within this triangle there is a spectacular deep that extends overall N75°E in a sinuous trend from that fracture zone to the triple junction, which is marked by an isolated pocket or median valley greater than 5000 m deep (Tapscott and others, in preparation).

The rough topography on the Southwest Indian Ridge contrasts markedly with the smoother, much blockier relief of the Southeast Indian Ridge. On the latter the contours are dominated by N45°E trending fracture zones and a 200 to 300 m deep that marks the axis at the crest of the ridge. The Central Indian Ridge is also characterized by a deep at the axis but the topography is more rugged and the ridge axis is more segmented by huge fracture zones that expose rocks of the lower crust (Engel and Fisher, 1975). This is especially true to the north of the area shown in Figure 1, notably for the Marie Celeste Fracture Zone at 18°S.

Away from the active ridge sections there are other topographic provinces of importance. East and southeast of Mauritius for several hundred kilometers the topographic relief is extreme, with elongated ridges and faulted slivers separated by flat floored basins of turbidites and volcanic ash. This ridge and pond topography trends nearly north-south in a large region west of 64°E, except for the sharply defined Rodriguez Ridge at about 20°S and a discordant knot near 23°S, 59°30'E. This area contrasts markedly with the

smooth volcanogenic apron surrounding and south of Réunion, and also with the sedimented and smoothed tract from Réunion south to the northeast-trending northern foothills of the Southwest Indian Ridge at 52°-59°E. South and southwest of the triple junction for a considerable distance are northeast-southwest trending ridges and swales whose origin is obscure, but which also occur northeast of the Southeast Indian Ridge as pictured on Figure 1.

MAGNETIC ANOMALIES AND SEISMICITY

Figure 2 portrays the residual magnetic anomalies (total field with IGRF removed for data prior to 1971; total field with IGRF + 400 gammas removed for data since then) along trace for all the available Scripps Institution of Oceanography, Woods Hole Oceanographic Institution, and Institut de Physique du Globe cruises. A few reconnaissance lines from CONRAD 16 and VEMA 20 of the Lamont-Doherty Geological Observatory are also shown. Anomalies in the area around the triple junction are not drawn. These data are shown at a larger scale elsewhere (Tapscott and others, in preparation). Also superimposed upon the lineations are the relocated earthquake epicenters from the ESSA earthquake tape between 1971 and 1976. These earthquakes were relocated by Sean Solomon of MIT.

FIGURE 2

Profiles of residual magnetic anomalies at right angles to track in the southwest Indian Ocean. All cruises after 1971 have 400 gammas added to the IGRF (IAGA, 1965). The magnetic anomalies in the area of the rectangle have been interpreted by Tapscott and others (in preparation). The circled crosses represent relocated earthquake epicenters, the relative size indicating magnitude. The black dots with lines through them represent magnetic anomalies. The heavy lines mark the active spreading centers and transform faults and the light dashed lines mark fracture zone traces. The hatched line marks the rough-smooth boundary around the Southwest Indian Ridge.

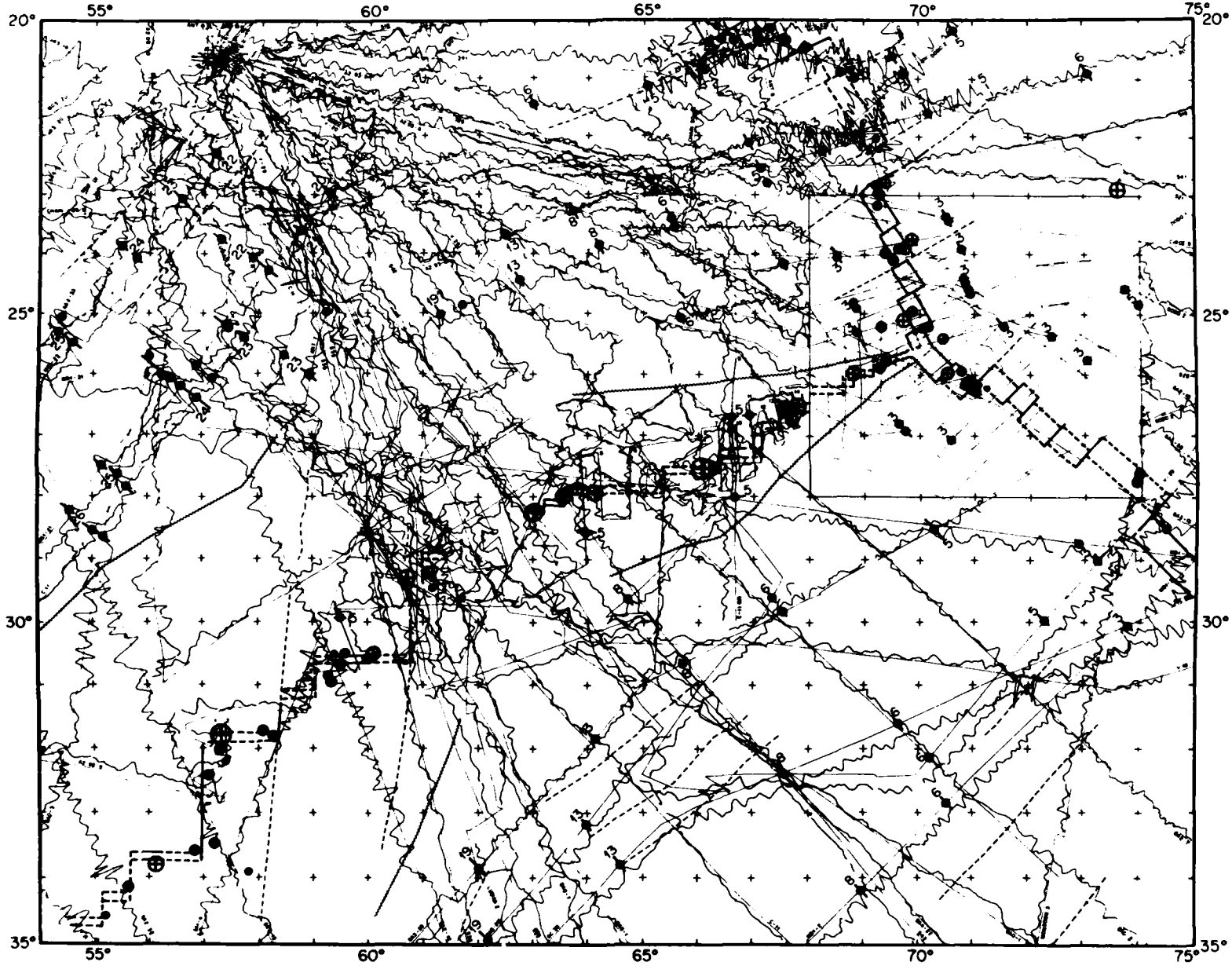
55°
60°
65°
70°
75°
20°
25°
30°
35°

Central Anomaly, Seismicity, and the Ridge Axis

On superimposing the magnetic anomaly and seismicity chart upon the topographic contours, in general the earthquake epicenters and the pronounced positive anomalies lie close to the elevated topography. When examined in detail both the center of the Central Indian and of the Southeast Indian Ridges are associated with a 500 m depression. The axis of the Southwest Indian Ridge is marked by a much more pronounced cleft that generally is deeper than 1000 m and in some localities extends to 2000 m. In the case of the Central and Southeast Indian Ridges these depressions correlate well with the center of the central magnetic anomaly and hence they are interpreted to mark the axis of spreading. In general, the offsets on the central anomalies in these two regions are small and few very deep transform faults are observed. However on the Central Indian Ridge at 20°S and 23°S and on the Southeast Indian Ridge at 26°S, 27°30'S and 28°30'S small but observable transform faults are revealed both by topography and by offsets of the magnetic lineations.

In contrast to the other ridge axis sections in this region, the Atlantis II and Melville Fracture Zones are spectacular features. They show a pronounced north-south trend in both the topography and the relocated epicenters. There probably are two north-south transform faults between them and together these four features offset the active

spreading centers 5° northward in an east-west distance of 4°. All the epicenters lie either on transform faults or spreading centers.

East of 61°E (Melville Fracture Zone) the morphology and activity of the ridge trend plainly N75°E overall. Though the general trend of the topography is northeast, the ridge is characteristically blocky, with generally east-west troughs joined and offset by broader north-south depressions. Between 66°E and 67°E there is a clear central magnetic anomaly associated with a deep depression in the topography. It is assumed that except for the area between 61°S and 63°E this depression marks the active spreading region, here a zone consisting of east-west trending spreading centers offset by short north-south transform faults. However, to be consistent one is constrained by the data control to assume that between 61° and 63°E the ridge axis likewise follows the central depression and hence runs about 30° oblique to the normal or at 60° to the direction of the transform faults.

Older Anomalies

The magnetic anomalies on the Southwest Indian Ridge are difficult to interpret owing to the slow spreading rate (<1 cm/yr) and the associated rough topography. Further complications arise because the axis consists of short sections of spreading ridge offset by fracture zones.

Thus it is difficult to obtain a magnetic profile that has not crossed a fracture zone. The ridge crest profiles that were run north-south on ATLANTIS II (AII) 93-5 and one carefully controlled line, MARION DUFRESNE (MD) 11-2, are presented as Figure 3. The latter line was run between two clearly identified central anomalies recorded by Atlantis II. An attempt was made to match the lineations on the ridge axis profiles with the standard block model and a 'contaminated' model. In the 'contaminated' model the box-like feature of blocks has been smoothed by a Gaussian filter of variable length (Tisseau, 1978). The Gaussian filter models the random nature of the intrusion process at the spreading center. The exact nature of the computation process can be found in Tapscott and others (in preparation). With the aid of the contamination model one is able to observe Anomaly 5 on both ends of the MD-11 profile, and on one or perhaps two of the AII 93-5 profiles. We were not able to identify with certainty any anomalies older than Anomaly 5.

The magnetic anomalies on the Central Indian Ridge are much easier to identify than those on the Southwest Indian Ridge because its spreading rate is faster and the topography less rough. A previous compilation by Fisher and others (1971) identified many anomalies, from the central anomaly to Anomaly 5 either side of the ridge axis. Here we present a more extensive compilation of the data but, except for

FIGURE 3

Residual magnetic anomaly profiles across the Southwest Indian Ridge (for position see numbers on profiles on Figure 2) projected onto 000° and compared with synthetics, skewed 60°, unaltered and contaminated by a 4 km Gaussian filter. Spreading rate 0.8 cm/yr.

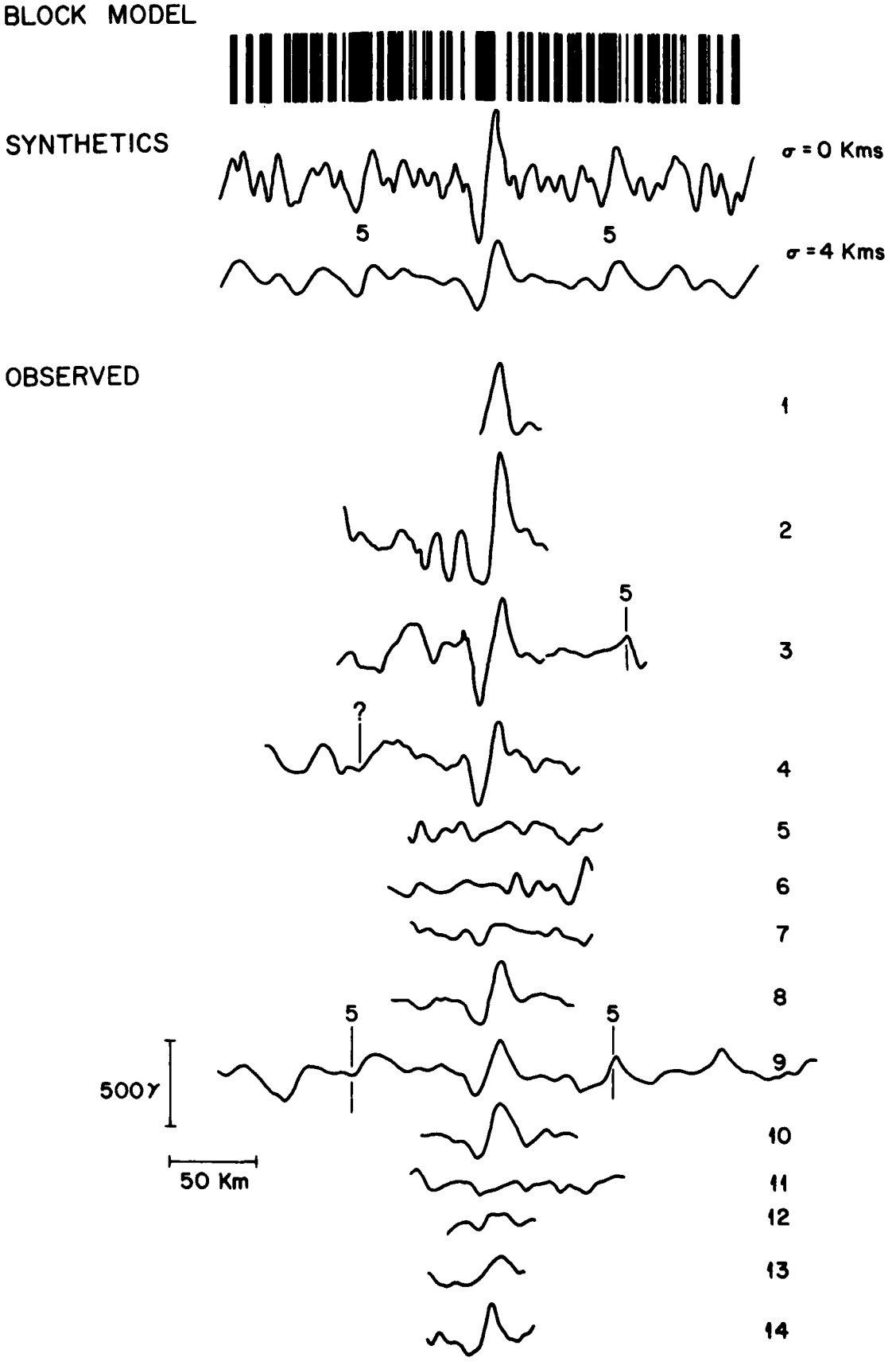
BLOCK MODEL
SYNTHETICS
σ = 0 Kms
5
5
σ = 4 Kms
OBSERVED
1
2
5
3
?
4
5
6
7
8
5
5
9
500γ
10
50 Km
11
12
13
14

the detailed survey near the triple junction, few new identifications. However one is able to recognize with more certainty than Fisher and others (1971) the transform faults and offsets on the lineations. In the present paper the major advance has been on anomalies older than Anomaly 5. AII 93-5, AII 93-6, and MD-11 profiles were run closely parallel to what was thought to be the direction of spreading. These lines were most successful, and on three profiles we identified with certainty anomalies 6, 8, 13 and possibly Anomaly 18 on two lines and on one, MD-11, anomalies 19 and 20 that obviously represent spreading at a much faster rate than the younger anomalies (Figure 4). Anomaly 6 also is recognizable on a VEMA-20 profile to the east of the ridge axis. From the presumed lineation of these anomalies and the apparent rate it is clear that the present phase of spreading extends back to at least the time of Anomaly 18 and probably until about Anomaly 19. At that time there must have been a major change in direction, following the formation of the northwest-southeast trending anomalies in the Madagascar Basin.

Of the three spreading centers, the Southeast Indian Ridge has by far the easiest anomalies to identify. Though there are considerably fewer tracks on this section of the ridge the trends and rates of spreading are very easily determined from the magnetic lineations. As all the profiles over the Southeast Indian Ridge shown here have

FIGURE 4

Residual magnetic anomaly profiles across the Central Indian Ridge, projected onto N060°E. These are compared with synthetics, skewed 30°, unaltered and contaminated by a 4 km Gaussian filter. Spreading rate 2.0 (anomalies 8 to 5) and 1.8 (anomalies 21 to 8) cm/yr.

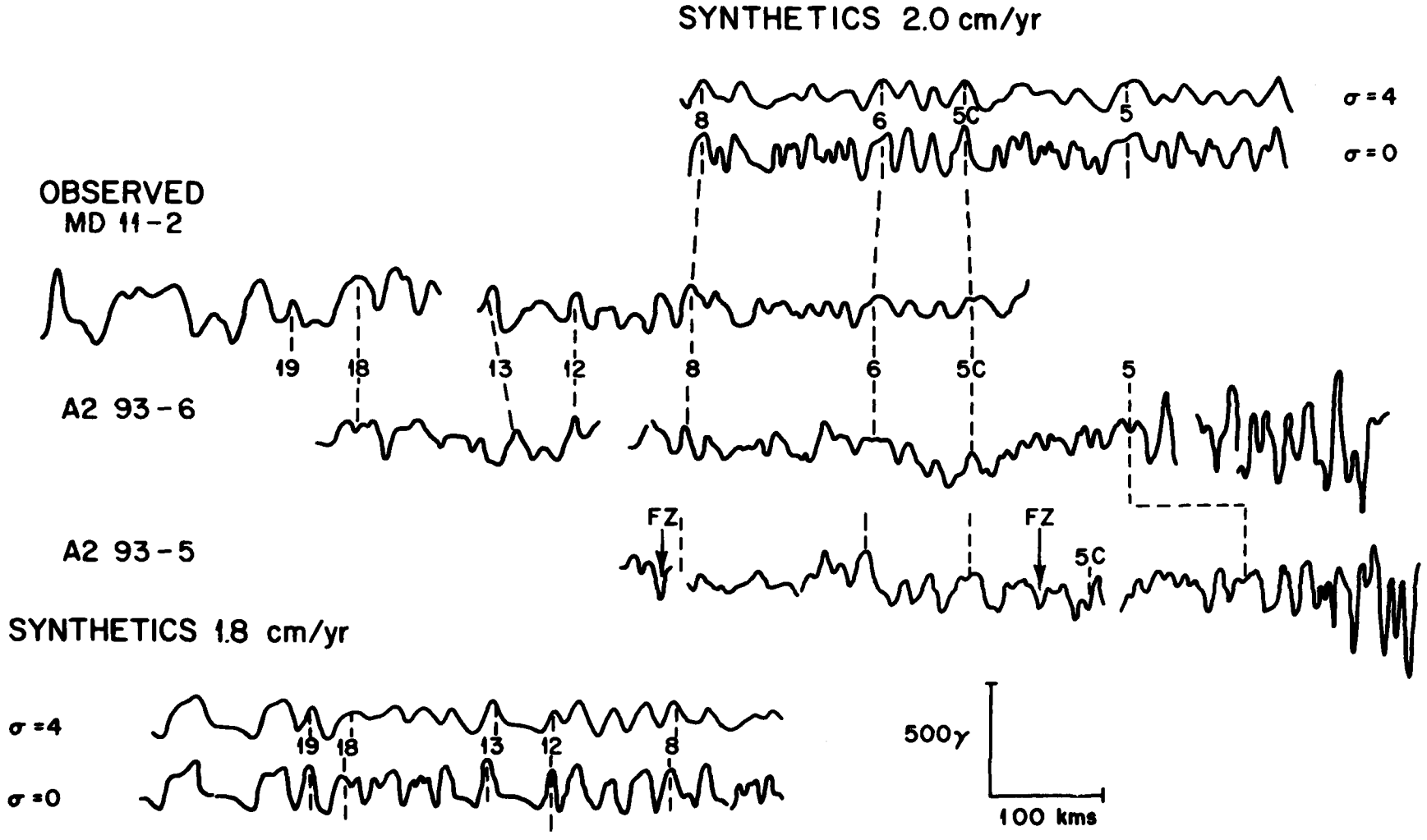
SYNTHETICS 2.0 cm/yr
σ=4
σ=0
8
6
5C
5
OBSERVED
MD 11-2
19
18
13
12
8
6
5C
5
A2 93-6
FZ
FZ
A2 93-5
5C
SYNTHETICS 1.8 cm/yr
σ=4
σ=0
19
18
13
12
8
500γ
100 kms

been discussed elsewhere we have not presented a figure of the projected anomalies. North of the ridge axis and just west of the Ninetyeast Ridge, Sclater and others (1976) reported a suite of anomalies 6 through 17 with one clear Anomaly 19 at 25°30'S and 85°E. To the south of the Southeast Indian Ridge anomalies 6, 8, 13 and 19 are all clearly identified on profiles presented by Schlich (1975). Also one may recognize in the topography possible fracture zones trending northeast-southwest at right angles to the proposed magnetic lineations. The magnetic lineations on the southeast branch reveal three main features. First, though the ridge has a relatively complicated blocky morphology, the ridge axis sections are much longer than the transform faults, and in general there is a relatively simple evolutionary history. Second, on the profiles both north and south of the ridge the direction of spreading and the rate of spreading changed at Anomaly 19 time. Finally, the identified anomalies 7 through 13 north of the ridge axis are about 1 1/2 degrees of latitude closer to the ridge axis than are those to the south. Preliminary comparison of profiles suggests that this is due to a general asymmetry by a jump or continuous asymmetric spreading between anomalies 5 and 6.

TECTONIC CHART

Figure 5 is a tectonic chart of the area between 15°S and 35°S, and between 54°E and 85°E, based upon the topographic and magnetic data presented in Figures 1 and 2 and that presented by Tapscott and others (in preparation) at the triple junction. For the areas outside these figures we complemented our data by accepting the interpretation of Schlich (1975) for the Mascarene and Crozet Basins, Fisher and others (1971) for the Central Indian Ridge, and Sclater and others (1976) and Sclater and Fisher (1974) for the Central Indian Ridge.

West of the Melville Fracture Zone at 61°E the Southwest Indian Ridge consists of a series of diffuse and not clearly identified spreading centers offset in significant degree by an en echelon suite of north-south trending transform faults. East of the Melville Fracture Zone the ridge becomes a tenuous set of east-west trending spreading centers offset by short and difficult to identify north-south transform faults. The center of spreading is remarkably well delineated by the 4000 m contour (Figure 5).

The north-south trending fracture zones are spectacular in both depth and extent and their topographic expression can be extended to just south of the well-identified magnetic lineations in the Madagascar Basin. To the east of the Melville Fracture Zone this pronounced north-south grain

FIGURE 5

A tectonic chart of the area surrounding the Indian Ocean triple junction superimposed upon the 4000 m contour. The continuous or dashed lines represent the central anomalies. The single dashed lines represent active transform faults and fracture zones. The hatched line marks the boundary of the Southwest Indian Ridge. The black dots with lines through them are magnetic anomalies. The circled crosses are recent epicenters, relative size indicating magnitude.

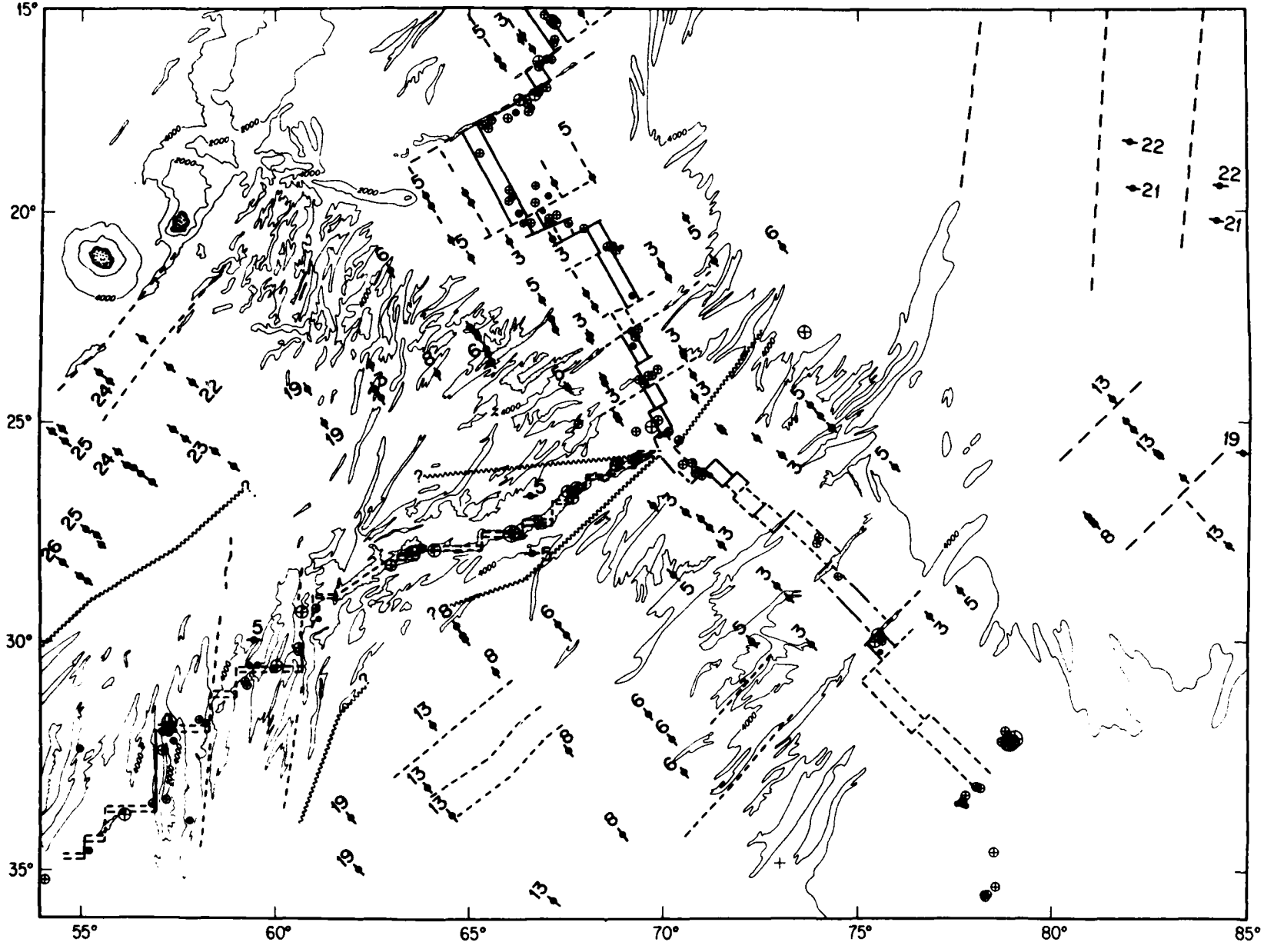
15°
20°
25°
30°
35°
55°
60°
65°
70°
75°
80°
85°

disappears. The trends well south of the Southwest Indian Ridge spreading center appear northeast-southwest in direction.

The rough to smooth topographic transitions north and south of the axes, that mark the presumed boundaries between the Southwest Indian Ridge and other ridges, have a complex character. Between the triple junction and the Melville Fracture Zone at 61°E the northern boundary runs east-west but is not very clear, whilst the southerly boundary runs southwest-northeast and is well-defined. The area enclosed by those boundaries is a right triangle, with the most acute apex at the triple junction. West of the Melville Fracture Zone the rough/smooth boundary between the Southwest Indian Ridge and the other two ridges trends at a much steeper angle both north and south of the ridge than to the east of 61°E.

The Central Indian Ridge, north of the Marie Celeste Fracture Zone at 18°S, is marked by very deep en echelon fracture zones with clearly identified and massively offset ridge segments between them. South of this fracture zone the ridge segments appear longer and the transform faults are less obvious on the topography. The magnetic anomalies can be traced with confidence to Anomaly 8 and with less confidence to Anomaly 19. However, between Anomaly 19 and Anomaly 21 time there is a striking change, since at 50 Ma (Anomaly 21) the spreading direction apparently was N35°E.

The Southeast Indian Ridge, in contrast, has the characteristic blocky morphology of relatively fast ($\sim$3 cm/yr) spreading centers though it still possesses a central valley. Most of the recent epicenters lie on transform faults and few lie on the active spreading center sections. A surprisingly large grouping of earthquakes is observed at 32°S and 79°E. These earthquakes apparently lie on an inactive section of a transform fault. Their origin and the explanation of the large number is unknown at this time. From the present back until approximately 44 Ma (Anomaly 19) the direction of spreading has been roughly constant at N45°E and the rate has remained between 2.5 and 3 cm/yr with some asymmetry. However, earlier than this, between 50 Ma (Anomaly 21) and 80 Ma (Anomaly 34) the spreading direction was very different, N05°E in the Central Indian Basin (McKenzie and Sclater, 1971), and N30°E in the Crozet Basin (Schlich, 1975), the apparent discrepancy in both trends being due to the curvature of the earth.

PRESENT PLATE MOTION: AFRICA/ANTARCTICA

One of the main objectives of this study was to determine an instantaneous pole of relative motion for Africa/Antarctica. To obtain this pole, we determined the positions along the plate boundary where we believed the directions of motion were well-known (Table 1; Fig. 6). These positions and

TABLE 1

Directions of Spreading on the Southwest Indian Ridge

Feature	Latitude	Longitude	Direction Observed	Direction Predicted	Date Source
Triple Junction (1)	25.60°S	70.00°E	01°±09°	358°	Tapscott and others (in prep.)
Spreading Center (2)	27.30°S	66.63°E	358°±05°	359°	This paper
Melville F.Z. (3)	30.00°S	60.75°E	354°±04°	01°	This paper
"58°E F.Z." (4)	31.70°S	58.35°E	02°±05°	02°	This paper
Atlantis II F.Z. (5)	33.00°S	57.00°E	0°±02°	02°	This paper
Prince Edward F.Z. (6)	46.00°S	35.15°E	17°±02°	15°	Bergh and Norton (1976)
Shaka F.Z. (7)	53.50°S	09.00°E	39°±02°	37°	Sclater and others (in press)
Islas Orcadas F.Z. (8)	54.25°S	06.00°E	40°±02°	40°	Sclater and others (in press)
Bouvet F.Z. (9)	54.25°S	02.00°E	45°±02°	44°	Sclater and others (1976)

Pole deduced from fracture zones: 8.4°N, 42.2°W, $\alpha 95 = 4.0°$

FIGURE 6

A comparison between predicted isochrons and observed magnetic lineations in the vicinity of the Indian Ocean Triple Junction. The isochrons were computed by rotating the present ridge axis by half the angle about the poles given in Table 2b. The dotted line represents the Melville Fracture Zone.

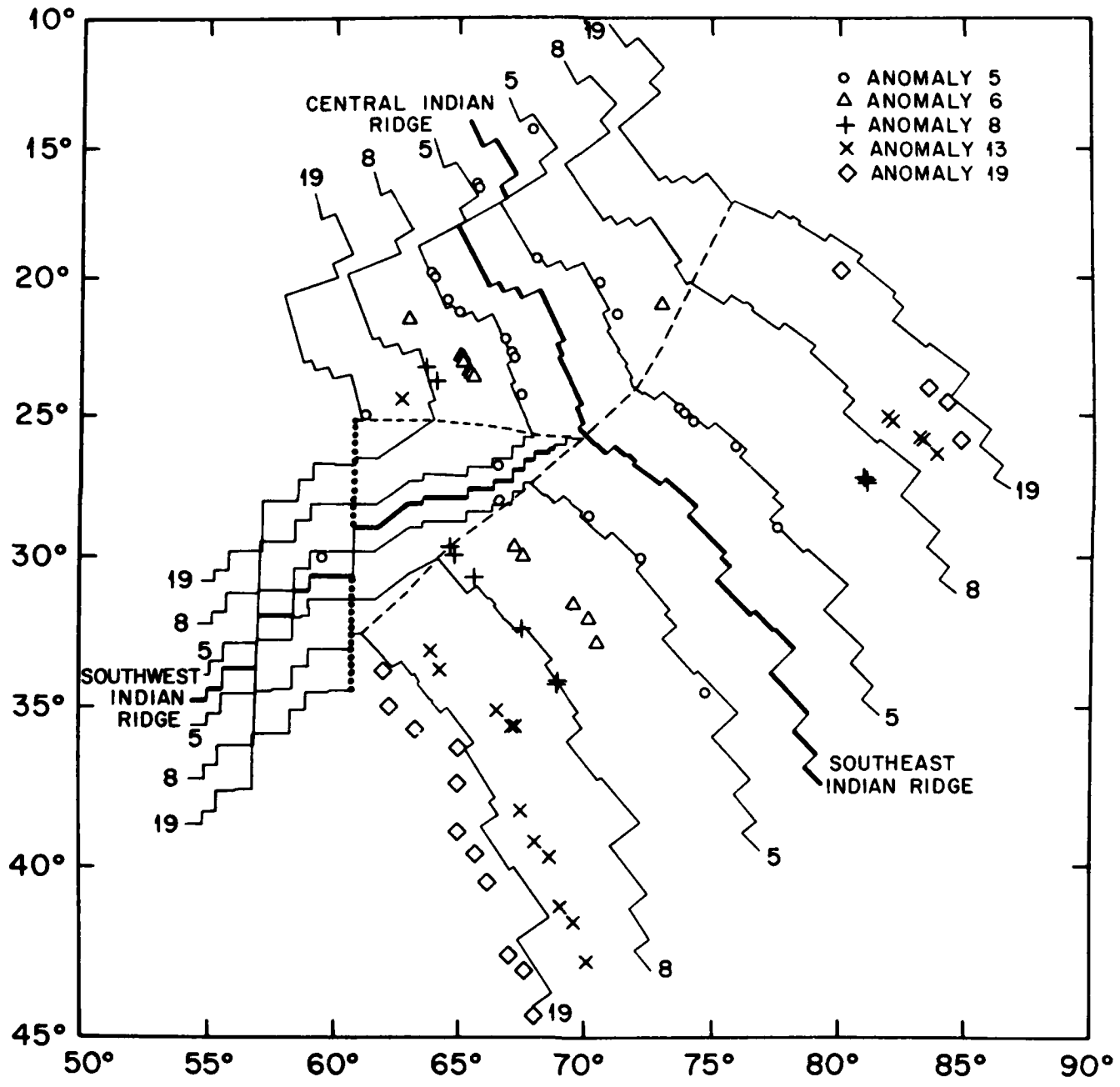
10°
15°
20°
25°
30°
35°
40°
45°
50°
55°
60°
65°
70°
75°
80°
85°
90°
ANOMALY 5
ANOMALY 6
ANOMALY 8
ANOMALY 13
ANOMALY 19
CENTRAL INDIAN RIDGE
SOUTHWEST INDIAN RIDGE
SOUTHEAST INDIAN RIDGE

directions were combined two at a time to determine the pole of a rotation which fit both points. Only positions separated by more than 4° in latitude were selected, and these were weighted according to the accuracy with which it was believed the direction was known. These statistics have a weighted mean of the individual poles of 8.4°N, 42.2°W, with an $\alpha 95$ of 4.0° and a rate of 0.15 degrees/my. A comparison of the directions predicted by this pole and those observed at the nine locations selected shows that none disagree by more than 02°. This fit is considered excellent and strikingly demonstrates that, at the level of accuracy at which we are operating, Africa appears to be a single plate and the Bouvet Triple Junction data is compatible with that from the Indian Ocean Triple Junction.

It is of interest to note that this mean pole lies more than 30° from that predicted by Minster and others (1974) for their global closure model. It also lies 15° away from the pole calculated by Forsyth (reported in Sclater and others, 1976) by closure around the Bouvet Triple Junction. However, it is remarkably close to that predicted by Chase (1972). Clearly some reanalysis of the closure models of Minster and others (1974) is needed before they are preferred over those of Chase (1972).

In an imminent paper Tapscott and others (in preparation) compiled 60 observations of rate and instantaneous direction

of relative motion for the South American, African, Indian, and Antarctic plates. They added to this set some observations from the Bouvet and Indian Ocean Triple Junctions and used a program written by Forsyth (1976) to find the best fit set of relative rotation vectors. They find an Africa/Antarctica pole at 5.6°N, 39.4°W with a rate of 0.15 degrees/my. It is gratifying to see how well this more general set gave almost the same pole for Africa/Antarctica as given by our independent calculation. Our pole, which agrees with the data and is consistent with those on four other plate boundaries, is to be preferred to that of Minster and others (1974).

TECTONIC HISTORY

The fracture zones on the Southwest Indian Ridge trend north-south and extend a considerable distance in this direction to the north of the active section. But no anomalies older than Anomaly 5 were identified on this ridge axis. Thus there is no possibility with the available data set of directly determining whether or not the present spreading regime has persisted since 44 Ma (Anomaly 19) as is observed on the Central Indian and Southeast Indian Ridges. However, we can indirectly resolve the spreading history of the Southwest Indian ridge by reconstructing the past position of the other two ridges. This is possible to the east of the Melville Fracture Zone because the southernmost Anomaly 19 on the

Central Indian Ridge lies directly north of the most northern Anomaly 19 in the Crozet Basin (Figure 5). Further, both anomalies lie just east of the Melville Fracture Zone and the gap between them encloses almost the entire region of rough topography between the Melville and the triple junction.

Norton and Sclater (in press) have used the closure of the Chagos Bank onto the Mascarene Plateau and alignment of the Vishnu Fracture Zone and Mauritius Trench to compute an Anomaly 16 (39 Ma) pole for the motion of Africa with respect to Australia. Weissel and others (1977) have used the magnetic anomalies between Australia and Antarctica to compute an Anomaly 18 pole for the motion of India with respect to Antarctica. It is apparent that since Anomaly 19 time the finite poles must have lain fairly close to the present poles for the motions to have remained so constant both in rate and in direction on the three ridge axes. As a consequence, one can assume these Africa/India and India/Antarctica poles to hold back to Anomaly 19 time (44 Ma) (Table 2a). One then computes a pole for the motion of Antarctica with respect to Africa. This lies close to the present pole. Rotating the present Central Indian Ridge axis by the Anomaly 19 pole for Africa/India gives a good fit to the observed Anomaly 19 in the Madagascar Basin. But rotating the Southeast Indian Ridge axis by the Weissel and others (1977) pole gives a very poor match, even after allowing some asymmetry.

TABLE 2a

Poles Computed From Tapscott and others (in preparation), Weissel and others (1977) and Norton and Sclater (in preparation)

		Antarctica/Africa S.W.I.R.			Africa/India C.I.R.			Antarctica/India S.E.I.R.		
Anomaly	Age	Lat.	Long.	Angle	Lat.	Long.	Angle	Lat.	Long.	Angle
5	9	7.8	-41.8	1.38*	15.5	48.6	5.7[1]	16.2	34.6	5.9[1]
19	44	3.1	-38.3	8.0*	13.3	54.1	23.5[2]	9.9	34.8	24.6[3]

*Resultant pole

[1]Pole from Tapscott and others (in preparation)

[2]Pole computed from Norton and Sclater (in press)

[3]Pole computed from Weissel and others (1977)

TABLE 2b

Poles Used for Reconstructing Position of Ridge Axis

		Antarctica/Africa S.W.I.R.			Africa/India C.I.R.			Antarctica/India S.E.I.R.		
Anomaly	Age	Lat.	Long.	Angle	Lat.	Long.	Angle	Lat.	Long.	Angle
5	9	8.4	-42.2	1.4[1]	16.0	48.3	5.8[2]	16.8	34.3	6.0*
8	27	8.4	-42.2	4.9[1,3]	16.0	48.3	15.1[2,3]	15.4	29.8	16.0*
19	44	8.4	-42.2	8.0[1,3]	16.0	48.3	23.2[2,3]	14.0	28.8	24.8*

*Resultant pole

[1]This paper

[2]Pole from Fisher and others (1971)

[3]Angle adjusted to superpose ridge axis on proper anomaly

In both tables for the poles of rotation, positive number indicate northern latitudes and eastern longitudes and a right-handed screw about an axis passing through the pole and the center of the earth.

The present data set are not good enough to obtain improved finite poles but they are good enough to demonstrate the general development of the triple junction. Thus in order to illustrate how the Southwest Indian Ridge has been created by the rapid eastward motion of the triple junction we opted for the simplest approach compatible with the data. First, we assumed that the present poles of relative motion between Africa and Antarctica and between Africa and India have remained fixed since 44 Ma (Anomaly 19). We justify this by the long, straight fracture zone traces observed on the Southwest Indian Ridge and by the major fracture zones on the Central Indian Ridge and the close agreement between the poles of Tapscott and others (in preparation) and Norton and Sclater (in press). For the 27 Ma (Anomaly 8) and 44 Ma (Anomaly 19) rotations for the Central Indian Ridge, we computed the angles of rotation by fitting the ridge axis to the observed anomalies 8 and 19. The angle of rotation for 9 Ma (Anomaly 5) on the Southwest Indian Ridge was obtained by assuming the present rate of spreading to have been constant from that time. The angle for the 44 Ma (Anomaly 14) rotation we determined by fitting the ridge axis to the rough-smooth topographic boundary just south of Anomaly 19 on the Central Indian Ridge, the assumption being that relative to Africa, 44 million years ago the triple junction lay directly north of the Melville fracture zone and just south of the observed Anomaly 19 on the MD-11 profile.

For the 27 Ma (Anomaly 8) rotation angle, we assumed a constant rate of spreading on the Southwest Indian Ridge between 44 Ma and 9 Ma. We believe this process does not introduce significant errors because the average rate for the 44 Ma rotation is only slightly greater than that for 9 Ma.

Using these six rotations we computed the poles and angles of relative rotation between India and Antarctica for 9 Ma, 27 Ma, and 44 Ma (Table 2b). These poles were checked by rotating the present ridge axis by half the total angle to either side to obtain predicted isochrons. The match to Anomaly 5 is excellent. For Anomaly 8 the overall angle is too small, but satisfactory, but spreading has been strongly asymmetric and there is considerably more ocean south of the ridge than north of it between anomalies 5 and 8. For Anomaly 19 the asymmetry is still in existence but the overall angle, given the simplicity of the method used to obtain it, is surprisingly good.

With these poles, one rotates the Southwest Indian and Central Indian Ridges, as well as the Southeast Indian Ridge, about the present ridges by half the rotation angles of the respective 9 Ma, 27 Ma, and 44 Ma rotations. Some interesting points for the development of the Southwest Indian Ridge become apparent after these rotations. For example, the most northerly Anomaly 8 in the Crozet Basin and the shape

of the rough-smooth boundary between the Southwest Indian and Southeast Indian Ridges demonstrates that the Southeast Indian Ridge has shortened only very little since 44 Ma (Anomaly 19). Because one knows with some precision the amount by which this ridge has shortened with time, one can determine the amount that the Central Indian and Southwest Indian Ridges have changed in length. Both the Central Indian and Southwest Indian Ridges have increased in length, the Southwest Indian Ridge by 1000 kms and the Central Indian Ridge by 550 kms. The increase in length of the Southwest Indian Ridge since 44 Ma (Anomaly 19) is greater than the 800 kms it has opened. It is this relatively rapid eastward motion of the Indian Ocean Triple Junction and the relatively slow north-south spreading on the Southwest Indian Ridge that creates the triangle of rough topography with the apex at the triple junction. The right-sided western boundary of the triangle is the Melville Fracture Zone. This suggests most strongly that this phase of eastward drift of the triple junction started immediately after the formation of the Melville Fracture Zone and the abrupt change of spreading on the Central and Southeast Indian Ridges at 44 Ma.

The general trend of the Southwest Indian Ridge is oblique to the Melville and Atlantis II fracture zones. The trace of the triple junction is east-west on the African

plate and northeast on the Antarctic plate. West of the Melville Fracture Zone the trend of the Southwest Indian Ridge is even more oblique, and if the same model holds it is tempting to suggest that this rough/smooth boundary observed between the Southwest Indian Ridge and the Madagascar Basin is the trace of the triple junction on the African plate between anomalies 25 and 19.

DEVELOPMENT OF THE TRIPLE JUNCTION

There are considerable uncertainties in both the lengths of the individual ridge axis sections chosen and the poles used for the rotations. Thus one cannot give an exact representation of the evolution of the triple junction. On the other hand, we believe that for the most part it has had a stable RRR configuration. It is easy to see on the tectonic history diagram (Fig. 6) that at 9 Ma, (Anomaly 5), 27 Ma (Anomaly 8), and 44 Ma (Anomaly 19) the ridge axes all meet at a point without the necessity of transform offsets.

The tectonic diagram has been used to construct a mean velocity triangle for this time span (Figure 7a). This triangle enables one to discuss the general evolution of the triple junction. Assuming these mean directions and symmetric spreading at right angles to the spreading centers, the triple junction (J, Figure 7a) on the velocity diagram should move southeastward down the Southeast Indian Ridge as time passes.

FIGURE 7

a. A velocity diagram of the Indian Ocean triple junction during phases of normal RRR evolution. For symmetric and non-oblique spreading, the velocity of the junction is given by J. To maintain an approximately constant length for the Southeast Indian Ridge, the triple junction must periodically jump to the northwest along the direction of that ridge, creating transform faults on the Southwest and Central Indian Ridges (light dashed lines).
b. A schematic representation of the trace of migration of the triple junction on the three plates, assuming frequent ridge jumps.
c. A velocity diagram of the Indian Ocean triple junction assuming oblique spreading on the Central and Southwest Indian Ridges. The motion of the junction J causes the length of the Southeast Indian Ridge to decrease only very slowly compared to the situation in Figure 7a.
d. A schematic representation of the trace of the triple junction on the three plates.

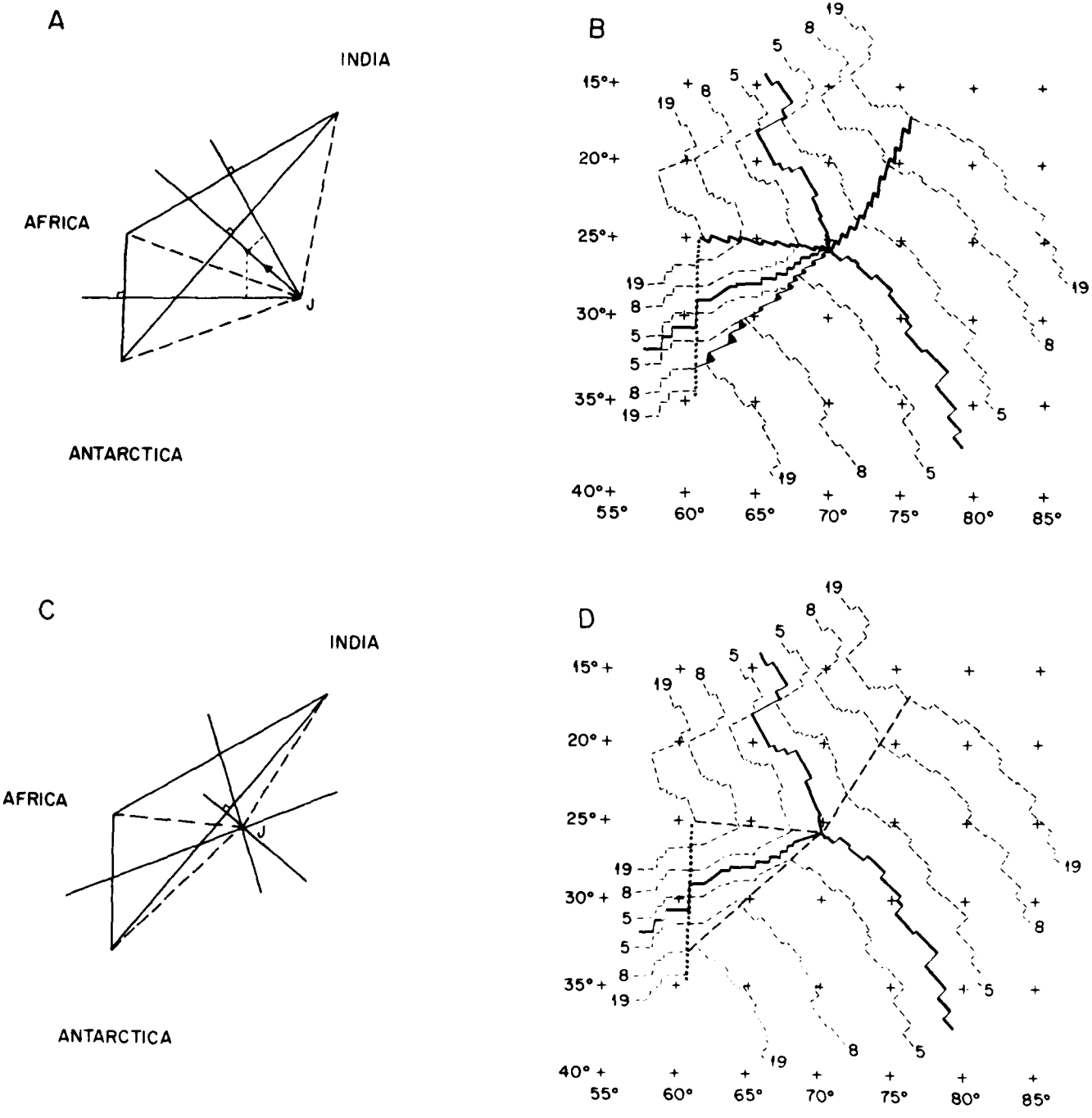
A
INDIA
AFRICA
J
ANTARCTICA
B
19
8
5
15°+
20°+
25°+
30°+
35°+
40°+
55°
60°
65°
70°
75°
80°
85°
C
INDIA
AFRICA
J
ANTARCTICA
D

Thus as one goes back in time and reverses the effect, the Southeast Indian Ridge should increase in length. This is not observed; on the contrary, the Southeast Indian Ridge has remained almost exactly the same length between 44 Ma and present.

There are two simple ways in which the Indian Ocean triple junction can evolve and maintain the Southeast Indian Ridge at an almost constant length. In the first the RRR junction develops smoothly for a short time as J in Figure 7a. Then the triple junction jumps northwest up the southeast branch and fracture zones are formed on the Southwest and Central Indian Ridges. The frequency and magnitude of these jumps is such that the length of the Southeast Indian Ridge never changes by a significant amount. Because the jump causes some of the African plate to be added to the Antarctic plate, the traces of this jump are more pronounced on the Antarctic plate than on the African plate. Also since some of the crust created on the African plate by the Central Indian Ridge is added to the Indian plate, the jumps leave a distinctive zig-zag shape of the triple junction on the Indian plate. A schematic development of the triple junction is shown as Figure 7b. Note the zig-zag nature of the east-west boundary of the trace of the triple junction on the African plate and the extra crust observed on the Antarctic plate.

An alternate and mechanically more simple scheme for the development of the triple junction is for spreading on

the Central Indian and Southwest Indian Ridges to be oblique rather than at right angles to the transform faults. In this case the extension of the three ridge axes can be made to fit close to the mid-point of the motion between India and Antarctica and the velocity triangle resembles Figure 7c. This triple junction is stable and the Southeast Indian Ridge becomes shorter only very slowly as time passes. The trace of the triple junction on the three plates is simple, with no necessity for jumps and offsets (Figure 7d). In the actual Southwest Indian Ridge, oblique spreading does not occur well away from the triple junction. It is possible that the obliquity could decrease with increasing distance from the triple junction. One can obtain the same result by asymmetric rather than oblique spreading on the Southwest Indian and Central Indian Ridges. Such strong asymmetry can be ruled out by the symmetric magnetic anomalies observed on the Central Indian and Southwest Indian Ridges.

On the present Southwest and Indian Ridge the topographic data (Figure 1) suggest strongly that there is oblique spreading at 61°E to 63°E and normal spreading at most other places, except possibly close to the triple junction. Further, there appears to have been both oblique and normal spreading on the Southwest Indian Ridge in the past. Though it will be difficult to differentiate between these two extreme cases, and in the limit of small ridge jumps they are the same,

it is worthwhile to enumerate some of the differences expected if the ridge jumps are large.

In the ridge-jumping/normal spreading model, one would expect the following features:

(1) as many fracture zones on the Central Indian Ridge as on the Southwest Indian Ridge during the eastward movement of the triple junction.

(2) rough but continuously lineated topography, associated with the jump, on the trace of the junction on the Antarctic plate.

(3) rough and discontinuously lineated topography along the trace on the African plate.

(4) less rough but still observable topographic expression on the Indian plate.

In the case of oblique spreading, one would anticipate (a) smooth traces on all three plates of the junction. Further (b) the anomalies on the Southwest Indian Ridge would be subdued and oblique near the traces of the triple junction and finally, (c) the anomalies on the Central Indian Ridge would be oblique near the traces of the triple junction. This obliquity would be small and may not be detectable without a detailed survey.

CONCLUSIONS

Between 54°E and 61°E the Southwest Indian ridge is dominated by a suite of en echelon north-south topographic gashes. East of 61°E to the Indian Ocean triple junction the major feature is a triangular region of rough topography with a sinuous northeast trending depression running from the north-south trending gashes to the eastern apex. We show that this depression probably marks the axis of a spreading center and that spreading occurs approximately north-south at a rate of 0.8 cm/yr. Further, we have found that the directions of motion predicted for the Africa/Antarctica boundary at the Bouvet and Indian Ocean triple junctions are compatible. Thus the Southwest Indian Ridge is a continuous boundary between only two plates. The directions and rates of motion at both triple junctions and those inferred from transform faults and magnetic anomalies between them give a pole for the present motion of Africa/Antarctica at 8.4°N, 42.4°W. This pole is close to that of Chase (1972) but more than 30° from that predicted by Minster and others (1974) in their respective global closure models.

A major change of spreading direction from north-south is northeast-southwest occurs in the Indian Ocean at the time of Anomaly 19 (44 Ma). We have shown that from this time until the present the position of the poles of relative motion between the African, Indian, and Antarctic plates

change remarkably little. We use this information and the magnetic anomalies to construct a tectonic history of the three major plate boundaries, the Central, Southwest, and Southeast Indian Ridges, at the time of anomalies 19, 8, and 5 (44 Ma, 27 Ma, and 9 Ma; Figure 8). In our initial reconstruction the Central and Southeast Indian Ridges meet the Southwest Indian Ridge at the Melville Fracture Zone at 61°E. The right triangular region of rough topography between this fracture zone and the triple junction is created by the rapid eastwards motion of this junction and slow spreading on the Southwest Indian Ridge. In the development of the triple junction the Southeast Indian Ridge remains almost constant in length. With present information it is not possible to determine whether this results predominantly from spreading normal to the transform faults on the Southwest Indian Ridge and continuous jumps to keep the Southeast Indian Ridge constant or to oblique spreading on both the Southwest Indian and Central Indian Ridges. We believe that the triple junction probably evolves in both modes.

FIGURE 8

The position of the Central, Southeast, and Southwest Indian Ridges with respect to a fixed Africa at the time of anomalies 19(A), 8(B), 5(C), and at present (D). Also shown are the rotated and present positions of the observed anomalies (symbols as for Figure 6). The continuous lines represent the inferred position of anomalies 19,8,and 5 on the reconstructions. They were determined by rotating the individual ridge axes through the appropriate rotation angle. On the Anomaly 19 reconstruction (A) the magnetic anomalies from the Indian plate (black) overlap those from the Antarctic plate but do not match the inferred position of the ridge axis. This implies that the pole we used for India/Antarctica for this reconstruction is reasonable and that more crust has been created south of the axis than to the north.

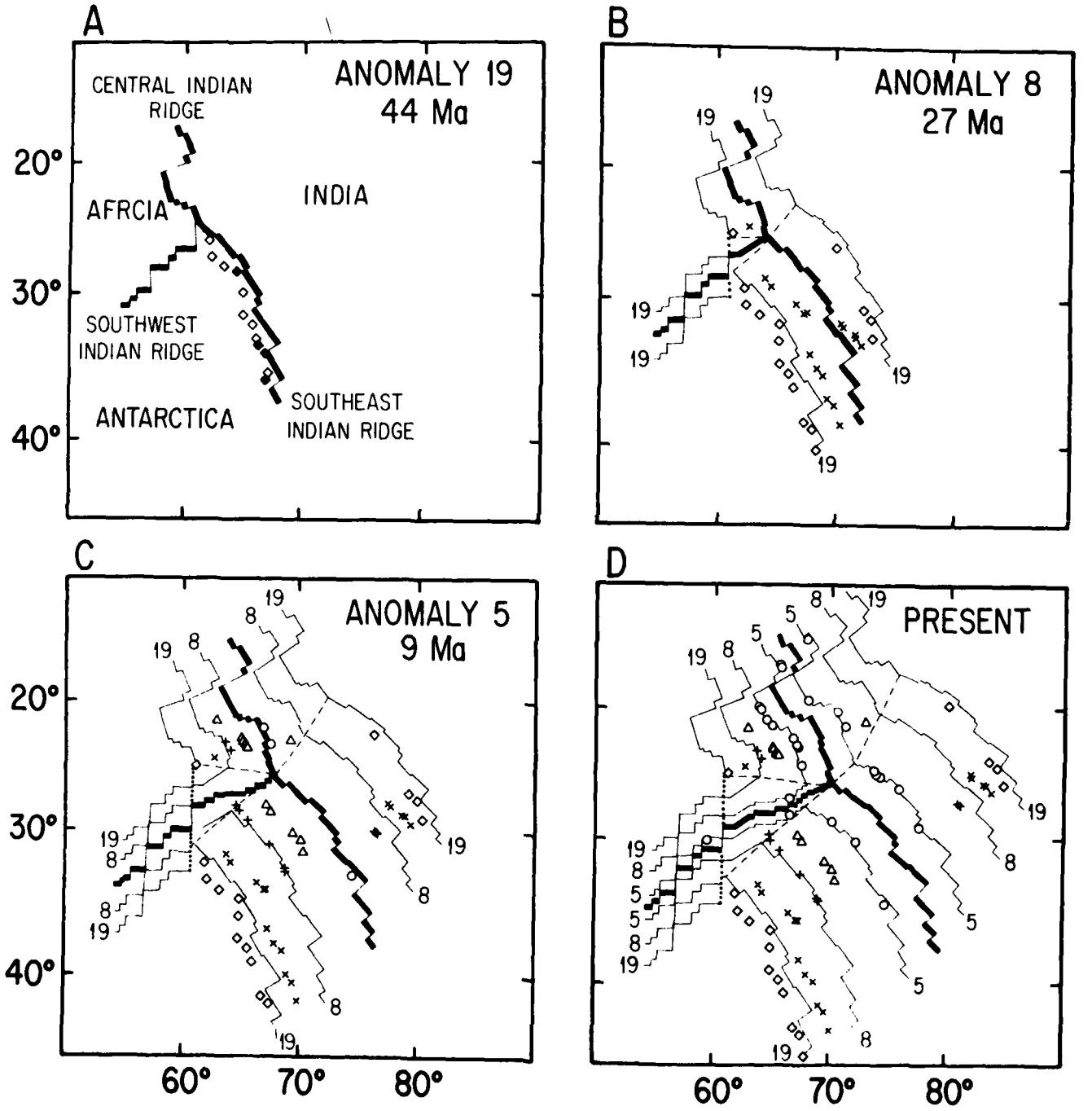
A
ANOMALY 19
44 Ma
CENTRAL INDIAN
RIDGE
INDIA
AFRCIA
SOUTHWEST
INDIAN RIDGE
SOUTHEAST
INDIAN RIDGE
ANTARCTICA
20°
30°
40°
B
ANOMALY 8
27 Ma
C
ANOMALY 5
9 Ma
D
PRESENT
60°
70°
80°

ACKNOWLEDGEMENTS

We thank the captains and crews of the research vessels Melville, Argo, and Atlantis II, the M/V Marion Dufresne, and our shipboard colleagues for their help and cooperation that made this work possible.

This work was supported by Office of Naval Research Contracts N00014-75-C-0291 with the Massachusetts Institute of Technology and N00014-74-C-0262; NR083-004 with the Woods Hole Oceanographic Institution and N00014-75-C-0152 with the Scripps Institution of Oceanography, and by the Centre National de la Récherche Scientifique and Terres Australes et Antarctiques Françaises who provided ship time for the French Indian Ocean program.

REFERENCES

Bergh, H.W., and Norton, I.O., 1976, Prince Edward Fracture Zone and the evolution of the Mozambique Ridge: Journal of Geophysical Research, v. 81, p. 5221-5239.

Chase, C.G., 1972, The N plate problem of plate tectonics: Royal Astronomical Society Geophysical Journal, v. 29, p. 117-122.

Engel, C.G., and Fisher, R.L., 1975, Granitic to ultramafic rock complexes of the Indian Ocean Ridge System, Western Indian Ocean: Bulletin of the Geological Society of America, v. 86, p. 1553-1578.

Fisher, R.L., Sclater, J.G., and McKenzie, D.P., 1971, Evolution of the Central Indian Ridge, Western Indian Ocean: Bulletin of the Geological Society of America, v. 82, p. 553-562.

Fisher, R.L., Bunce, E.T., and others, 1974, Initial Reports of the Deep Sea Drilling Project, vol. 24, Washington, DC, (U.S. Government Printing Office), 1183 p.

Forsyth, D.W., 1975, Fault plane solutions and tectonics in the South Atlantic and Scotia Sea: Journal of Geophysical Research, v. 80, p. 1429-1443.

IAGA Commission 2 Working Group 4, 1969, Analysis of the Geomagnetic Field, International Geomagnetic Reference Field, 1965.0: Journal of Geophysical Research, v. 74, p. 4407-4408.

McKenzie, D. and Sclater, J.G., 1970, The evolution of the Indian Ocean since the late Cretaceous: Royal Astronomical Society Geophysical Journal, v. 25, p. 437-528.

Minster, J.B., Jordan, T.H., Molnar, P., and Haines, E., 1974, Numerical modeling of instantaneous plate tectonics: Royal Astronomical Society Geophysical Journal, v. 36, p. 541-576.

Norton, I.O., 1976, The present relative motion between Africa and Antarctica: Earth and Planetary Science Letters, v. 33, p. 219-230.

Norton, I.O., and Sclater, J.G., 1978, A model for the evolution of the Indian Ocean and the breakup of Gondwanaland: Journal of Geophysical Research (in press).

Schlich, R., 1975, Structure et Age de l'Ocean Indien Occidental: Société Géologique de France, Memoire Hors-Série, no. 6, 103 p.

Schlich, R., and Patriat, P., 1971, Anomalies magnétiques de la branche est de la dorsale médio-idienne entre les iles Amsterdam et Kerguelen: Comptes Rendus Academy of Science, Paris, v. 272, p. 773-776.

Sclater, J.G., Luyendyk, B.P., and Meinke, L., 1976, Magnetic lineations in the southern part of the Central Indian Basin: Bulletin of the Geological Society of America, v. 87, p. 371-378.

Sclater, J.G., and Fisher, R.L., 1974, The evolution of the East Central Indian Ocean with emphasis on the tectonic setting of the Ninetyeast Ridge: Bulletin of the Geological Society of America, v. 85, p. 683-702.

Sclater, J.G., Bowin, C., Hey, R., Hoskins, H., Peirce, J., Phillips, J., and Tapscott, C., 1976, The Bouvet Triple Junction: Journal of Geophysical Research, v. 81, p. 1857-1869.

Sclater, J.G., Dick, H., Norton, I.O., and Woodroffe, D., 1978, Geophysical and petrological study of the Antarctic plate boundary east and west of Bouvet Island: Earth and Planetary Science Letters, v. 37, p. 393-400.

Tapscott, C., Patriat, P., Fisher, R.L., Sclater, J.G., Hoskins, H., and Parsons, B., 1978, The Indian Ocean Triple Junction (in preparation).

Tisseau, J., 1978, Etude structurale du Golfe d'Aden et du bassin de Somalie: Thèse de Doctorat de 3eme cycle, Université de Paris.

Warren, B.A., 1978, Bottom water transport through the Southwest Indian Ridge: Deep-Sea Research, V. 25, p. 315-321.

Weissel, J.K., and Hayes, D.E., 1972, Magnetic anomalies in the southeast Indian Ocean, in Hays, D.E., ed., Antarctic Oceanology II: The Australian-New Zealand Sector, Washington, DC, American Geophysical Union Antarctic Research Series, v. 19, p. 165-196.

Weissel, J.K., Hayes, D.E., and Herron, E.M., 1977, Plate tectonic synthesis: the displacements between Australia, New Zealand, and Antarctica since the Late Cretaceous; Marine Geology, v. 25, p. 231-277.

CHAPTER 3

THE INDIAN OCEAN TRIPLE JUNCTION

THE INDIAN OCEAN TRIPLE JUNCTION *

Christopher Tapscott	Department of Earth and Planetary Sciences Massachusetts Institute of Technology Cambridge, MA 02139 and Woods Hole Oceanographic Institution Woods Hole, MA 02543
Philippe Patriat	Laboratoire de Géophysique Marine Institut de Physique du Globe de Paris Saint-Maur-des-Fossés, FRANCE
Robert L. Fisher	Scripps Institution of Oceanography La Jolla, CA 92093
John G. Sclater	Department of Earth and Planetary Sciences Massachusetts Institute of Technology Cambridge, MA 02139
Hartley Hoskins	Woods Hole Oceanographic Institution Woods Hole, MA 02543
Barry Parsons	Department of Earth and Planetary Sciences Massachusetts Institute of Technology Cambridge, MA 02139

* Submitted to Journal of Geophysical Research.

ABSTRACT

The boundaries of three plates, Africa, India, and Antarctica, meet in a triple junction in the Indian Ocean near 25°S, 70°E. Using observed bathymetry and magnetic anomalies, we locate the junction to within 5 km and show that it is a ridge-ridge-ridge type. Two of the ridges are normal spreading centers with well-defined median valleys, but one, the Southwest Indian Ridge (SWIR), has a peculiar morphology in the vicinity of the triple junction, that of an elongate triangular deep with the junction at its apex. The floor of this deep represents crust formed at the SWIR, and the morphology results from the evolution of the triple junction. We determine directions and rates of spreading on all three ridges, and poles of relative motion for all plate pairs. Though we cannot determine the precise stability conditions at the triple junction, we are able to map the evolution of the junction over the last 10 million years. We detect and discuss topographic expressions of the triple junction traces on the three plates.

INTRODUCTION

The central Indian Ocean triple junction, the meeting point of the African, Indian, and Antarctic plates, is located near 25°S, 70°E. Previously, little has been known about the area in which the Central (CIR), Southeast (SEIR) and Southwest (SWIR) Indian ridges join, as there have been few properly oriented ship tracks through the region. Until recently, there has not even been any reliable indirect evidence (through global closure calculations) of the local spreading direction of the SWIR (Minster et al., 1974; Chase, 1972). Since the SWIR is spreading slowly, at less than 10 mm/yr (Bergh and Norton, 1976), its data are often difficult to interpret, and the more well-constrained observations possible at the triple junctions at either end can be important additions to our knowledge. It was largely for this reason that Sclater et al. (1976) studied the Bouvet Triple Junction at the South Atlantic terminus of the SWIR, and that we began the present study of the Indian Ocean Triple Junction.

The data presented here come principally from legs 5 and 6 of R/V Atlantis II cruise 93 from February through April of 1976. The survey was designed to delineate the tectonic history within 250 km of the triple junction by running five or more lines spaced at a few tens of kilometers across each of the three ridges approximately parallel to their spreading

directions. By utilizing already existing data as well (Figure 1), we have compiled a detailed geophysical survey within a roughly 500 km square around the triple junction. Using topographic and magnetic data from these cruises, we locate the triple junction to within 5 km and show that the instantaneous relative velocity triangle closes and that the junction is of the ridge-ridge-ridge (RRR) type. We then examine the tectonic history of the region over the past 10 million years, showing that it is consistent with observations elsewhere along the same plate boundaries and in particular with those at the Bouvet Triple Junction. Finally, we discuss the implications of the observed relative motions of the plates and the junction over the past 10 million years.

TOPOGRAPHY

Topographic information from recent satellite navigated cruises of the Scripps Institute of Oceanography and the Institute de Physique du Globe de Paris have been combined with that of the Atlantis II survey. To these have been added older tracks from the SIO expeditions DODO (1964) and CIRCE (1968) and the Institute de Physique du Globe. We have contoured the data in intervals of 500 m corrected for the local sound velocity profile, and the resulting topographic chart (Figure 2) shows several features of interest to good advantage.

FIGURE 1

The ship tracks on which we base our study of the Indian Ocean triple junction. The solid lines represent the AII-93 track, and the dotted lines represent other tracks. The open circles with crosses denote teleseismically located earthquake epicenters (1964-1976) and indicate the general location of the ridge axes. The letters designate AII-93 profiles discussed in the text.

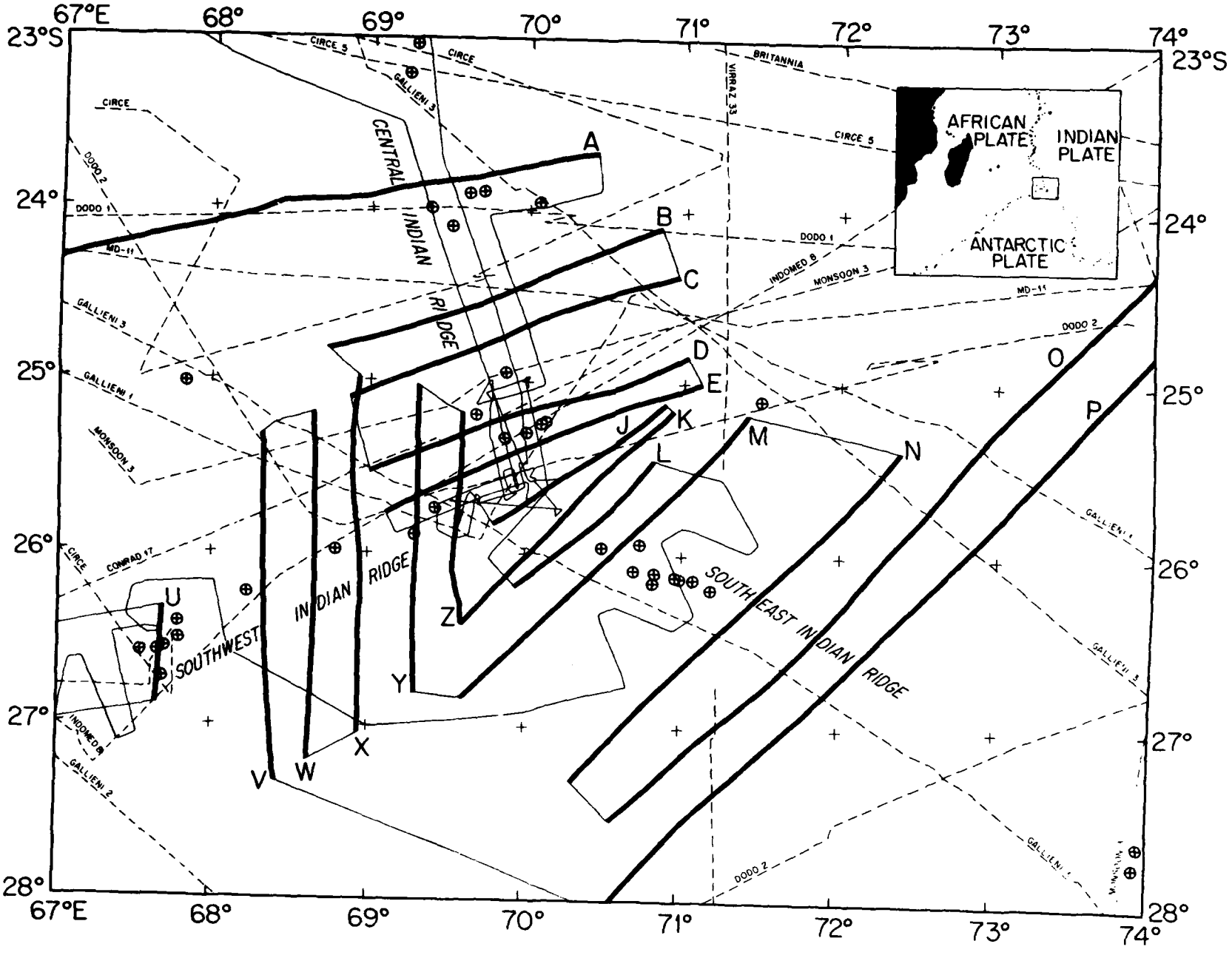
67°E
68°
69°
70°
71°
72°
73°
74°
23°S
24°
25°
26°
27°
28°
CIRCE
CIRCE 5
GALLIENI 3
BRITANNIA
VIRAZ 33
DODO 2
DODO 1
MD-11
CENTRAL INDIAN RIDGE
INDOMED 8
MONSOON 3
GALLIENI 1
CONRAD 17
INDIAN RIDGE
SOUTHWEST
SOUTHEAST INDIAN RIDGE
GALLIENI 2
A
B
C
D
E
J
K
L
M
N
O
P
U
V
W
X
Y
Z
AFRICAN PLATE
INDIAN PLATE
ANTARCTIC PLATE

FIGURE 2

Bathymetry in the area of the Indian Ocean triple junction. Depths are in corrected meters, and the contour interval is 500 m. Ship tracks are shown as dotted lines. Contours by R. L. Fisher.

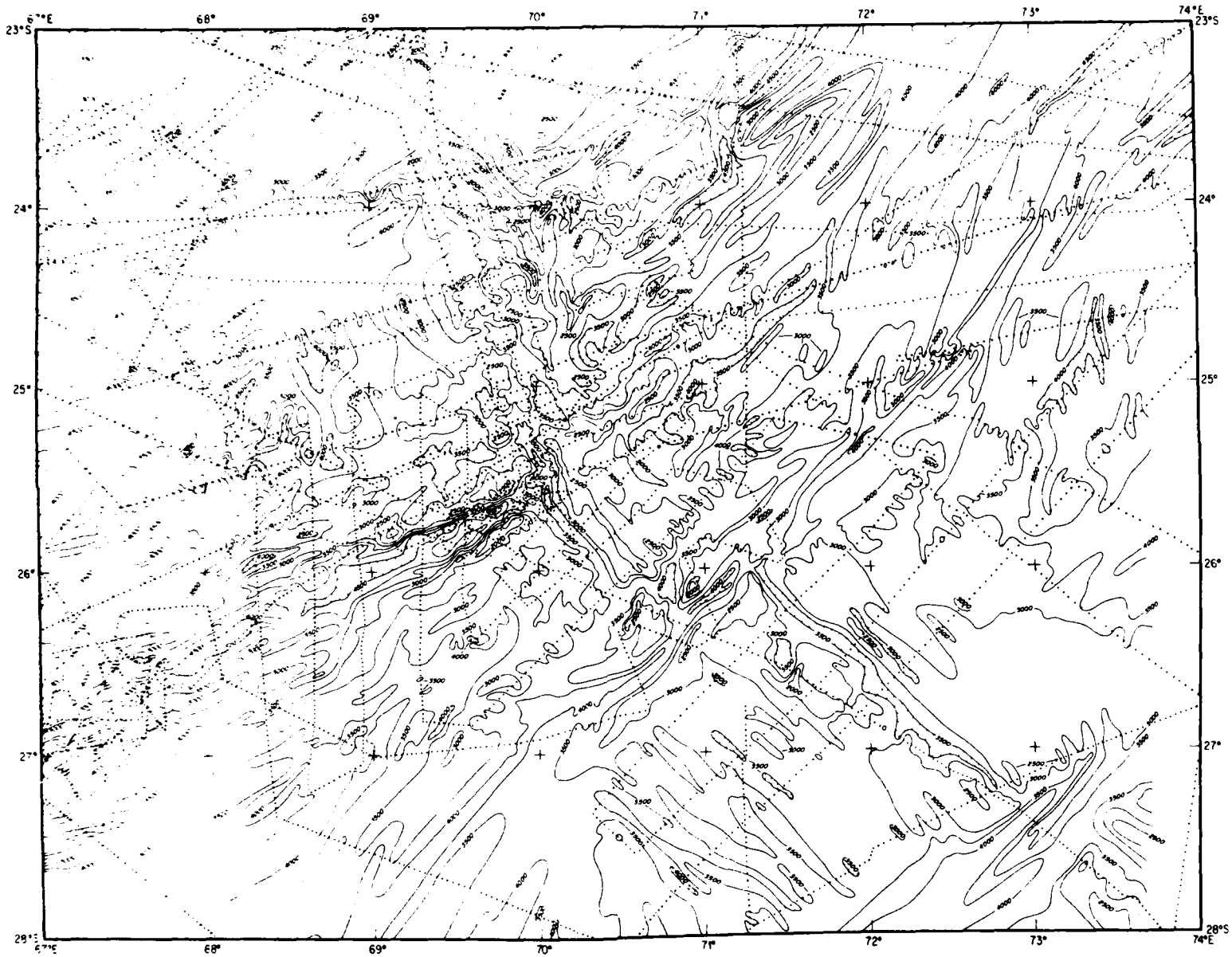
67°E
68°
69°
70°
71°
72°
73°
74°E
23°S
24°
25°
26°
27°
28°S

One can clearly see the three plate boundaries meeting in a triple junction near 25.7°S, 70°E, and the junction appears at first glance to be of the RRR type. The morphologies of the three spreading centers are of markedly different character, however.

The SEIR, which separates the Indian and Antarctic plates, has the morphology of a "classic" spreading ridge. It is characterized by smooth, blocky relief trending sub-parallel to a well-defined median valley offset at intervals by deep linear fracture zones. These fracture zones, which dominate the tectonic grain of the ridge, trend about N45°E and occur at 70.5°E, 71°E, and 73°E. They offset the ridge axis in a left-lateral sense and are associated with about 2000 m of relief. The transform at 71°E has a 60 km offset and constrains the local direction of relative motion between the Indian and Antarctic plate to be within 2° of 047°. Between the fracture zones, and oriented perpendicular to their trend, lie linear sections of spreading ridge, their axes marked by a median valley about 500 m deep (Figure 3a) and well-delineated by the 3500 m isobath (Figure 2). Additional minor transform faults may offset the median valley by small amounts. Beyond the rift valley mountains, the sea floor deepens gradually in a subdued, blocky fashion from about 2500 m depth to about 3500 m depth 300 km from the axis. We have compared the profile

FIGURE 3a

Bathymetric and magnetic profiles across the Southeast Indian Ridge projected onto a heading of N45°E. See Figure 1 for profile locations. The expected range of bathymetric values for a ridge spreading at 30 mm/yr according to the relation of Parsons and Sclater (1977) is shown. Also shown are the magnetization sequence according to the time scale of LaBrecque et al. (1977) and the phase shifted anomaly sequence calculated for a flat layer source extending from 3500 to 4000 m depth, both before and after convolution with a Gaussian filter of 2.5 km standard deviation. The stippled band through the magnetic and bathymetric profiles indicates the inferred region of Bruhnes age crust. FZ indicates an inferred fracture zone.

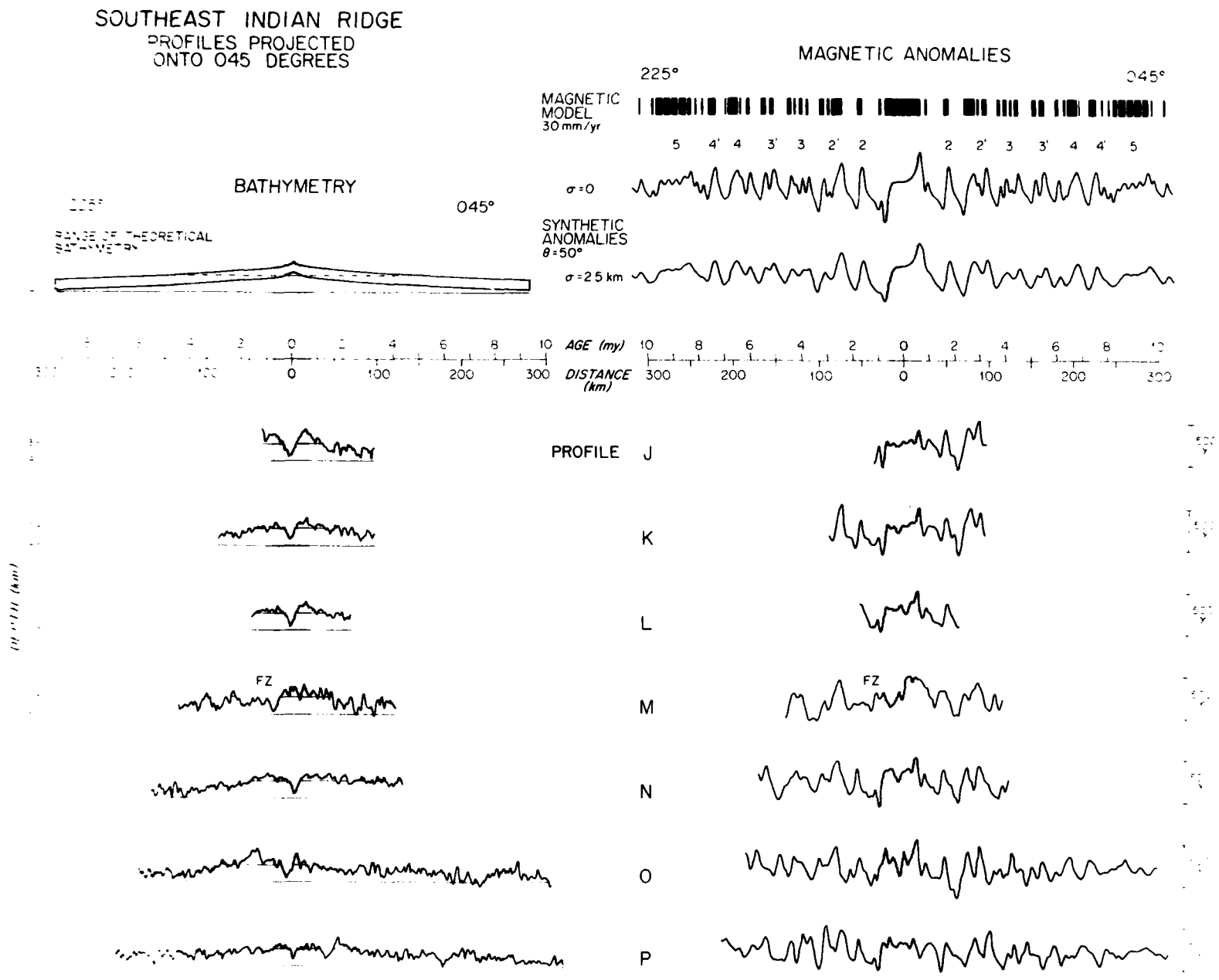
SOUTHEAST INDIAN RIDGE
PROFILES PROJECTED
ONTO 045 DEGREES
BATHYMETRY
045°
RANGE OF THEORETICAL BATHYMETRY
MAGNETIC ANOMALIES
225°
045°
MAGNETIC MODEL 30 mm/yr
5 4' 4 3' 3 2' 2 2 2' 3 3' 4 4' 5
σ=0
SYNTHETIC ANOMALIES θ=50°
σ=2.5 km
AGE (my)
DISTANCE (km)
PROFILE
J
K
L
M
N
O
P
FZ
FZ

of the ridge to the age-depth relation of Parsons and Sclater (1977) and find them consistent to within the 300 m amplitude of the short wavelength relief. In brief, the SEIR has all the morphologic aspects of an archetypal mid-ocean spreading center.

The topography of the CIR is more rugged and variable and less well-defined than that of the SEIR. Since it is spreading more slowly than the SEIR (25 mm/yr as compared to 30 mm/yr) this is in keeping with the general observation that rougher topography is associated with slower spreading ridges. The median valley of the CIR, delineated by the 3500 m contour and trending approximately N30°W, is clearly visible from the triple junction to 24.5°S, growing generally shallower toward the north (Figure 2). North of 24.5°S the median valley may still be traced, but less obviously. Bathymetric profiles across the ridge (Figure 3b) show that the valley exists and is 200 m to 300 m deep, but that its width and its absolute depths are quite variable, making it difficult to follow on a contour chart. Near 25.2°S, 70°E the CIR median valley is offset 20 km in a right-lateral sense by a small transform fault trending 059° $\pm$ 4°. This gives a reasonably well constrained measure of the local direction of relative motion between the African and Indian plates. There are no other clearly defined transform faults on the CIR within 300 km of the triple junction, though at 22.5°S, just to the north

AD-A089 103 WOODS HOLE OCEANOGRAPHIC INSTITUTION MASS F/G 8/7
THE EVOLUTION OF THE INDIAN OCEAN TRIPLE JUNCTION AND THE FINIT--ETC(U)
SEP 80 C R TAPSCOTT N00014-74-C-0262
UNCLASSIFIED WHOI-80-37 NL

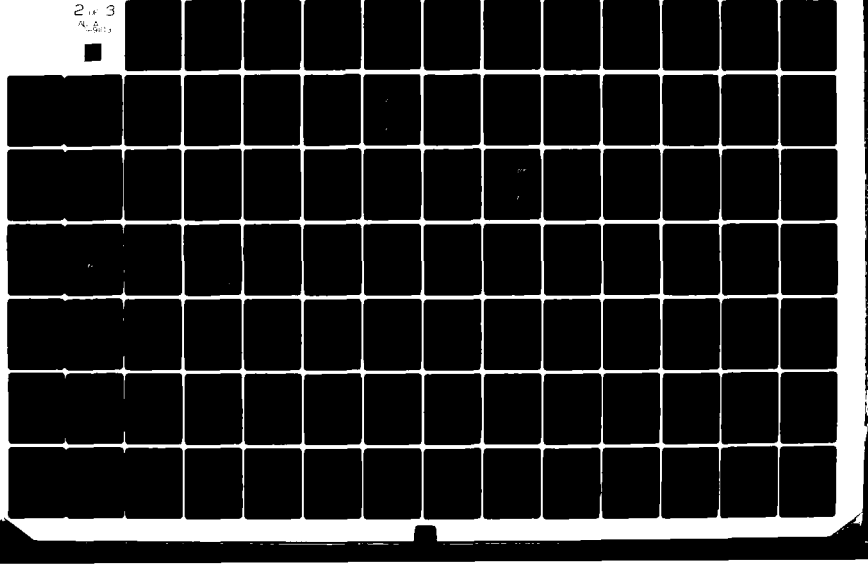

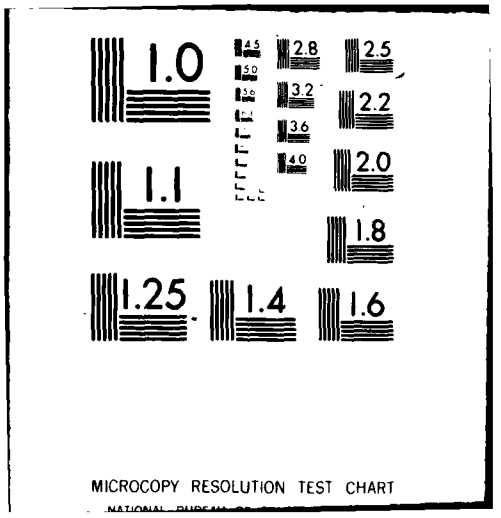
1.0
1.1
1.25
1.4
1.6
1.8
2.0
2.2
2.5
2.8
3.2
3.6
4.0
4.5
5.0
5.6
MICROCOPY RESOLUTION TEST CHART

FIGURE 3b

As in Figure 3a, but the profiles are across the Central Indian Ridge and are projected onto a heading of N60°E. The models are for a spreading rate of 25 mm/yr. The dashed portions of profiles E are over crust thought to have been formed at the Southeast and Southwest Indian Ridges.

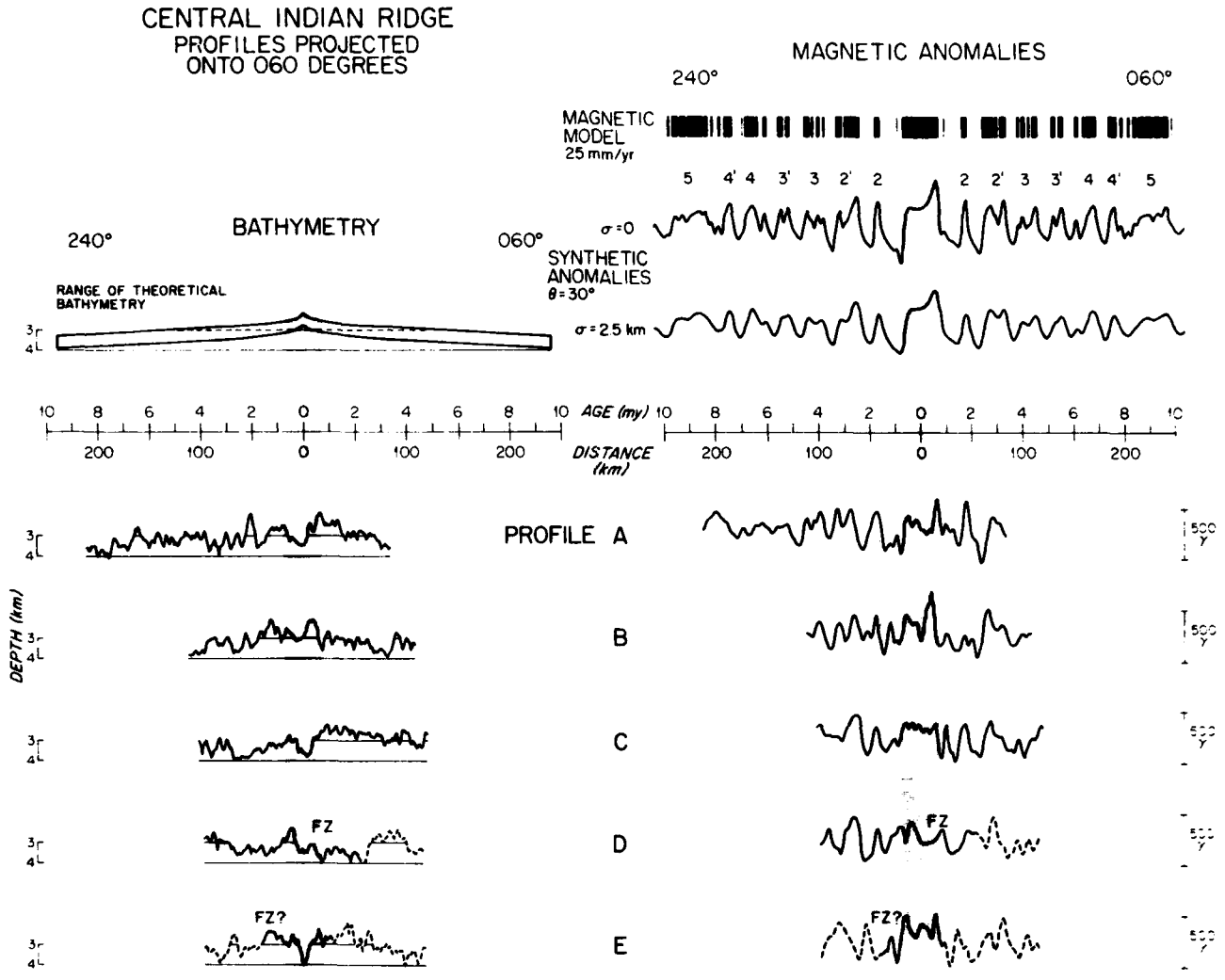
CENTRAL INDIAN RIDGE
PROFILES PROJECTED
ONTO 060 DEGREES
MAGNETIC ANOMALIES
240°
060°
MAGNETIC MODEL 25 mm/yr
5 4' 4 3' 3 2' 2 2 2' 3 3' 4 4' 5
BATHYMETRY
240°
060°
σ=0
SYNTHETIC ANOMALIES θ=30°
RANGE OF THEORETICAL BATHYMETRY
σ=2.5 km
10 8 6 4 2 0 2 4 6 8 10 AGE (my)
200 100 0 100 200 DISTANCE (km)
PROFILE A
B
C
D
E
FZ
FZ?
DEPTH (km)
500 γ

of the area of Figure 2, lies the southernmost of the major fracture zones mapped by Fisher et al. (1971). Between this and the 25.2°S transform fault are two offsets of the median valley at 24.2°S and 24.6°S. These offset the axis by only 10 km and have little topographic expression, though their existence is confirmed by magnetic data. In summary, the morphology of the CIR is similar to that of SEIR. It consists of segments of spreading centers (with median valleys) oriented at right angles to the direction of relative plate motion. The relatively confused topography, however, does not allow one to rule out a slight obliquity of spreading, perhaps by as much as 10°.

The morphology of the SWIR stands in marked contrast to that of the CIR and the SEIR. It appears as a great triangular chasm whose floor, at about 4500 m depth, is flanked north and south by 2000 m high linear mountain ridges (Figure 2). The ridges converge eastward toward the most acute apex of the triangle, located at the triple junction. The extreme relief across this spreading center is seen dramatically in profile (Figure 3c). The active spreading center and its recently created sea floor are up to 2000 m deeper than predicted by the Parsons and Sclater (1977) equation. The precise positions and trends of ridge axis segments are not at all well-defined by the rough topography of the SWIR, though the general

FIGURE 3c

As in Figure 3a, but across the Southwest Indian Ridge and projected onto a heading of N0°E. The models are based on a spreading rate of 8 mm/yr, and the magnetized layer is taken to lie between 4000 and 4500 m depth. The dashed portions of the profiles are over crust thought to have been formed at the Central and Southeast Indian Ridges.

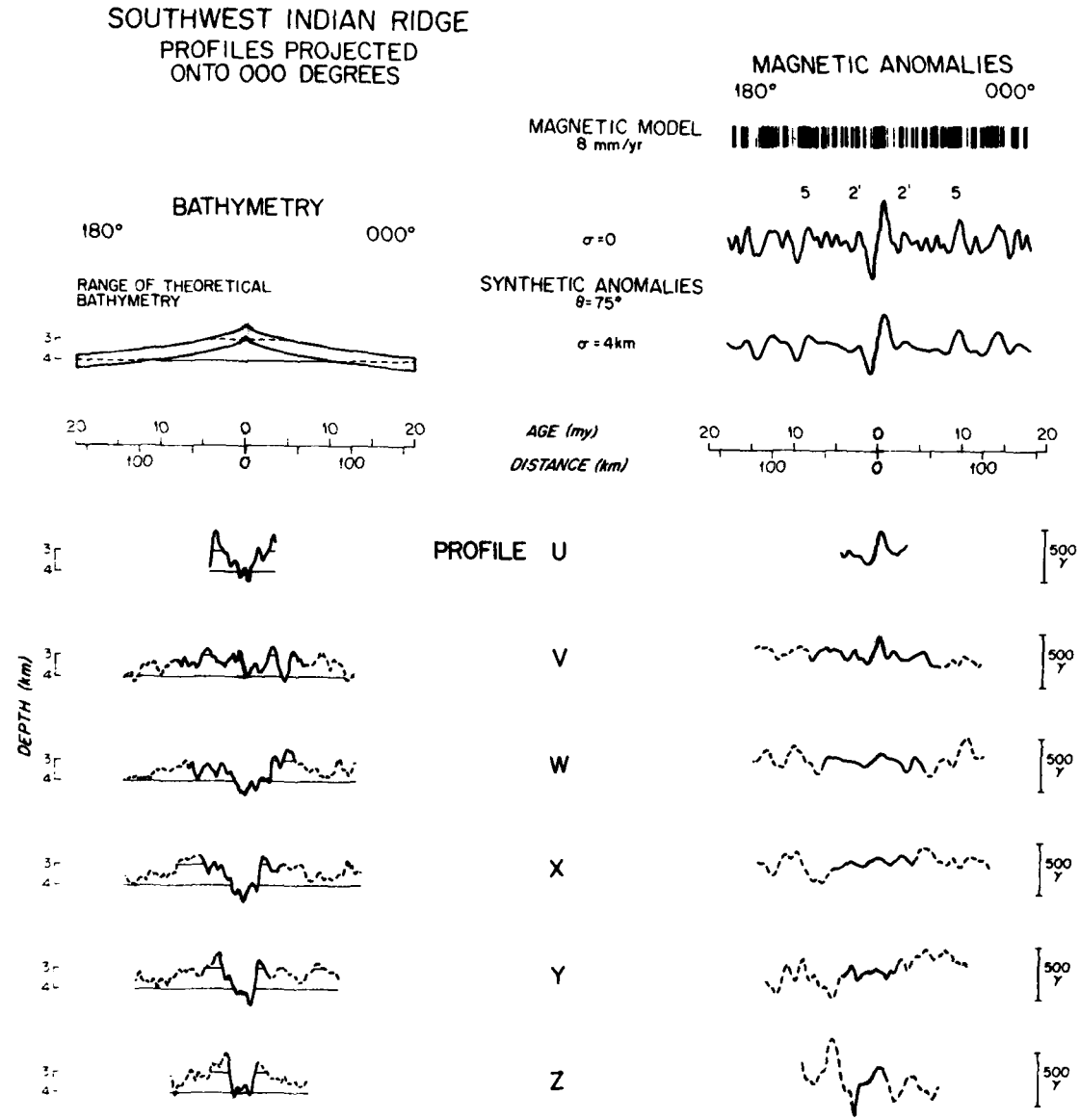
SOUTHWEST INDIAN RIDGE
PROFILES PROJECTED
ONTO 000 DEGREES
MAGNETIC ANOMALIES
180°
000°
MAGNETIC MODEL
8 mm/yr
5 2' 2' 5
BATHYMETRY
180°
000°
σ=0
RANGE OF THEORETICAL
BATHYMETRY
SYNTHETIC ANOMALIES
θ=75°
σ=4km
3
4
20 10 0 10 20
100 0 100
AGE (my)
DISTANCE (km)
20 10 0 10 20
100 0 100
PROFILE U
V
W
X
Y
Z
DEPTH (km)
500 γ

topographic grain trends about N70°E. Neither are there any obvious fracture zone traces within 300 km of the triple junction with which the local direction of relative motion between the African and Antarctic plates might be determined. There are a few vague indications of a north-south grain, the most prominent being the N3°W trending widening of the central deep at 68.8°E, but these are no more than merely suggestive. Farther to the west, however, Sclater et al. (in preparation) have mapped the Atlantis II and Melville fracture zones at 57.5° and 60.5°E respectively. These are long, deep fracture zone traces of large offset and trend within 2° of north-south, and this direction of relative plate motion may be taken to be close to that nearer the triple junction. Assuming this direction of spreading, it is not obvious from the morphology whether the SWIR is dominated by en echelon ridge segments spreading normal to their strike or by segments spreading obliquely. Both interpretations can be supported by various aspects of the rough topography.

The confluence of these three spreading centers, each of different character, marks the site of the triple junction near 25.7°S, 70°E. Here the continuous median valley of the Central and Southeast Indian Ridges (delineated by the 3500 m contour in Figure 2) deepens and changes trend in a distinct bend. Just at this bend, the 4500 m depths of the SWIR approach the CIR-SEIR median valley, separated from it by a

sill of about 3300 m depth in a narrow east-west trending channel. The intersection of this channel and the CIR-SEIR median valley marks the site of the triple junction.

MAGNETIC ANOMALIES

During R/V Atlantis II cruise 93 the total geomagnetic field strength was observed continuously. From this we subtracted the International Geomagnetic Reference Field (IGRF) to obtain the magnitude of the residual geomagnetic field, profiles of which across the three ridges are shown in Figures 3a, 3b, and 3c. For each ridge, the profiles have been projected along the approximate direction of spreading. Also displayed is a synthetic magnetic anomaly profile for each ridge derived from the geomagnetic reversal time scale of LaBrecque et al. (1977) and a two-dimensional flat layer model of 500 m thickness at the average depth of each ridge. We have modeled the "contamination" of the magnetic signal caused by the finite width of the active zone of intrusive and extrusive addition of crustal material (Atwater and Mudie, 1973) by convolving the block model magnetization with a gaussian filter of standard deviation similar to that of the injection process (Schouten and Denham, in preparation; Tisseau, 1978). The effect of contamination is, of course, greater at lower spreading rates because of the narrower width of single-polarity blocks. One also expects the standard deviation of

the gaussian filter to increase with decreasing spreading rate as the plate motions become slower and perhaps therefore more episodic, increasing the temporal contribution to the variability of the magnetization (Schouten and Denham, in preparation).

The magnetic anomalies along the SEIR are excellently formed (Figure 3a) in that one may easily correlate and identify them almost everywhere. The only notable exception is the disturbance of the central portion of profile M which may be explained by the probable occurrence of a fracture zone. The standard deviation of the gaussian contamination is quite small, being 2 km or less, and the phase shift of the magnetic anomalies is close to the 50° value expected for blocks oriented along N45°W at this location. On the northeastern ends of profiles O and P one sees the complete anomaly sequence since Anomaly 5 (9 Ma). Spreading has been nearly symmetric at a half-rate close to 30 mm/yr during this period and particularly since the time of Anomaly 2' (3 Ma). During the latter period the only evident complications are the previously mentioned fracture zone in profile M and an inferred ridge jump in profile P at or about the time of Anomaly 2. The period previous to 3 Ma is only seen well on profiles O and P. There were slight asymmetries of spreading and a slightly higher average spreading rate than more recently, between 31 and 32 mm/yr. Overall, however, the profiles show that

magnetically, as well as morphologically, the SEIR is a classic example of a simple symmetric spreading center.

Just as the CIR is morphologically more complex than the SEIR, so also are its magnetic anomalies more difficult to interpret than those of the SEIR. They are less distinct and are of more variable shape (Figure 3b), and seem consistent with a zone of emplacement with a standard deviation of between 2 and 3 km. Their phase shift is impossible to determine accurately, but appears close to the 30° expected of a ridge trending N30°W. In spite of these difficulties, many anomalies may be correlated and identified, and as a whole the profiles indicate that the CIR has been spreading with little or no asymmetry at a half rate of about 25 mm/yr since the time of Anomaly 2' (3 Ma) or perhaps Anomaly 3 (4 Ma). Each profile has some complications, however, and we have little information about the spreading rate before 4 Ma. Profile E shows higher spreading rate and considerable asymmetry, but it may cross a transform fault near its center, and its outer portions are over crust formed at the Southwest and Southeast Indian spreading centers. Profile D runs obliquely across the 25.2°S transform fault. Lines C, B, and A indicate symmetric spreading at about 25 mm/yr since time of Anomaly 2' (3 Ma) or perhaps Anomaly 3 (4 Ma). The western end of profile A extends to Anomaly 5 (9 Ma). Beyond Anomaly 3' (5.3 Ma), it indicates a slower

spreading rate of 20 mm/yr, in excellent agreement with the rate from 21 Ma to 9 Ma that Sclater et al. (in preparation) find for the western side of the CIR (based in part on the same line). It is questionable, however, whether this reflects a slower rate of opening or is an effect of asymmetric spreading. The data of Fisher et al. (1971) do not indicate any significant asymmetry, but neither do they indicate any significant change in rate. Over the last 4 million years, in any case, the Central Indian Ridge near the triple junction has been spreading symmetrically at near constant rate.

The magnetic anomalies along the SWIR are very subdued and difficult to interpret (Figure 3c). The central anomaly is clearly recognizable only on profiles U and V, as is (probably) Anomaly 2' both to the north and the south of the axis. Indications of a more subdued central anomaly are present on profiles W and X. These lines are consistent with observations made on the SWIR between 57°E and 68°E by Sclater et al. (in preparation), which demonstrate that the SWIR has been spreading in a north-south direction at a half-rate of 8 mm/yr since at least 10 Ma. We may identify several of the reasons for the poor quality of the magnetic anomalies. The slow spreading rate, particularly when coupled with gaussian contamination of 3 to 4 km standard deviation, leads to low amplitude, indistinct magnetic anomalies. The phase shift is

high, consistent with the 75° expected for a normally spreading ridge. Either closely spaced fracture zones must exist, disturbing the two-dimensional magnetic patterns, or the ridge must spread obliquely near the triple junction (also with the possibility of fracture zones). This would have the effect of reducing the spreading rate normal to ridge strike and thus decrease the resolution of the anomalies. The phase shift expected for this configuration would be within a few degrees of that for the normal spreading case.

In summary, the profiles across the SWIR, together with those of Sclater et al. (in preparation), indicate that the African-Antarctic relative motion has been progressing at a half rate of close to 8 mm/yr near the triple junction. Since 10 Ma, this rate has changed very little, and spreading has been nearly symmetric, but the data do not allow confident measurement of departures from these norms. Finally, it is interesting to note that only the central portions of the profiles of Figure 3c are over crust created at the Southwest Indian spreading center, and this portion narrows as one approaches the triple junction. Crust under the southern ends of the profiles was created at the SEIR, and the magnetic profiles Z, Y, X and W show respectively parts of anomalies 2', 3, 3' and possibly 4 created at that ridge.

TECTONICS

The magnetic anomaly profiles of the AII-93 lines and of other cruises in the area are plotted at right angles to the ship's track and are displayed in Figure 4 superimposed on selected bathymetric contours. Also shown are identifications of anomalies 1 through 5, as well as the locations of fracture zones inferred from the bathymetry and magnetics.

The local evolution of the Southeast Indian Ridge is well-defined by the data and appears to have been predominantly one of symmetric spreading at right angles to ridge strike at nearly constant rate and direction. Here the tectonic history is displayed almost in its entirety, and such subtleties as the pre-anomaly 2 ridge jump at 72°E are evident.

The CIR evolution, though generally well laid out, is somewhat less clear. The line placement and the quality of the magnetics are such that possible small obliquities and asymmetries of spreading can not be resolved, particularly in the older anomalies and very near the triple junction. This question has profound implications for the evolution of the triple junction.

Except for the region of AII-93 profile V near 68.4°E, the tectonic structure of the SWIR is not readily resolved. One can form some idea of the position of the spreading axis from the magnetics and bathymetry and map its approach to the

FIGURE 4

Magnetic anomaly profiles along track superimposed on the generalized bathymetry in the triple junction area. The lightly shaded regions are shallower than 3000 m, and the stippled regions are deeper than 3500 m in the Central and Southeast rift valleys, and deeper than 4500m in the Southwest rift valley. Anomaly identifications are indicated by heavy lines and numbers. Fracture zones are also indicated. The heavy dashed lines represent the approximate extent of crust formed at the Southwest Indian spreading center. The earthquake epicenters shown in Figure 1 appear as circles.

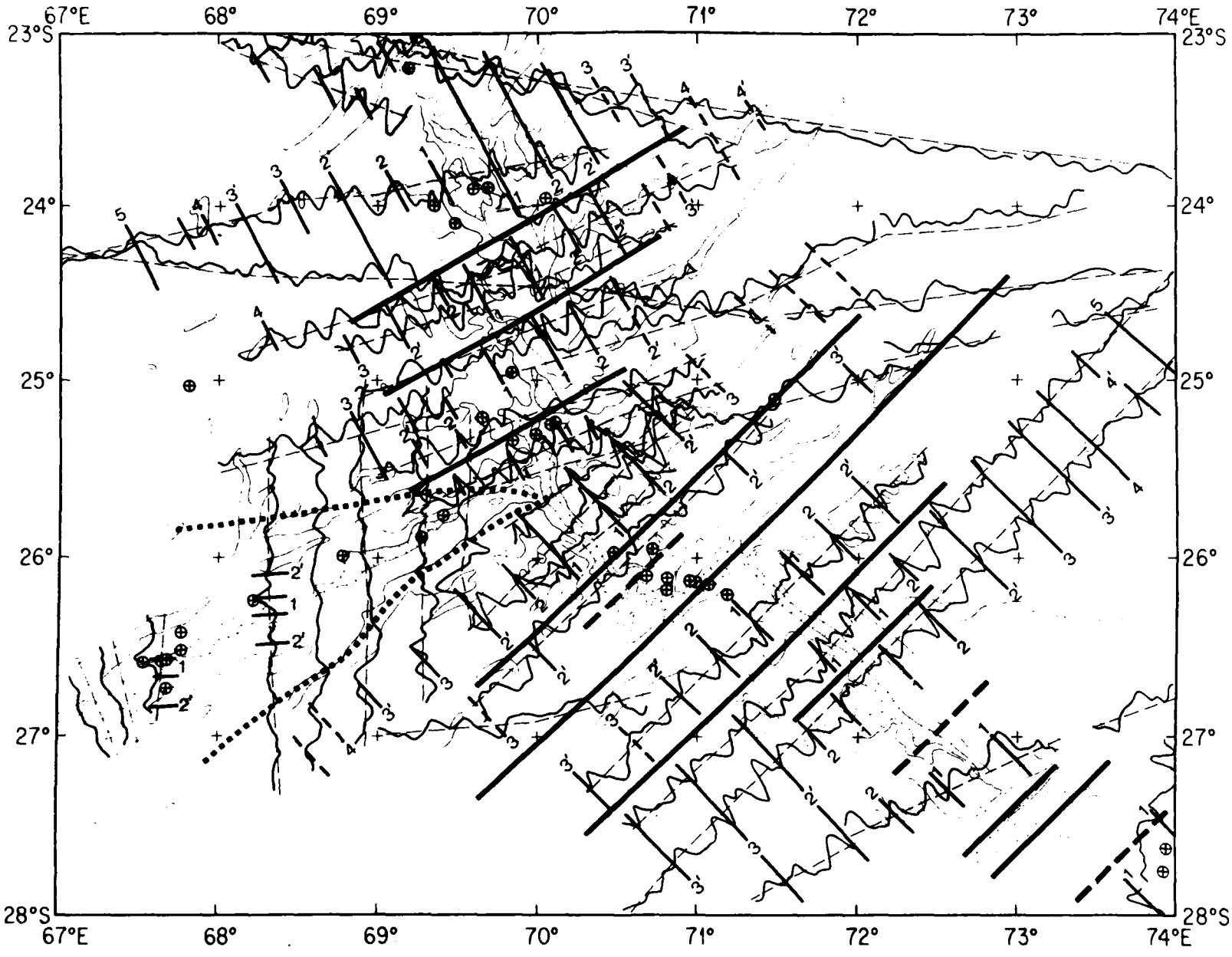
67°E
68°
69°
70°
71°
72°
73°
74°E
23°S
24°
25°
26°
27°
28°S

CIR-SEIR axis. Some fracture zones are indicated, but the actual trend of the spreading axis is not obvious. The extent of the SWIR regime is constrained by the presence of CIR and SEIR generated crust to the north and south of the southwest axis. The boundaries of this triangular region on the African and Antarctic plates are indicated by the rough-smooth transition in bathymetry and the approximately congruent smooth-rough transition in magnetic texture.

The tectonic diagram of Figure 4 serves to locate the triple junction within a few kilometers of 25.66°S, 70.06°E. Here the SWIR deep joins by means of an east-west trending channel with the continuous CIR-SEIR median valley at the site of the bend in the latter. Congruent with the morphologic bend is the angle in the trend of the CIR-SEIR central anomaly. The topographic and magnetic data together show that the three ridges meet in a RRR triple junction at that point, and the magnetic data indicate a stable evolution of the junction over the past few million years.

It is significant that the tectonic information (Figure 4) gives no indication whatsoever of a local system of microplates such as postulated by Barberi and Varet (1977) for the incipient triple junction at the head of the East African rift system; the Indian Ocean triple junction is indeed a junction of three plates. It is peculiar, however, that the

bathymetric expression of the Southwest Indian spreading center is not more clearly continuous with those of the Central and Southeast branches. Perhaps the more slowly spreading Southwest axis does not exist continuously as an identifiable feature in the young, thin crust near the triple junction, but manifests itself only during especially active pulses of motion between the African and Antarctic plates.

INSTANTANEOUS RELATIVE PLATE MOTIONS

Local Relative Plate Motions and the Velocity Diagram

Table 1 lists the directions and rates of the relative motions among the African, Indian, and Antarctic plates derived from bathymetric and magnetic data near the triple junction. The large uncertainties ascribed to the Africa/Antarctica values arise from the fact that the best information along this boundary comes not from the immediate neighborhood of the triple junction, but from 500 to 1500 km to the west. Preferred estimates of these errors are about half the given magnitude, but since most of the data are not of local origin one must allow for greater possible discrepancy. The information in Table 1 defines the velocity triangle of the triple junction (Figure 5a). The triangle is closed well within the uncertainties of the measurements, indicating that the local relative plate velocities have been

TABLE 1. Observed Relative Motions at the Indian Ocean Triple Junction

Plate Boundary	Source Data	Direction, deg.	Full Rate, mm/yr
Africa/India	25.2°S fracture zone AII-93 profiles A, B, C	059° ± 4°	49 ± 3
India/ Antarctica	71°E fracture zone AII-93 profiles J, K, L, N, O	047° ± 2°	59 ± 2
Africa/ Antarctica	Melville and Atlantis II fracture zones AII-93 profiles U and V and Sclater et al. (in preparation)	000° ± 10°	16 ± 5

FIGURE 5

a. A vector diagram of the relative plate velocities at the triple junction. Stipple areas represent the limits of the possible errors in the vectors. The error at the African end of the Africa/Antarctica vector is the compound error of that vector and the India/Antarctica vector. The lines representing the best estimates of the vectors have been emphasized. Directions are given in degrees east of north, and full rates are given in mm/yr.

b. The heavy lines represent the vector diagram of the relative plate velocities at the triple junction calculated from the instantaneous relative angular velocity vectors computed in this paper. These are superimposed on the best estimate vectors and associated regions of error of Figure 5a.

VECTOR DIAGRAM

(a) OBSERVED VELOCITIES

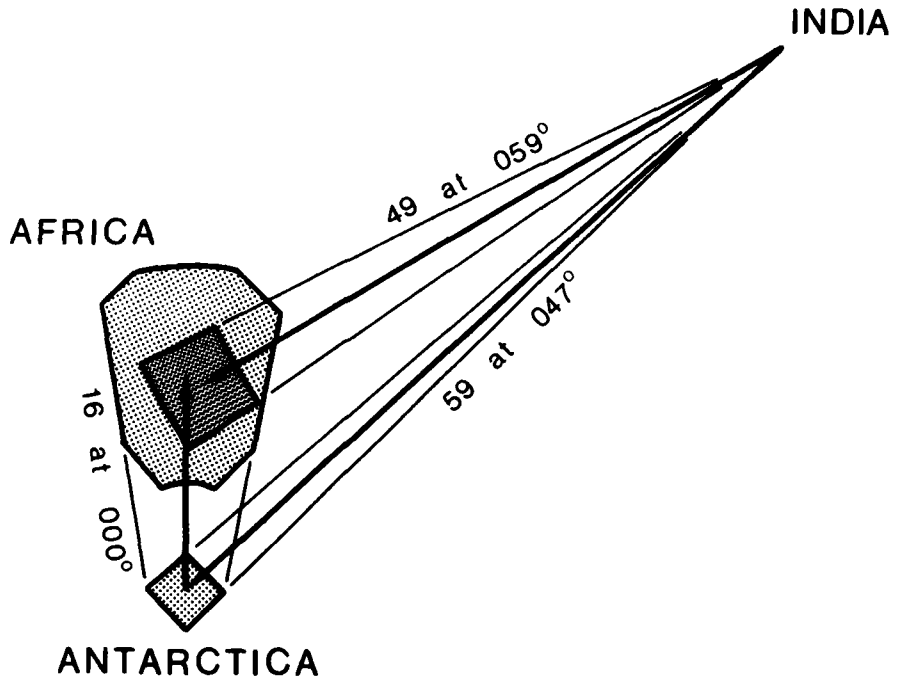

(b) CALCULATED VELOCITIES

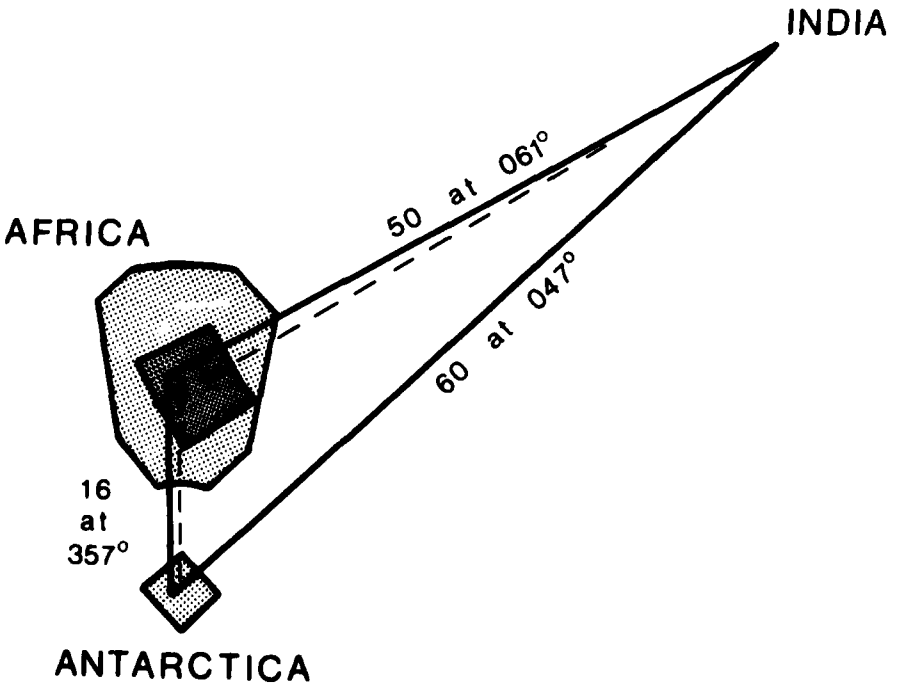

correctly deduced. In viewing the velocity triangle, one sees clearly the striking similarity of the Africa/India and Antarctica/India motions and the markedly contrasting slowness of the north-south Africa-Antarctica motion, even allowing for errors in the velocities.

The Global Solution and the Instantaneous Poles

Under the rigid plate hypothesis, one can reduce the uncertainties in an observation of relative plate motion by using a larger set of observations to determine the instantaneous relative angular velocity vector which describes the relative rotation of the plates. Using the method of Forsyth (Forsyth, 1975; Sclater et al., 1976), we determined the internally consistent set of relative rotation poles which best fit published observations of the direction and rate of the present relative motion across the common boundaries of the African, Indian, Antarctic, and South American plates (Table 2). These poles are given in Table 3, and the values one calculates for the data using these poles are included in Table 2.

In general, the poles determined here fall quite close to other published poles (Table 3), the only notable exception being the Africa/Antarctica pole, for which there is considerable dispersion among various determinations. Our pole at 5.6°N, 39.4°W falls 35° from that calculated by Minster et al.

TABLE 2. Computation of Instantaneous Poles

Plate Boundary	Source	Position N.Lat.	Position E.Long.	Observed Direction Θ	Observed Rate mm/yr	Observed Uncertainty	Calculated Direction Θ	Calculated Rate mm/yr
Africa/ India	2	11.0	57.5	30		5	28	12
	3	-9.0	67.5	52		4	52	36
	3	-14.0	66.0	58		3	59	39
	3	-16.0	66.5	60		5	60	41
	3	-17.5	66.0	63		3	62	42
	3	-20.0	67.0	60		10	62	45
	3	-20.0	68.0	63		10	60	45
	1	-25.2	70.0	59		5	61	50
	4	7.0	60.0		26	4	38	17
	4	4.5	62.25		28	4	40	21
	4	4.0	63.5		29	4	39	22
	3	-10.25	66.5		38	4	55	36
	3	-12.0	66.0		38	4	58	38
	3	-13.0	66.5		38	4	58	39
	3	-20.0	66.0		41	4	63	44
	3	-20.75	68.0		45	5	61	46
	3	-22.25	69.0		46	3	60	48
	1	-23.8	69.6		50	2	60	49
	3	-24.0	70.0		51	4	60	49
	1	-24.5	69.8		50	2	60	50
	1	-24.75	69.8		50	2	61	50
	3	-25.0	70.0		49	4	61	50
India/ Antarctica	1	-26.2	71.0	47		5	46	60
	4	-38.0	78.0	48		15	45	68
	4	-39.0	78.0	42		15	45	68
	4	-40.0	82.0	39		15	42	70
	4	-42.0	85.0	34		15	40	71
	4	-45.0	96.0	29		15	32	73
	5	-49.0	125.0	7		5	11	72
	6	-62.0	156.0	-22		15	-21	64
	1	-25.9	70.35		58	2	47	60
	1	-26.2	71.5		59	2	46	61
	1	-26.4	71.9		59	2	45	61
	4	-27.0	73.0		64	6	45	62
	4	-31.0	76.0		60	6	44	65
	4	-38.0	78.0		70	4	45	68
	4	-44.0	94.0		74	5	33	72
	7	-50.0	114.0		74	4	18	73
	5	-49.0	125.0		74	4	11	72
	7	-50.5	134.0		74	6	3	70
	8	-62.0	158.0		68	4	-23	64

TABLE 2 (continued)

Plate Boundary	Source	Position N.Lat.	Position E.Long.	Observed Direction Θ	Observed Rate mm/yr	Observed Uncertainty	Calculated Direction Θ	Calculated Rate mm/yr
Africa/	9	-54.25	2.0	45		2	45	16
Antarctica	10	-54.25	6.0	40		2	41	16
	10	-53.5	9.0	39		2	38	16
	11	-46.0	35.15	17		2	15	17
	10	-33.0	57.0	0		2	1	16
	10	-31.7	58.35	2		5	1	16
	10	-30.0	60.75	-2		5	0	16
	1	-25.8	69.6	0		10	-3	16
	9	-54.6	0.0		16	4	47	16
	9	-54.0	4.0		16	4	43	16
	11	-45.0	36.0		16	8	14	17
	1	-25.8	69.6		16	5	-3	16
Africa/	12	10.8	-42.3	92		4	93	28
South	12	10.2	-40.9	94		5	92	29
America	12	9.4	-40.0	92		5	92	29
	12	8.8	-38.7	92		10	91	29
	12	7.6	-36.6	91		10	89	30
	13	-0.1	-18.0	78		5	78	34
	13	-1.1	-14.0	76		4	76	34
	9	-54.5	-1.0	65		10	69	35
	14	-7.0	-13.0		40	4	76	36
	15	-28.3	-13.0		39	4	77	39
	15	-30.5	-14.0		40	4	77	39
	15	-38.2	-15.0		40	4	78	39
	9	-54.5	-1.0		32	4	69	35
South America/	9	-55,7	-3.0	85		2	85	20
Antarctica	9	-55.5	-1.5		18	3	85	21
	9	-56.0	-4.5		18	3	85	20

Source 1 is this paper; 2, Matthews (1966); 3, Fisher et al. (1971); 4, McKenzie and Sclater (1971); 5, Weissel and Hayes (1974); 6, Hayes and Connolly (1972); 7, Weissel and Hayes (1972); 8, Falconer (1972); 9, Sclater et al. (1976); 10, Sclater et al. (in preparation); 11, Bergh and Norton (1976); 12, Heezen et al. (1964a); 13, Heezen et al. (1964b); 14, van Andel and Moore (1970); 15, Dickson et al. (1968).

TABLE 3. Comparison of Observed and Predicted Relative Motions at the Indian Ocean and Bouvet Triple Junctions

Plate Boundary	Observed Motions: Indian Ocean Direction Θ	Observed Motions: Indian Ocean Rate mm/yr	Observed Motions: Bouvet* Direction Θ	Observed Motions: Bouvet* Rate mm/yr	Pole Position and Rate: Source	N.Lat.	E.Long.	Deg/my	Predicted Motions: Indian Ocean Direction Θ	Predicted Motions: Indian Ocean Rate mm/yr	Predicted Motions: Bouvet Direction Θ	Predicted Motions: Bouvet Rate mm/yr
Africa/ India	59	49			1	15.5	48.6	0.63	60.7	50.5		
					2	16	48	0.62	60.4	50.3		
					3	15	48	0.633	59.7	50.6		
					4	18.7	44.8	0.58	58.5	49.9		
					5	17.3	46.0	0.644	58.9	54.0		
India/ Antarctica	47	59			1	16.2	34.6	0.66	46.7	59.6		
					2	11	32	0.64	39.9	56.2		
					3	16	24	0.650	37.8	63.3		
					4	10.7	31.6	0.67	39.3	58.9		
					5	18.7	32.7	0.67	46.9	62.7		
Africa/ Antarctica	0	16	45	16.6	1	5.6	-39.4	0.15	-3.4	15.7	48.0	15.5
					2	-16	-38	0.18	-22.4	19.8	38.6	14.9
					3	4	-51	0.262	-10.6	25.3	36.1	27.7
					4	-19.0	-13.3	0.19	-14.7	20.5	69.9	12.8
					5	9.5	-41.7	0.149	-0.6	15.2	47.4	15.8
					6	23.4	-49.4	0.166	11.5	15.1	46.4	18.5
					7	8.4	-42.4	0.15	-2.0	15.3	46.2	15.9
Africa/ South America			65	32.0	1	57.4	-37.7	0.35			68.8	34.9
					2	58	-37	0.37			69.4	36.8
					3	66	-29	0.344			76.7	32.2
					4	57.4	-37.5	0.37			68.9	36.9
					5	66.6	-37.3	0.356			73.3	32.9
					6	58.2	-38.2	0.358			68.8	35.5
South America/ Antarctica			85	18.0	1	82.5	-30.4	0.28			84.4	20.8
					2	87	-30	0.36			87.6	24.5
					3	64	-107	0.330			44.7	21.7
					4	77.7	-101.8	0.38			68.5	24.0
					5	87.7	75.2	0.302			93.8	19.6
					6	78.9	-0.8	0.244			89.9	19.6

Source 1 is this paper; 2, McKenzie and Sclater (1971); 3, Chase (1972); 4, Minster et al. (1974); 5, Minster and Jordan (1978); 6, Forsyth (reported in Sclater et al., 1976); 7, Sclater et al. (in preparation).

*From Sclater et al. (1976)

(1974) and 20° from that calculated by Forsyth (reported in Sclater et al., 1976). It is remarkably close to that derived by Minster and Jordan (1978) and Sclater et al. (in preparation), being 5° and 4° distant from these, respectively. The calculation in the latter paper is based upon much the same SWIR data as the present calculation, though the method of computation is different. As these three calculations are to date the only ones based upon all the currently available data along the Africa/Antarctica plate boundary, and in view of the fact that they arrive at virtually the same Africa/Antarctica pole in spite of differing methods and constraints, one must accept that pole in preference to earlier determinations.

Finally, we note that a better fit to the data could not be obtained by allowing Africa to behave as independent Nubian and Somalian plates with slight extension across the East African rift system. This is in agreement with the findings of Sclater et al. (in preparation). Evidently, any incipient plate separation in East Africa has not yet had an impact on the global tectonic system measureable at the scales investigated here. We did not consider the possibility that the Indian plate might in fact be two plates in slight relative motion across the Ninetyeast Ridge as proposed by Stein and Okal (1978). Because most of the fracture zones

along the India/Antarctica boundary are poorly surveyed, the data used here are inadequate to resolve this question.

The Calculated Velocity Diagram

Table 3 lists the relative plate velocities at the site of the Indian Ocean triple junction calculated from the poles derived here. When one plots these as a vector diagram superimposed on the observed velocities and uncertainties (Figure 5b), one sees that the predicted relative motions agree excellently with observations in the neighborhood of the triple junction. The agreement, well within the uncertainties of the observations, demonstrates the consistency of the triple junction data with other measurements of the relative motions among these plates and validates the assumption of rigid plate behavior. We feel confident that the errors in the local relative plate velocities calculated here are small, perhaps 2° in direction and 2 mm/yr in magnitude. Therefore, in the following discussion of the stability and evolution of the triple junction, we take the velocity triangle of Figure 5b to represent exactly the instantaneous relative plate velocities at the triple junction. Any inaccuracy introduced by this simplifying assumption will be small.

STABILITY AND CONFIGURATION

The topographic and magnetic data presented here (Figure 4) indicate that the Indian Ocean triple junction is a RRR type. Furthermore, it appears to be stable in the sense of McKenzie and Morgan (1969), since its geometrical arrangement has persisted for a finite period of geologic time. From Figure 4, one sees that the configuration of the junction has remained largely unchanged for five to ten million years, and Sclater et al. (in preparation) present less detailed data indicating that the triple junction has evolved in much the same manner since 40 Ma.

Stability - Normal RRR

Where adequate to resolve the question, the sea-floor spreading data show that all three ridge axes are spreading symmetrically at right angles to their strikes. This is the situation encountered along the major portion of the world's mid-ocean rift system. Assuming this to hold rigorously, one can construct a stability diagram of the triple junction (Figure 6a) after McKenzie and Morgan (1969), using the velocity triangle of Figure 5b.

Figure 6a shows the junction to be stable, of course, as it must be under the assumptions. The speed of each of the three plates relative to the junction (J_n) is 34 mm/yr, and the traces of the junction on the Indian, Antarctic, and African plates have trends of N20°E, N74°E, and N102°E,

FIGURE 6

a. The stability diagram for the triple junction based on the vector diagram of Figure 5b, assuming symmetric spreading in all three ridge axes in directions normal to their trends. The lighter lines represent the frames of reference which are stationary with respect to each plate boundary. They intersect at the frame of reference J_n in which the triple junction is stationary. Dashed lines represent the motion of each of the three plates with respect to the triple junction

b. The stability diagram as in Figure 6a, but allowing oblique spreading on the Central and Southwest Indian Ridges to match the observed trends of the triple junction traces on the African and Antarctic plates. The triple junction is stationary in frame of reference J_o.

STABILITY DIAGRAM

(a) NORMAL RRR

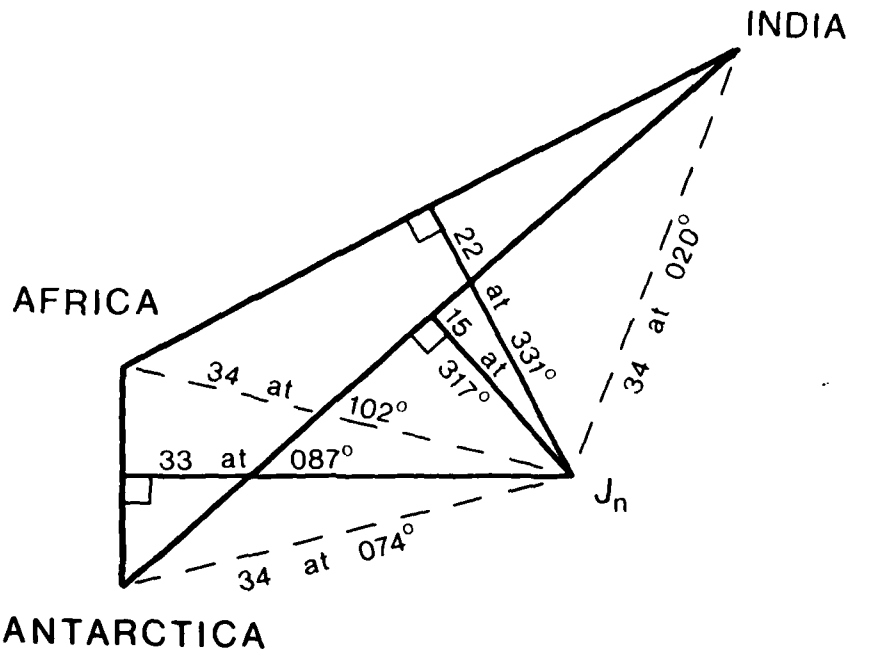

(b) OBLIQUE RRR

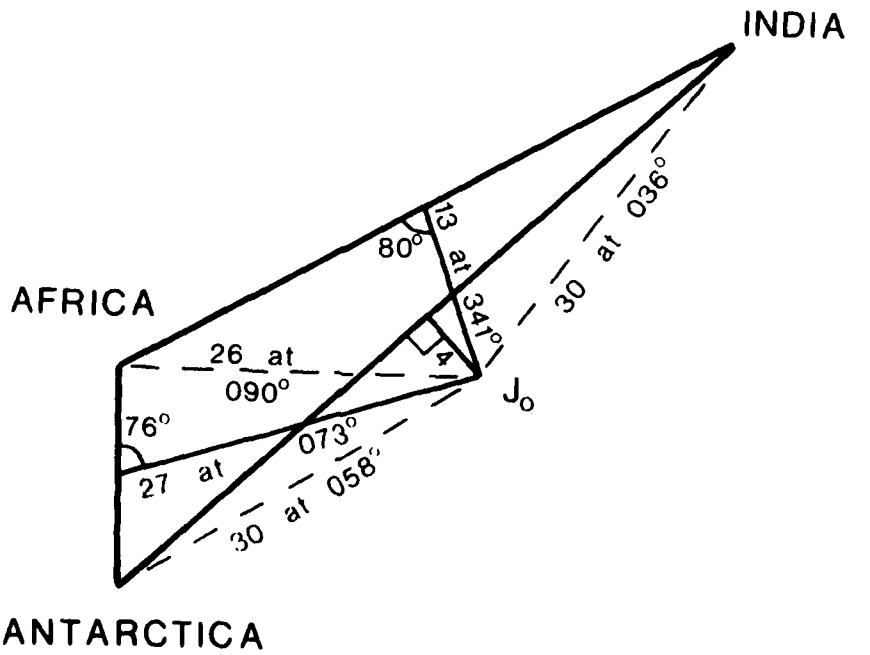

respectively. These traces are the sutures between crust formed at different plate boundaries. One notes that as the triple junction evolves, the Central and Southwest Indian Ridges grow longer by 22 mm/yr and 33 mm/yr respectively, while the SEIR shortens at a rate of 15 mm/yr. The rapid lengthening of the SWIR compared to its spreading rate causes the acute triangular morphology on that branch, with the rough SWIR-created crust enclosed by the converging triple junction traces on the African and Antarctic plates.

Formally, Figure 6a represents the instantaneous relative velocities precisely at the site of the triple junction. This is geophysically inappropriate, however, and it is more proper to consider the Figure to represent an average over a relatively short period of time and a relatively small area, say about one million years and a few tens of kilometers square. When viewed in this manner, the stability diagram of Figure 6a cannot alone account for the data in the area of the triple junction. The topographic and magnetic features interpreted as marking the boundaries between sea floor created at the SWIR and sea floor created at the CIR and SEIR trend roughly N90°E and N60°E respectively, (Figure 4), not the N102°E and N74°E shown on the stability diagram. Furthermore, the magnetic anomaly data (Figure 4) clearly demonstrate that the length of the SEIR has changed relatively little over the last five to ten million years,

certainly not by the 75 to 150 km decrease predicted by a simplistic application of Figure 6a. One may account for these observations in a number of ways, but they first lead one to consider another quasi-instantaneous stability diagram.

Stability - Oblique RRR

Based upon the crustal boundary trends on the African and Antarctic plates and the nearly constant length of the SEIR, one can redraw the stability diagram of the Indian Ocean triple junction (Figure 6b), imposing a stable condition on the junction (J_o) by allowing the SWIR and the CIR to trend obliquely to their spreading directions. The geometry of sea floor evolution thus implied is in excellent accord with the general magnetic and topographic patterns observed, particularly along the Southwest branch. The small obliquity required, less than 15° on the SWIR and only 10° on the CIR, may well be consistent with observations very close to the triple junction.

One may achieve a similar result by introducing asymmetry of spreading rather than obliquity, but the degree of asymmetry required is excessive, especially in the SWIR, and may be ruled out by the available magnetic data. A lesser degree of asymmetry might still be present along with the obliquity, however. In any case, the weight of the evidence strongly suggests that the SEIR is spreading normally and symmetrically right up to the triple junction.

Other Configurations

Bathymetric and magnetic observations indicate that the Indian Ocean triple junction is a RRR junction, and this may be further confirmed by considerations of stability. One cannot obtain stable ridge-fracture-fracture (RFF) or ridge-ridge-fracture (RRF) triple junction structures consistent with the data.

In order that a RFF triple junction be stable, the ridge axis trend must pass through the opposite vertex of the velocity triangle. Reference to Figure 6 shows that this can be accomplished most easily by forcing the SWIR trend to pass through the Indian vertex, but even this demands more asymmetry and/or obliquity than the data will permit. Moreover, there is absolutely no sign of a fracture zone at the triple junction on the India/Antarctica plate boundary, which is the best defined of the three. Neither is there one on the Africa/India boundary. This rules out the possibility of a RFF junction.

Neither can the triple junction have a stable RRF configuration, since stability in this case requires that the two ridge axis trends intersect on the third side of the velocity triangle. Figure 6b shows that the SWIR and CIR trends might possibly intersect on the India/Antarctica side of the velocity triangle, but in an RRF configuration, that would imply a fracture zone on the India/Antarctica plate

boundary at the triple junction. Once again, there is no sign of this on the SEIR. This rules out a RRF structure and is further evidence that the Indian Ocean triple junction is in fact a stable ridge-ridge-ridge junction.

STRUCTURE NEAR THE TRIPLE JUNCTION

It is important to remember that the stability diagrams of Figure 6 represent quasi-instantaneous relationships actually at the triple junction. The pattern of sea-floor evolution with which we are comparing them, however, was laid down over a comparatively long period of time, about 10 million years, and in part was created quite far from the coeval triple junction. During most of this time the normal spreading situation of Figure 6a might have predominated, provided that periodically the triple junction jumped to the northwest along the trend of the Southeast Indian Ridge, creating fracture zones in the Central and Southwest branches. If the frequency and magnitude of these jumps were properly scaled, the time-averaged relationships would resemble those of Figure 6b and would account equally well for the general pattern of triple junction evolution.

In fact, Figures 6a and 6b represent end members of a continuum of configurations, any of which might dominate at various times. In order to determine the true configuration

and stability conditions prevailing at the Indian Ocean triple junction, one must examine in detail the structure of each of the three ridges as they approach the junction. The conclusion is critically dependent on the structures of the Central and Southwest branches particularly, and, unfortunately, the available data are insufficient to allow one to determine these structures to the desired precision.

The Southwest Indian Ridge

A closer examination of the magnetic and topographic information along the SWIR immediately reveals that it is unable to answer the question of spreading obliquity. One may easily interpret the data to be consistent with either extreme (Figure 7a and b). In general, the bathymetric contours suggest oblique spreading (Figure 7b) except in a section between 68°E and 69°E (across which runs the clearest magnetic profile). Also, there is an east-west (non-oblique) trending grain within 20 km of the triple junction. The resolving power of wide beam echo-sounding records is too low, however, to define the structure in adequate detail.

Sclater et al. (in preparation) show that farther to the west the SWIR trends perpendicular to its direction of spreading. This has no certain implications nearer the triple junction, however. It is possible that a given section of spreading center originates as an oblique spreading center at the triple

FIGURE 7

a. An interpretation of the Southwest Indian spreading center as a system of en echelon segments trending normal to their spreading direction. Shaded areas are shallower than 3000 m. Deeper contours within the spreading center area are shown at 500m intervals. Postulated fracture zones are indicated by heavy lines, and the postulated area of Bruhnes age crust is stippled. Heavy dashed lines represent the boundaries of crust created at the Southwest Indian Ridge.

b. An interpretation of the Southwest Indian spreading center as a system of spreading segments trending oblique to their direction of spreading. Features are as in Figure 7a.

(a) NORMAL

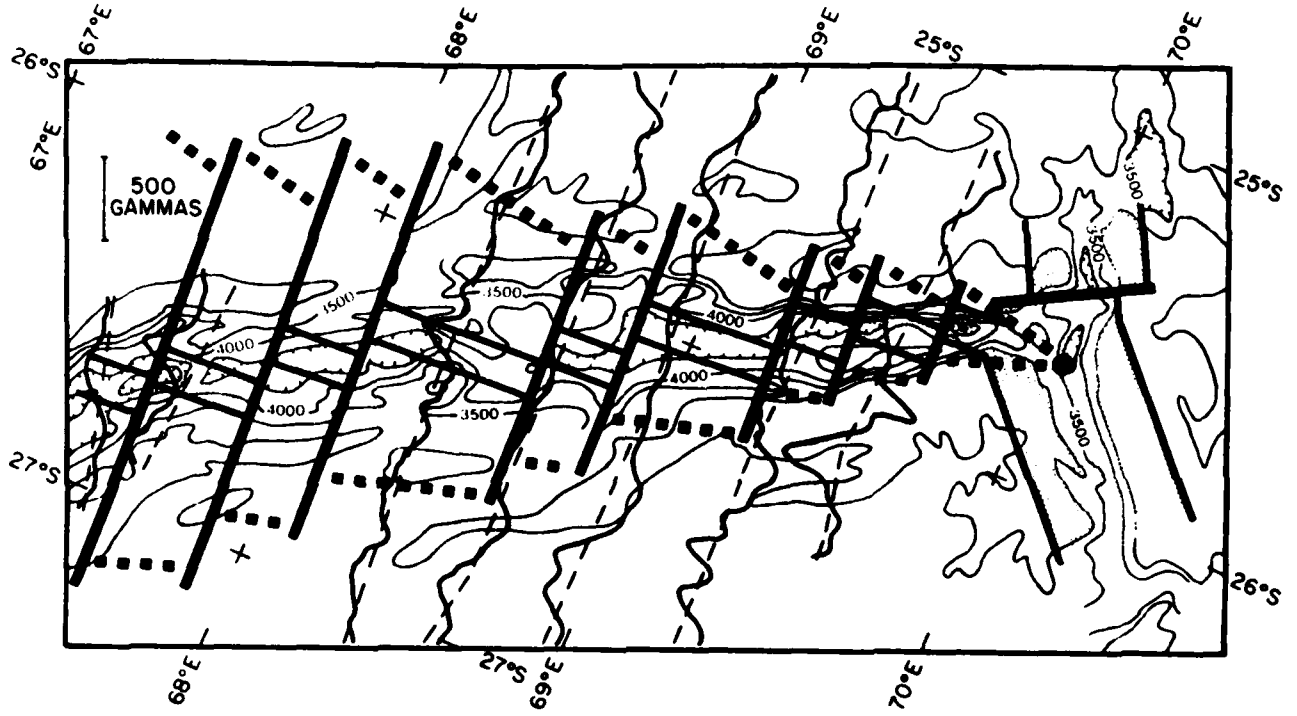

(b) OBLIQUE

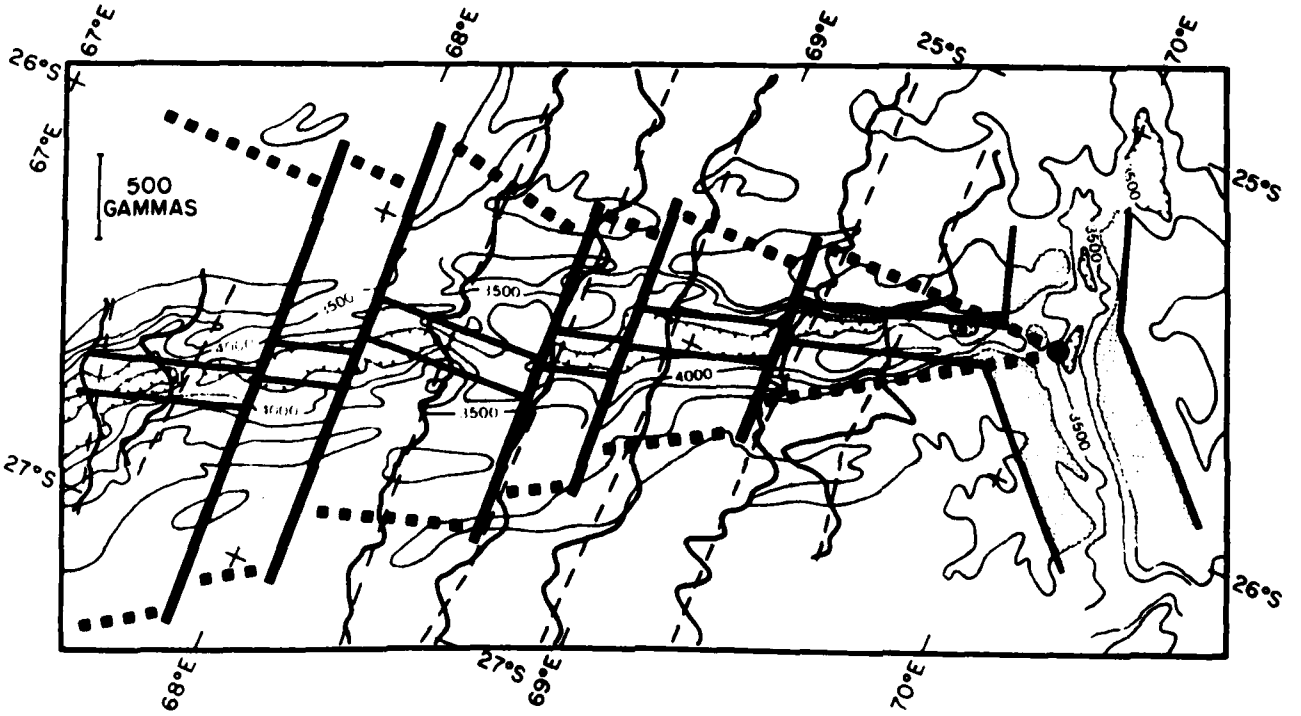

junction, and, as the evolving junction moves away toward the east, the section gradually reorients itself to lie perpendicular to its spreading direction.

The Central Indian Ridge

Although the magnetic anomaly data are better over the CIR than over the SWIR, it is again impossible to distinguish between normal and slightly oblique spreading near the triple junction. Both bathymetric contours and magnetic correlations suggest an oblique ridge orientation in the expected sense in the 20 km north of the triple junction (Figure 8). However, the bathymetry also suggests the presence of a small transform fault at 25.5°S (Figure 8) whose existence would invalidate the magnetic correlation. In the absence of a more detailed survey, the spreading center strike can be determined only to within a few degrees.

The Southeast Indian Ridge

Figure 8 demonstrates that as the SEIR approaches the triple junction, it is indeed spreading symmetrically in a direction normal to its strike. Moreover, the young magnetic anomalies on the Indian plate associated with the SEIR (anomalies 2 and 2') extend farther to the north than is consistent with the present length of the SEIR. This indicates that the steady shortening of the SEIR inferred from Figure 6a has been proceeding since 3 Ma. Magnetic anomalies on the Antarctic plate (Figure 4), however, show that this has not

FIGURE 8

A detail of the magnetic anomalies along track in the vicinity of the triple junction, superimposed on the bathymetric contours. Areas deeper than 3500 m in the axial valleys are shaded. The magnetic correlations are discussed in the text.

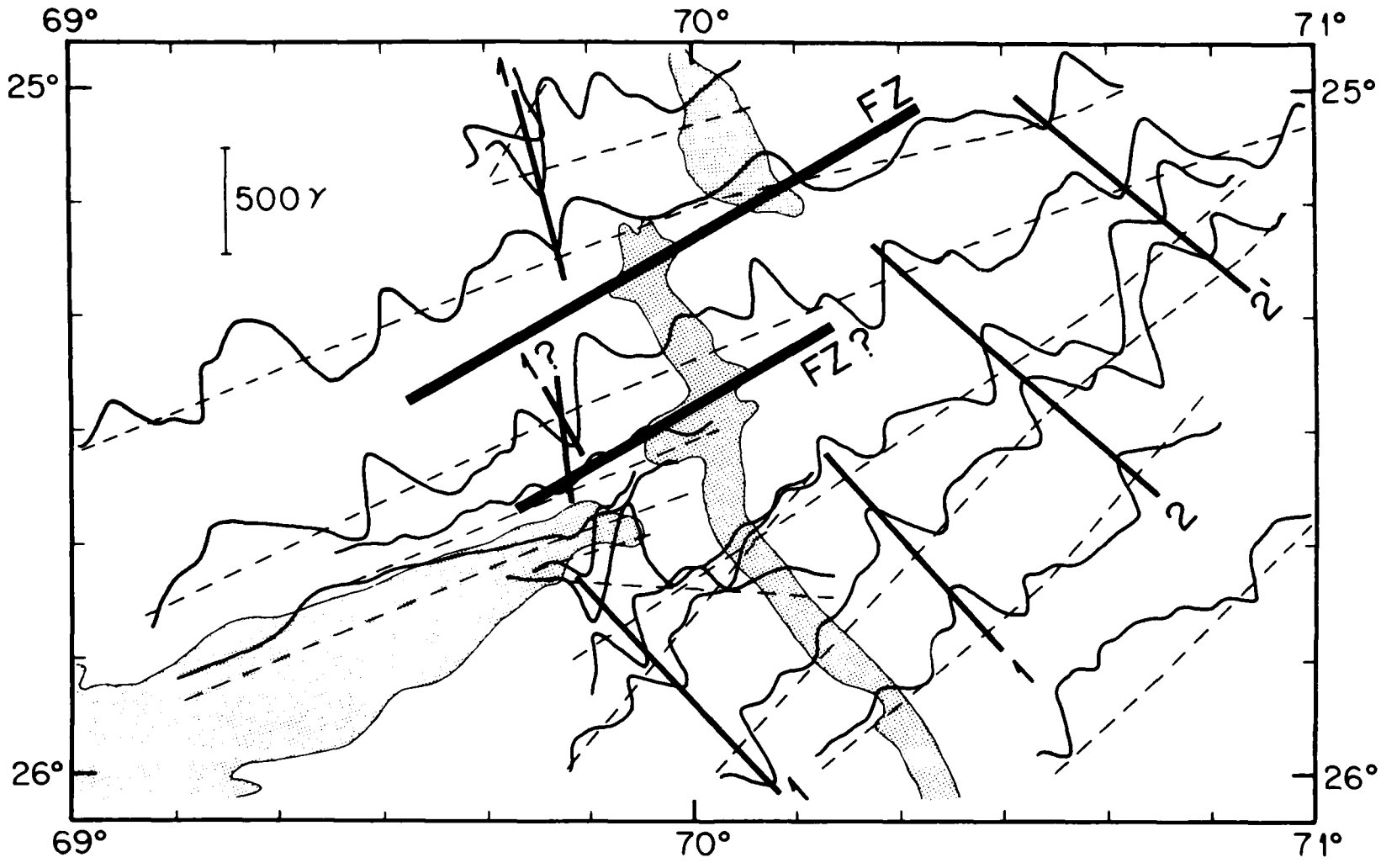
69°
70°
71°
25°
26°
500γ
FZ
FZ?
1
1?
2
2

continued uninterrupted since the time of Anomaly 3' (5 Ma). Some combination of ridge jumps and oblique spreading must have intervened.

EVOLUTION OF THE TRIPLE JUNCTION SINCE 10 Ma

In spite of not being able to determine the precise configuration of the triple junction, one can still map out the general evolution of the junction since 10 Ma. One may construct the regional pattern of crustal isochrons in the following manner.

First, one assumes that the poles and rates of the instantaneous relative rotations among the Indian Ocean plates determined here (Table 3) have remained constant since 10 Ma. This study shows the assumption is justified. Furthermore, Sclater et al. (in preparation) have shown that the poles in question have changed very little, if at all, since 40 Ma. Though it is geometrically impossible that all three poles remain fixed with respect to their associated plates for a finite period of time, the rotations since 10 Ma are small enough that the errors introduced by this simple scheme are insignificant. Next, each spreading axis, as delineated by the topographic and magnetic data, is rotated about its pole of opening to define the position of the plate boundary at various times in the past. These loci represent isochrons on the oceanic crust.

Figure 9 displays the pattern of one million year isochrons since 10 Ma superimposed on the 3000 m bathymetric contour. Symmetric spreading at constant rate has been assumed, except where ridge jumps occur on the SEIR. Comparison with Figure 4 shows this simple scheme to be an excellent representation of the tectonic history of the triple junction over the last ten million years. The figure is based upon a configuration of normally oriented ridge axes. Not shown is the pattern of isochrons produced by spreading obliquities near the triple junction. It is evident from Figure 7 that the two patterns are nearly identical except for details within the domain of the Southwest branch.

The traces of the triple junction separate crust formed at different ridges (Figure 9). Those on the African and Antarctic plates converge in an acute angle at the triple junction and enclose the triangle of crust formed at the SWIR. The geometry is a consequence of the rapid extension of the SWIR as the evolving triple junction moves swiftly eastward with respect to Africa (Figure 10). This is responsible for the principal topographic features along the Africa/Antarctica plate boundary between 67°E and the triple junction. The same process acting since 40 Ma has created the main topographic grain of the SWIR from as far westward as the Melville Fracture Zone at 61°E (Sclater et al., in preparation).

FIGURE 9

The isochron pattern produced by the evolving triple junction of normally spreading ridges superimposed on the generalized bathymetry. The isochrons are at 1 m.y. intervals, and their ages are given by the numbers. Crust formed since 1 Ma is stippled. Heavy lines represent fracture zones. Heavy dashed lines represent traces of the triple junction. The construction of the Figure is discussed in the text.

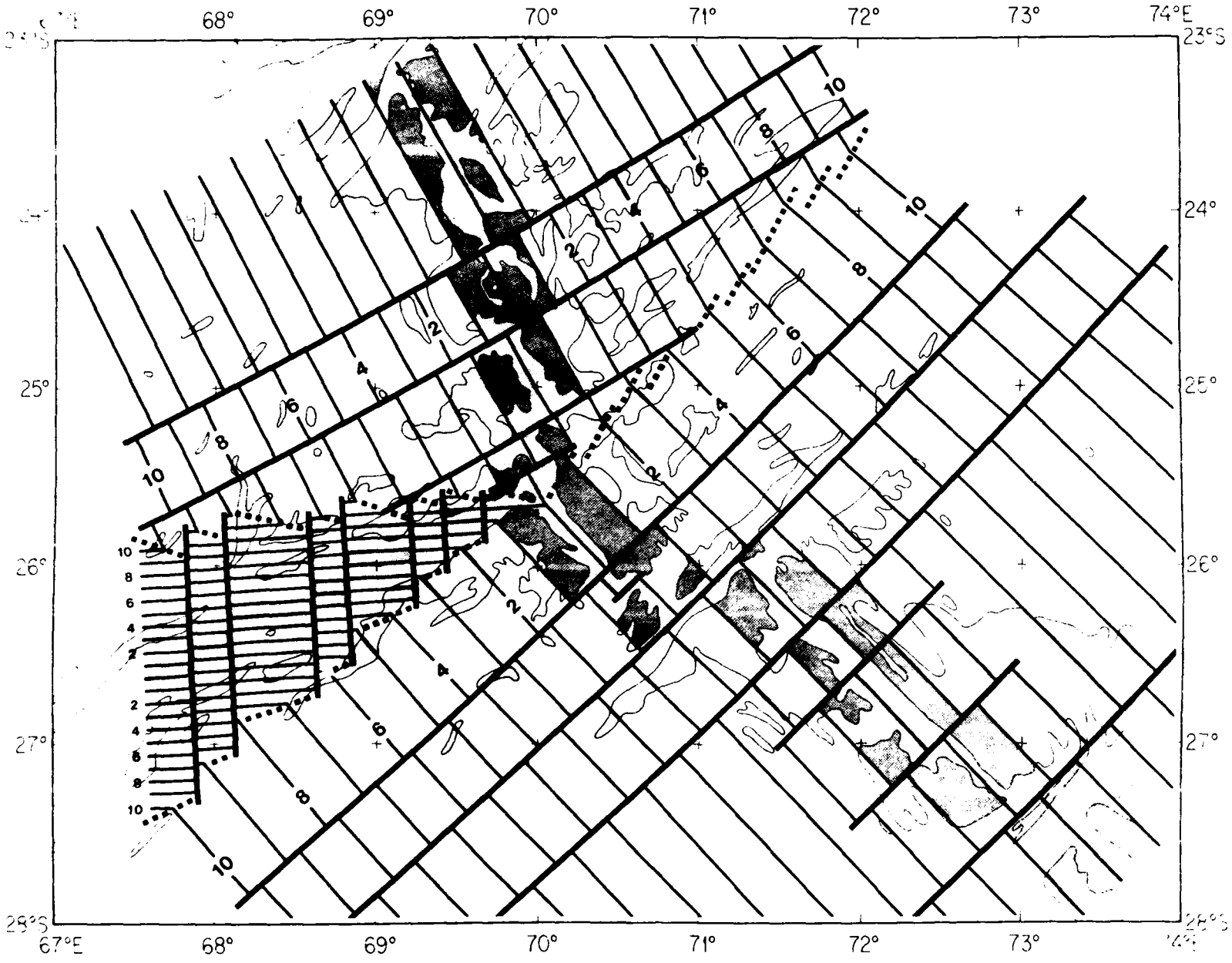
68°
69°
70°
71°
72°
73°
74°E
67°E
23°S
24°
25°
26°
27°
28°S

FIGURE 10

A schematic representation of the evolving Indian Ocean triple junction at times 8 Ma, 6 Ma, 4 Ma, and 2 Ma. The African plate has been held fixed in its present position. The isochrons are at 1 m.y. intervals, and in each reconstruction crust of less than 1 m.y. age is stippled.

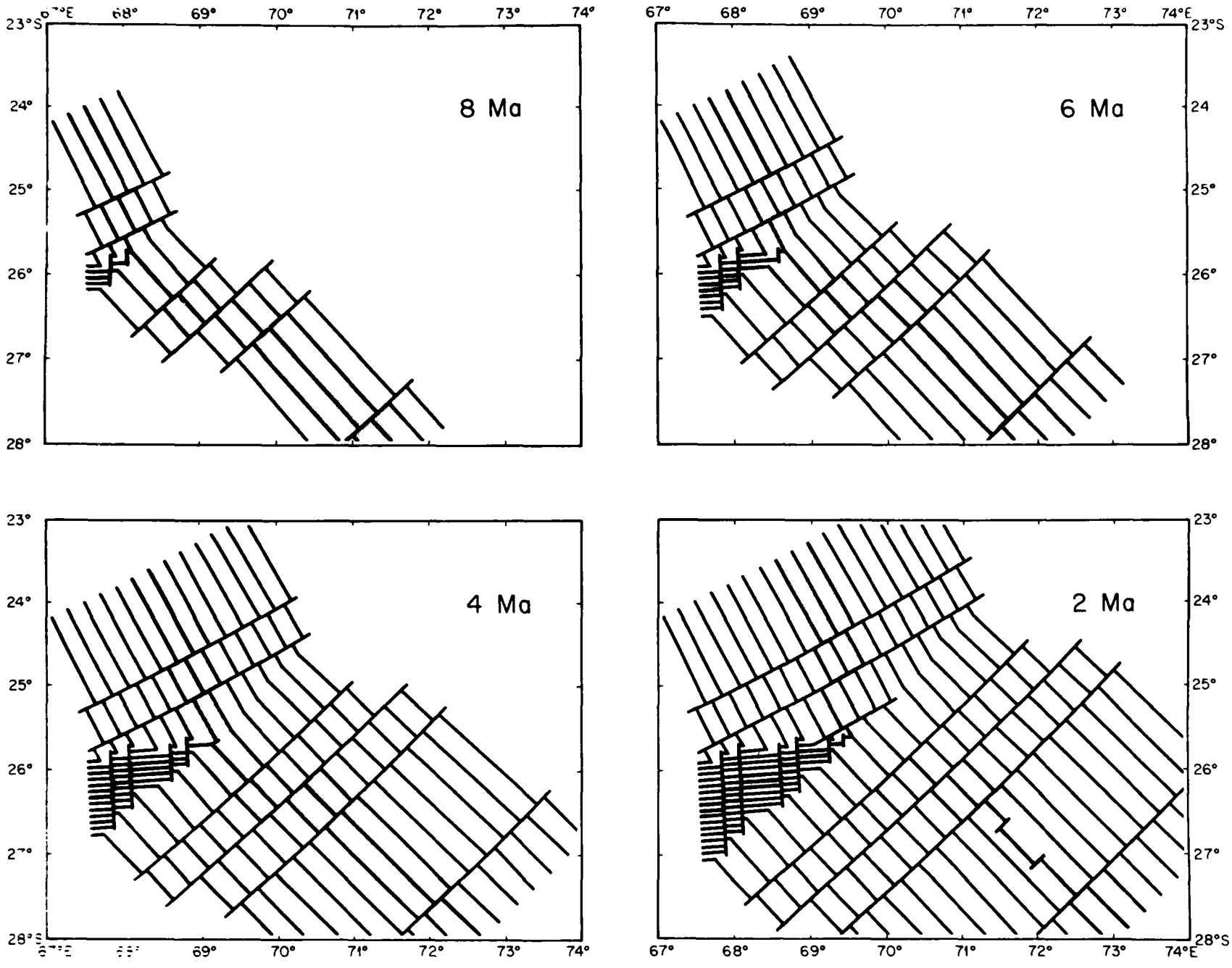
8 Ma
6 Ma
4 Ma
2 Ma
67°
68°
69°
70°
71°
72°
73°
74°E
23°S
24°
25°
26°
27°
28°S

The triple junction traces on the African and Antarctic plates are associated with broken yet lineated topographic highs, and so to a lesser degree is the trace on the Indian plate. There may be a causal relationship in this association, in that the highs may be an effect of the contrast between crust created at different spreading rates. Another possible cause for lineated highs along the triple junction traces is that they were built by excess magmatism at or near the triple junction in a process similar to the construction of aseismic ridges. Phillips and Tapscott (in preparation) postulate a similar origin for the Yermak Plateau and the Morris Jessup Rise in the Arctic Ocean.

SUMMARY

We have located the Indian Ocean triple junction to within 5 km and have shown it to be a ridge-ridge-ridge junction. We have succeeded in determining the instantaneous relative angular velocity vectors of the Indian Ocean plates and have calculated the velocity triangle of the triple junction. Unfortunately, our inability to determine the detailed structure of the Southwest Indian Ridge prevents us from determining the true stability conditions of the junction. Both postulated configurations have probably prevailed at different times.

Regardless of the precise structure of the triple junction, we have been able to map its evolution and have demonstrated that the morphology of the Africa/Antarctica plate boundary in the region is a direct consequence of that evolution. Finally, we have pointed out the intriguing possibility that the triple junction traces on the three plates may have topographic expression.

ACKNOWLEDGEMENTS

We would like to thank Captain D.F. Casiles, the crew, and the scientific party of the R/V Atlantis II for their effective execution of the scientific program, and the personnel of the Digital Data Library of the Woods Hole Oceanographic Institution, who performed the final editing and processing of the data. This work was supported by the Office of Naval Research contract N00014-75-C-0291 with the Massachusetts Institute of Technology, N00014-74-C-0262 with the Woods Hole Oceanographic Insitution, and N00014-75-C-0152 with the Scripps Institution of Oceanography.

REFERENCES

Atwater, T., and J.D. Mudie, Detailed near-bottom geophysical study of the Gorda Rise, J. Geophys. Res., 78, 8665-8686, 1973.

Barberi, F., and J. Varet, Volcanism of Afar: Small scale plate tectonics implications, Geol. Soc. Amer. Bull., 88, 1251-1266, 1977.

Bergh, H.W.,and I.O. Norton, Prince Edward Fracture Zone and the evolution of the Mozambique Basin, J. Geophys. Res., 81, 5221-5239, 1976.

Chase, C.G., The N plate problem of plate tectonics, Geophys. J. Roy. Astron. Soc., 29, 117-122, 1972.

Dickson, G.O., W.C. Pitman, and J.R. Heirtzler, Magnetic anomalies in the Atlantic Ocean and ocean floor spreading, J. Geophys. Res., 73, 2087-2100, 1968.

Falconer, R.K.H., The Indian-Antarctic-Pacific triple junction, Earth Planet. Sci. Lett., 17, 151-158, 1972.

Fisher, R.L., J.G. Sclater, and D. McKenzie, Evolution of the Central Indian Ridge, Western Indian Ocean, Geol. Soc. Amer. Bull., 82, 553-562, 1971.

Forsyth, D.W., Fault plate solutions and tectonics of the South Atlantic and Scotia Sea, J. Geophys. Res., 80, 1429-1443, 1975.

Hayes, D.E., and J.R. Connolly, Morphology of the Southeast Indian Ocean, Antarctic Oceanology II: The Australian New Zealand Sector, ed. D.E. Hayes, Am. Geophys. Un., Washington, DC, 125-145, 1972.

Heezen, B.C., E.T. Bunce, J.B. Hersey, and M. Tharp, Chain and Romanch fracture zones, Deep Sea Res., 11, 11-33, 1964.

Heezen, B.C., R.D. Gerard, and M. Tharp, The Vema fracture zone in the equatorial Atlantic, J. Geophys. Res., 69, 733-738, 1964.

LaBrecque, J.L., D.V. Kent, and S.C. Cande, Revised magnetic polarity time scale for Late Cretaceous and Cenozoic time, Geology, 5, 330-335, 1977.

Mathews, D.H., The Owen fracture zone and the northern end of the Carlsberg ridge, Phil. Trans. Roy. Soc., 259, 172-186, 1966.

McKenzie, D.P., and W.J. Morgan, Evolution of triple junctions, Nature, 224, 125-133, 1969.

McKenzie, D., and J.G. Sclater, The evolution of the Indian Ocean since the Late Cretaceous, Geophys. J. Roy. Astron. Soc., 25, 437-528, 1971.

Minster, J.B., and T.H. Jordan, Present-day plate motions, J. Geophys. Res., 83, 5331-5354, 1978.

Minster, J.B., T.H. Jordan, P. Molnar, and E. Haines, Numerical modeling of instantaneous plate tectonics, Geophys. J. Roy. Astron. Soc., 36, 541-576, 1974.

Parsons, B., and J.G. Sclater, An analysis of the variation of ocean floor bathymetry and heat flow with age, J. Geophys. Res., 82, 803-827, 1977.

Phillips, J.D., and C. Tapscott, The evolution of the Atlantic Ocean north of the Azores, in preparation.

Schouten, H. and C.R. Denham, Modeling the oceanic magnetic source layer and the likelihood of mixed polarity in oceanic basement drill cores, in preparation.

Sclater, J.G., C. Bowin, R. Hey, H. Hoskins, J. Peirce, J. Phillips, and C. Tapscott, The Bouvet Triple Junction, J. Geophys. Res., 81, 1857-1869, 1976.

Sclater, J.G., R.L. Fisher, P. Patriat, C. Tapscott, and B. Parsons, The Eocene to present development of the Southwest Indian Ridge, a consequence of the evolution of the Indian Ocean Triple Junction, in preparation.

Stein, S., and E.A. Okal, Seismicity and tectonics of the Ninetyeast Ridge area: Evidence for internal deformation of the Indian Plate, J. Geophys. Res., 83, 2233-2245, 1978.

Tisseau, J., Etude structurale du Golfe d'Aden et du bassin de Somalie, Thèse de Doctorat de 3eme cycle, Université de Paris, 1978.

Van Andel, T.H., and T.C. Moore, Magnetic anomalies and sea-floor spreading rates in the northern South Atlantic, Nature, 226, 328-330, 1970.

Weissel, J.K., and D.E. Hayes, Magnetic anomalies in the southeast Indian Ocean, Antarctic Oceanology II: The Australian - New Zealand Sector, ed. D.E. Hayes, Am. Geophys. Un., Washington, DC, 165-196, 1972.

Weissel, J.K., and D.E. Hayes, The Australian-Antarctic discordance: new results and implications, J. Geophys. Res., 79, 2579-2587, 1974.

CHAPTER 4

THE FINITE ROTATIONS OF A THREE PLATE SYSTEM

THE FINITE ROTATIONS OF A THREE PLATE SYSTEM WITH APPLICATIONS TO THE LABRADOR SEA

C. Tapscott

Department of Earth and Planetary Sciences
Massachusetts Institute of Technology
Cambridge, MA 02139 and
Woods Hole Oceanographic Institution
Woods Hole, MA 02543

ABSTRACT

A method is presented for determining the best reconstruction of the past relative positions of three tectonic plates around a triple junction according to a fitting criterion applied to sea-floor spreading data. The method enables one to set confidence limits on the optimal set of internally consistent finite rotations based upon the probable errors in the data. The technique is illustrated by reconstructions of the plates about the now extinct Labrador Sea triple junction at the times of anomalies 21 (50 Ma) and 24 (56 Ma).

INTRODUCTION

Over the last several million years the relative motions of the lithospheric plates have been the principal mechanism shaping the face of the earth. For this reason, one of the major thrusts of geophysical research since the advent of the new global tectonics has been toward determining as accurately as possible the relative positions of the plates at various times in the past. Early in this endeavor, Bullard et al. (1965) recognized that, by a theorem due to Euler, such plate reconstructions could be described in terms of finite rotations about axes passing through the center of the earth. The problem of reconstructing the past relative positions of two plates is then the problem of discovering the finite rotation that best brings into coincidence two patterns, one on each plate, that represent the adjacent edges of the plates at the time for which the reconstruction is valid. Many such reconstructions have been made fitting together the margins of the Gondwana continents (e.g., Bullard et al., 1965; Smith and Hallam, 1970) and magnetic anomaly isochron lineations and fracture zone traces in the ocean basins (e.g., McKenzie and Sclater, 1971; Pitman and Talwani, 1972).

No two plates exist in isolation. All pairs are part of the global system, and all the pairwise relative rotations form an internally consistent set if the plates are indeed rigid bodies. All closed cyclic products of relative rotations must result in unity. The interdependence of the finite rotations provides additional constraints which can be an advantage in seeking the best reconstruction, in that a paucity of data

between two plates can sometimes be overcome by enlarging the system to include three or more plates around one or more triple junctions. With adequate data, one may test the validity of the rigid plate hypothesis for the plates involved in such a multiple plate system, questioning it if no acceptable reconstruction can be achieved.

This paper extends the fitting technique of Hellinger (1979) to deal with three plates around a triple junction. The method presented here enables one to find, with a minimum of effort, the internally consistent set of finite rotations describing the best possible reconstruction of a three plate system according to the fitting criterion. Perhaps most important, Hellinger's (1979) technique allows one to set statistically meaningful limits on the region of valid rotation tensors. The three plate method is illustrated by reconstructions of the plates around the Labrador Sea triple junction at the times of Anomaly 24 (56 Ma) and Anomaly 21 (50 Ma).

THE METHOD

The best fit of patterns depends on the statistical criterion defining the quality of the fit. Criteria commonly used include the simple but effective method of "eyeballing" the patterns, variations on minimizing the sum of the squares of the distances of each point from the other lineation (Bullard et al., 1965; Pilger, 1978), and minimizing the overlap and underlap area between the patterns (McKenzie and Sclater, 1971). These techniques have both advantages and disadvantages relative

to one another. All have the common disadvantage that they fail to take account of the known uncertainties in the data. Hellinger (1979) has recently introduced a method correcting this shortcoming, and, moreover, Hellinger's technique uses the data and their uncertainties to set statistically meaningful limits on the region of valid finite rotations.

The technique is particularly well-suited to the type of data usually encountered in sea-floor spreading studies. The data must satisfy the following conditions or assumptions (Hellinger, 1979):

1. The patterns or lineations to be matched on the two plates are known only at a finite number of discrete points (shiptrack crossings of magnetic anomalies or fracture zones).
2. The location of each datum is uncertain (to the limit of resolution in interpretation) and the distribution of errors may be adequately described by a bivariate-normal probability density function. These errors are uncorrelated.
3. The data on each plate may be divided into a number of sections (e.g., a fracture zone trace or a magnetic anomaly lineation between adjacent fracture zones), each of which may be well-represented by a segment of a great circle.
4. One may identify a one-to-one correspondence between the sections of data on one plate and those on the other plate.

The simplest and most readily calculated criterion of fit applicable to the method (criterion Φ_o in Hellinger, 1979) is easily described. After a trial rotation, the best fit great circle is calculated for each section of data (now the united set of data from both plates, see Figure 1), weighting each point according to its uncertainty. The proper great circle is that which minimizes the sum of the squares of the weighted distances of the points from the plane of the great circle. The measure of the misfit of each section is just this sum of squared, weighted distances, and the measure of misfit of the reconstruction is the sum of the measures of the individual sections. That is, if there are n_{ij} points in section j on plate i, then the measure of misfit of that section for a rotation r is

$$\Phi_{oj} = \sum_{k=1}^{n_{1j}} (\hat{p}_j \cdot \hat{s}_{1jk})^2 \sigma_{1jk}^{-2} + \sum_{k=1}^{n_{2j}} (\hat{p}_j \cdot r\hat{s}_{2jk})^2 \sigma_{2jk}^{-2} , \quad (1)$$

where $\hat{p}_j$ is the unit vector perpendicular to the plane of the best fit great circle of section j, the $\hat{s}_{ijk}$ are the unit vectors through the data points of section j on plate i, and the σ_{ijk} are the standard deviations of their error distributions, scaled to a unit sphere. If there are a total of J sections, then the measure of misfit for the reconstruction defined by the rotation r is

$$\Phi_o = \sum_{j=1}^{J} \Phi_{oj} . \quad (2)$$

The best reconstruction is the one which minimizes this measure of misfit. The method makes minimal assumptions about the actual shape of the ancient plate boundary and is well-suited

FIGURE 1

A schematic diagram illustrating the method of pattern fitting. The data on one plate are shown as circles and on the other plate as squares, and corresponding sections of data are indicated before rotation. After a trial rotation, great circles are fit to each section of plate boundary, using the data from both plates. After Hellinger (1979).

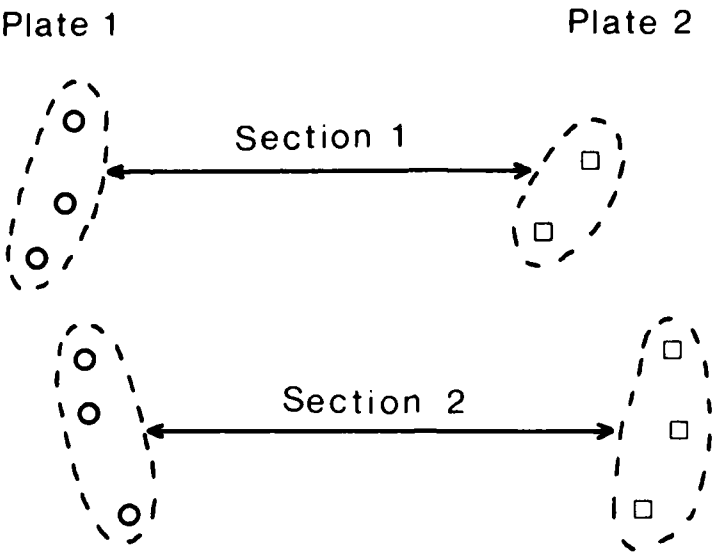

Before Rotation

The Best Fit
Great Circles:

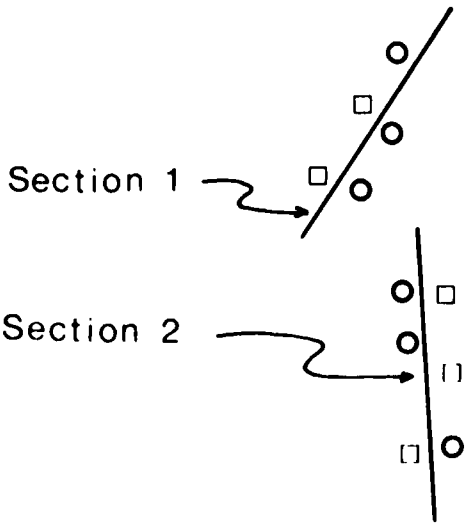

After Rotation

to the sparse data sets often encountered in investigations of sea-floor spreading.

The measure of misfit of a reconstruction of several plates is merely the sum of the measures of misfit of each plate pair. This paper presents a computer program (Appendix) which calculates the measure of misfit for a reconstruction of a three plate system and searches for the interdependent set of finite relative rotations describing the best reconstruction according to criterion Φ_o (Hellinger, 1979). This technique provides a valuable tool for reconstructing the past relative positions of several tectonic plates and for defining the confidence limits we may set on our knowledge of their relative motions.

THE LABRADOR SEA - ANOMALY 24

Srivastava (1978) has presented the results of a geophysical survey in the Labrador Sea and has identified several marine magnetic anomaly lineations,giving a set of finite rotations which restore the Greenland, North American, and Rockall plates to their relative positions at the time of Anomaly 24 (56 Ma). Phillips and Tapscott (in preparation) also present a set of finite rotations for the same purpose, basing their study solely on published data from the North Atlantic Ocean (Laughton, 1971; Johnson et al., 1972; Johnson and Egloff, 1973; Vogt and Avery, 1974; Kristoffersen and Talwani, 1977).

After compiling a data set of locations of Anomaly 24

from these sources (Table 1, Figure 2), one may apply the criterion of fit described above to both sets of rotations (Table 2). Overall, the rotations of Srivastava (1978) yield a much smaller measure of misfit, though those of Phillips and Tapscott (in preparation) produce a slightly better fit for the Greenland-Rockall and North America-Rockall boundaries. This is obvious when one plots the reconstructions (Figures 3 and 4). The Phillips and Tapscott (in preparation) rotations take North America much too close to Greenland, while the Srivastava (1978) rotations move Rockall slightly too far toward the west. By arbitrarily fixing the Greenland-North America and Greenland-Rockall poles and making slight adjustments in the angles of rotation, one may significantly improve both reconstructions, though that derived from Srivastava (1978) is clearly superior.

Starting from this point and searching for the best set of finite rotations (down to a resolution of 0.25° in pole location and 0.01° in rotation angle), one finds a minimum in the measure of misfit for a set including a Greenland-North America pole close to that of Srivastava (1978). The other two rotation poles, however, have moved toward the northwest, giving a much better fit of Rockall to the Greenland-North America combination (Table 2, Figure 5). The set of finite rotations derived here clearly yields an improved reconstruction about the Labrador Sea triple junction for Anomaly 24 time.

Having discovered the optimal set of finite rotations for the data, one may determine the confidence limits on the finite rotation poles. One method of doing this is to apply the

TABLE 1. Anomaly 24 Locations Used in this Study

Section	N. Lat.	W. Long.	N. Lat.	W. Long.	Section	N. Lat.	W. Long.	N. Lat.	W. Long.
	Greenland Plate		North American Plate			Greenland Plate		Rockall Plate	
1	57.80	45.40	55.92	46.87	1	58.21	43.28	56.15	24.60*
	57.73	46.39	55.84	47.51		58.56	42.60	56.50	24.00*
						58.89	42.11	57.00	23.20*
2	58.01	47.39	56.10	48.76		59.70	41.00*	57.50	22.20*
	58.33	48.26	56.32	49.32		61.50	39.10*		
	58.47	49.01	56.51	49.84					
						North American Plate		Rockall Plate	
3	58.36	50.56	56.37	51.80					
	58.57	51.12	56.58	52.30	1	56.18	45.20*	56.00	25.40*
	58.77	51.56	56.80	52.80		55.79	45.25	55.00	25.90*
			57.01	53.23		54.91	45.16	54.60	26.20*
						53.91	45.15	53.15	26.15*
4	59.51	52.80	56.50	54.07		53.30	45.06	52.40	26.30*
	59.75	53.11	57.75	54.38					
	59.99	53.36	58.01	54.66					
	60.29	53.61	58.27	54.99					
	60.57	58.86	58.55	55.22					
5	60.70	54.63	58.73	55.85					
	60.99	54.91	58.98	56.18					
	61.24	55.22	59.24	56.47					

*From Phillips and Tapscott (in preparation). All other data are from Srivastava (1978). All data are estimated to be accurate to within 10 km.

FIGURE 2

Locations of Anomaly 24 along the margins of Greenland (circles), North America (squares), and Rockall Bank (stars) used in this study. Corresponding sections of data are indicated by joined balloons. The positions of the continental masses are indicated by shading the regions within the 1000 fathom bathymetric contour. The data and sources are listed in Table 1.

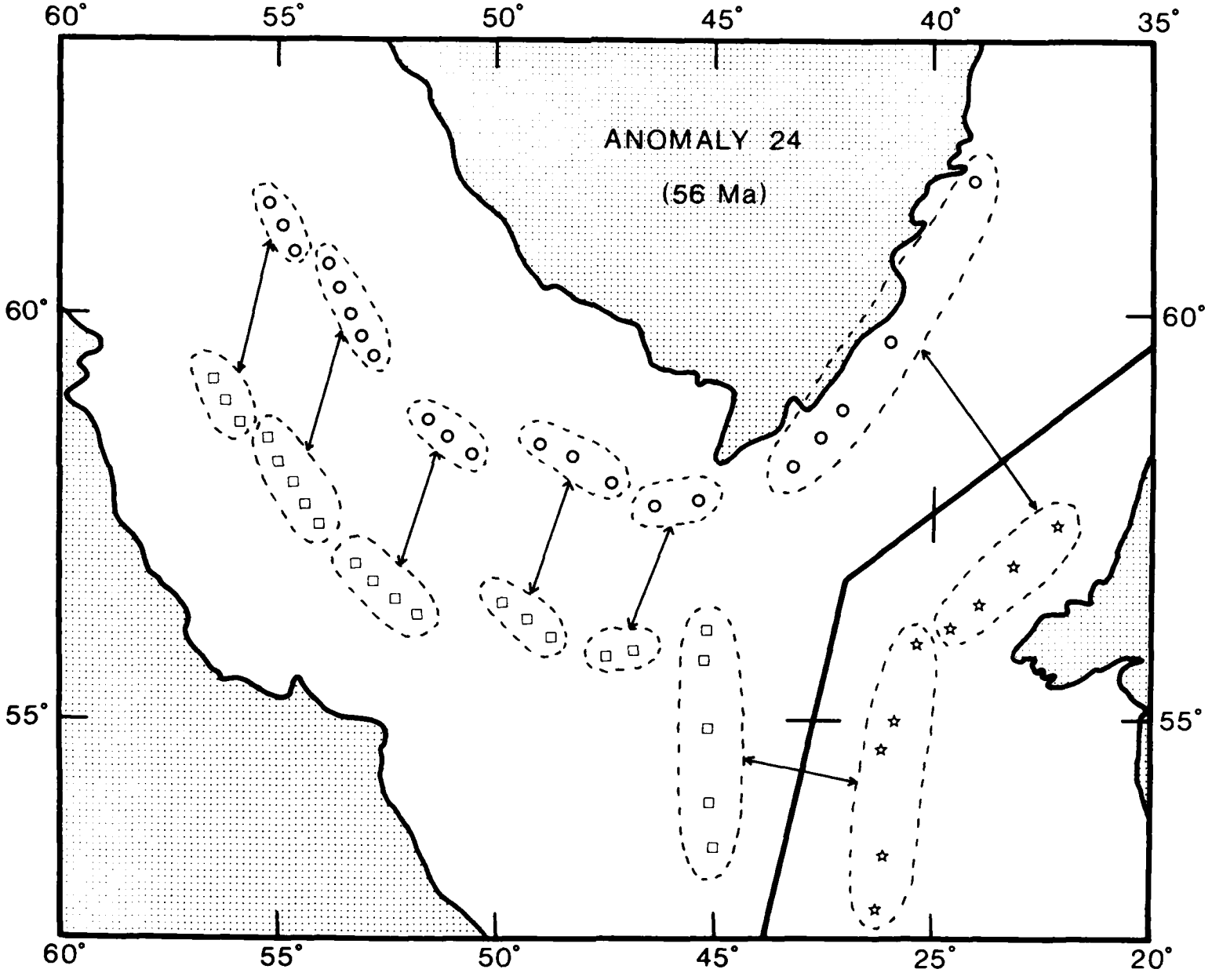
60°
55°
50°
45°
40°
35°
ANOMALY 24
(56 Ma)
60°
55°
60°
55°
50°
45°
25°
20°

TABLE 2. Comparison of the Quality of Reconstructions for Anomaly 24.

Source	Plate Pair*	Finite Rotation N. Lat.	E. Long.	Angle	Relative Measure	Total Relative Measure
Srivastava (1978)	N/G	26.0	1.5	-2.80	5.23	
	R/G	50.2	130.9	-10.97	18.9	91.2
	R/N	40.0	145.0	-11.40	67.0	
Phillips and Tapscott (in prep.)	N/G	-9.1	25.6	-3.22	542	
	R/G	35.6	127.9	-9.86	13.0	584
	R/N	35.4	147.8	-11.15	29.1	
Revised after Srivastava (1978)	N/G	26.0	1.5	-2.80	5.23	
	R/G	50.2	130.9	-10.77	13.9	46.7
	R/N	39.8	145.2	-11.20	27.6	
Revised after Phillips and Tapscott (in prep.)	N/G	-9.1	25.6	-2.37	100	
	R/G	35.6	127.9	-10.11	39.0	180
	R/N	35.8	142.7	-10.97	41.3	
This paper	N/G	22.0	4.0	-2.62	5.30	
	R/G	63.6	120.6	-12.01	13.7	35.2
	R/N	56.2	141.0	-11.90	16.2	
This paper (two plates)	N/G	23.5	2.5	-2.69	5.00	—

*N/G signifies North American relative to Greenland;
R/G, Rockall relative to Greenland;
R/N, Rockall relative to North America.

FIGURE 3

A reconstruction of Anomaly 24 about the Labrador Sea triple junction according to Srivastava's (1978) rotations. Symbols are as in Figure 2.

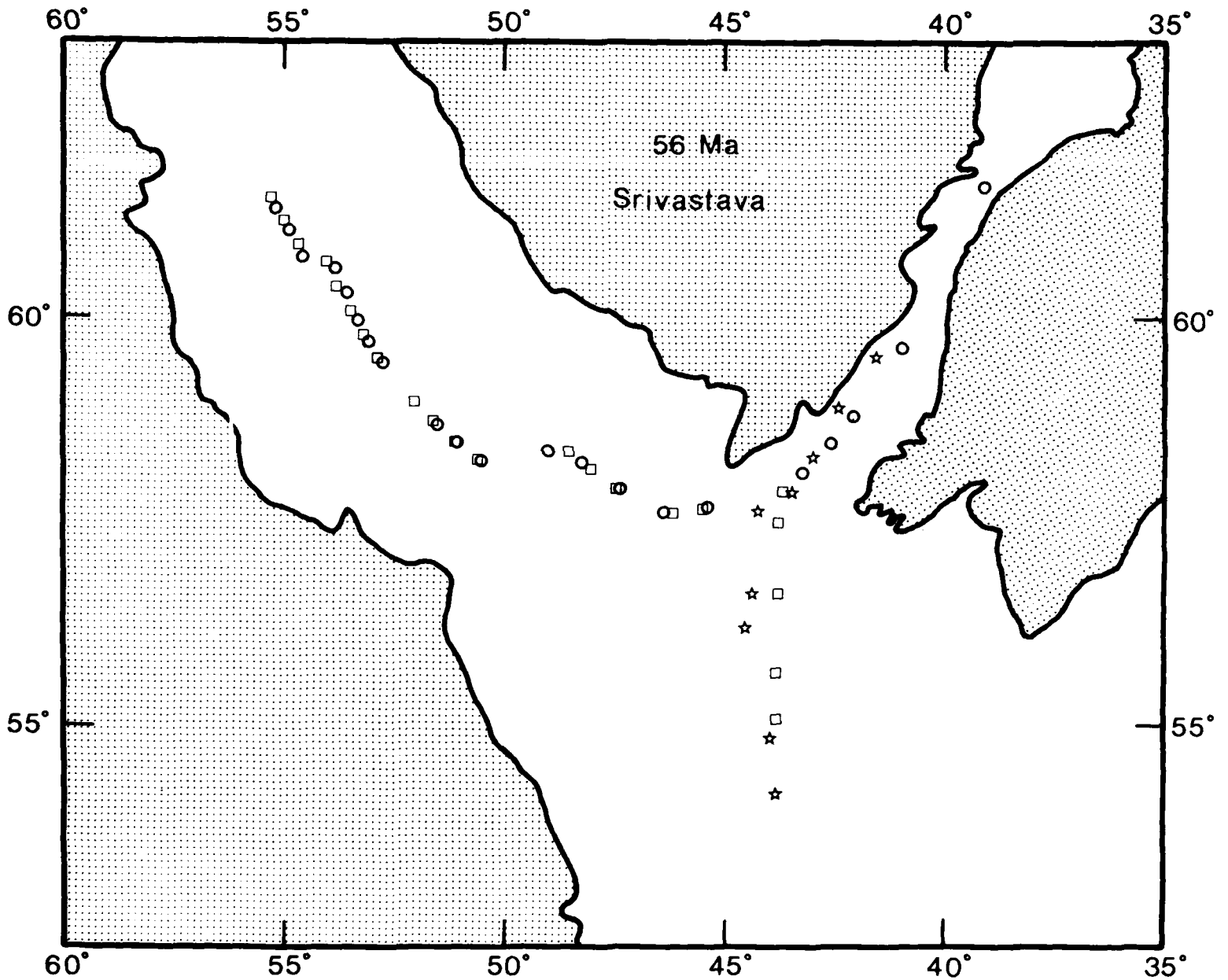
60°
55°
50°
45°
40°
35°
56 Ma
Srivastava
60°
55°

FIGURE 4

A reconstruction of Anomaly 24 about the Labrador Sea triple junction according to rotations of Phillips and Tapscott (in preparation). Symbols are as in Figure 2.

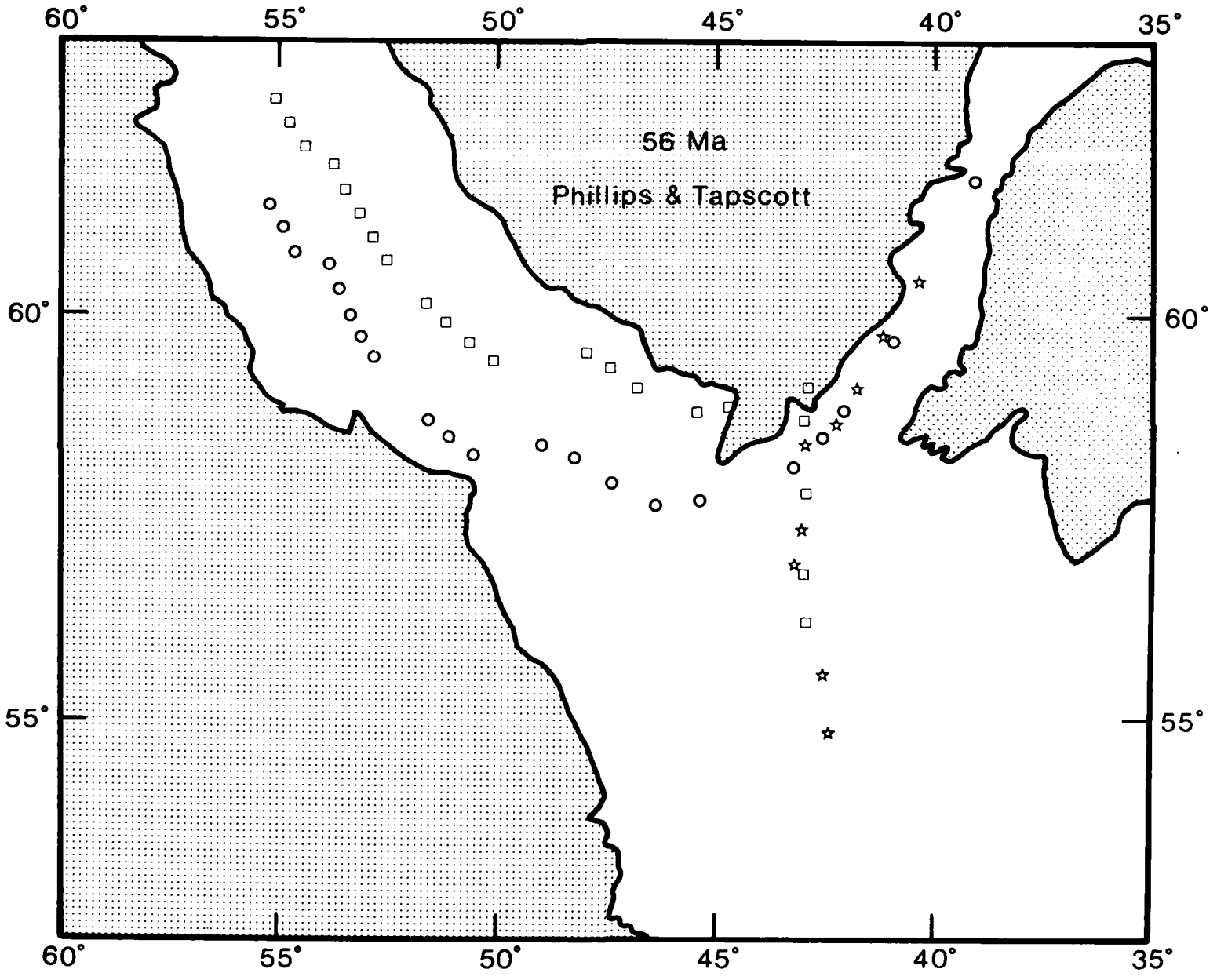
60°
55°
50°
45°
40°
35°
56 Ma
Phillips & Tapscott
60°
55°

FIGURE 5

A reconstruction of Anomaly 24 about the Labrador Sea triple junction using the rotations derived in this paper. Symbols are as in Figure 2.

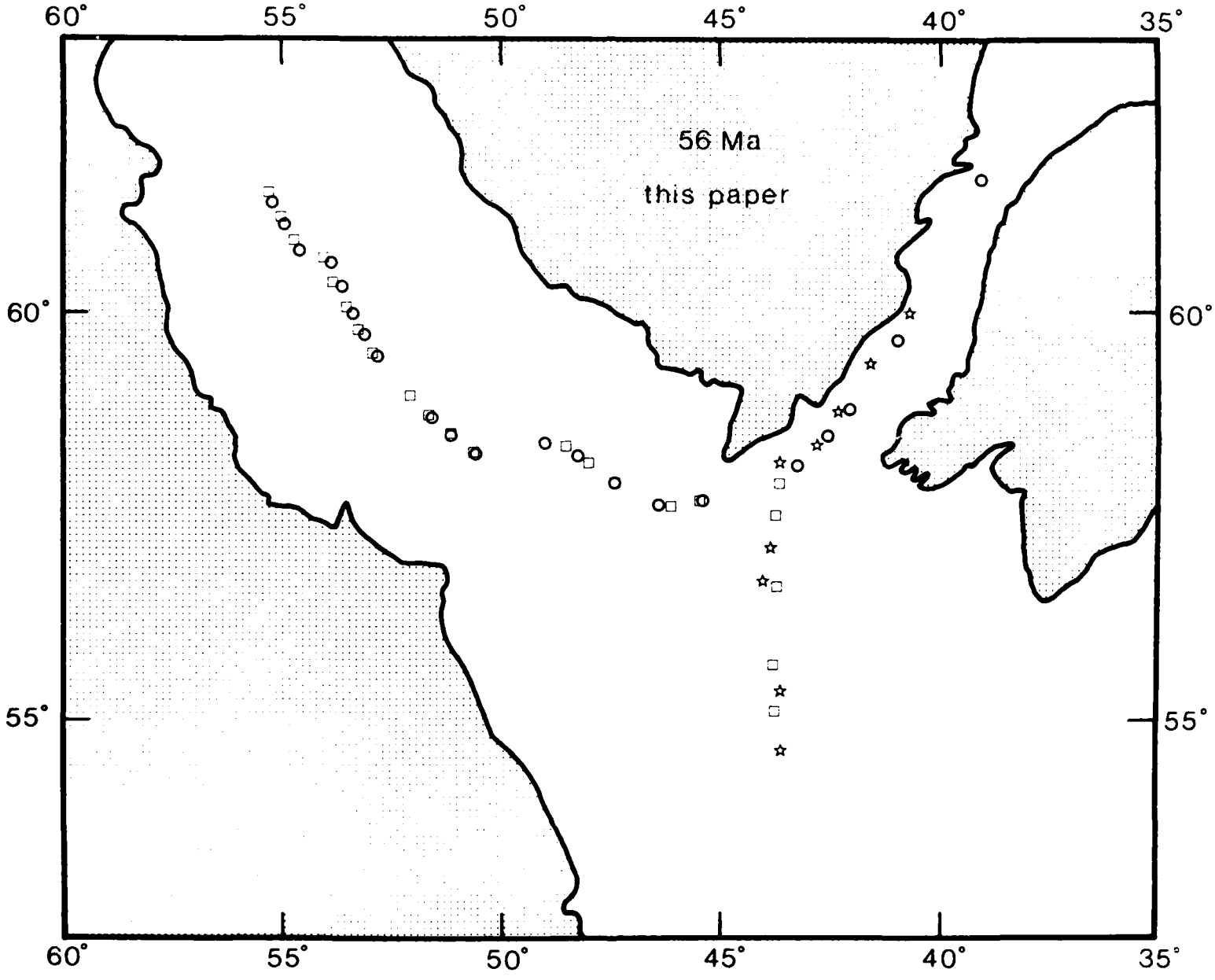
60°
55°
50°
45°
40°
35°
56 Ma
this paper
60°
55°

rigorous and exhaustive technique of Hellinger (1979) to each plate boundary in turn. A somewhat more qualitative but no less useful determination of the regions of confidence may easily be made by exploring a few rotations in the neighborhood of the best-fit set. In the present study, for example, the testing of a few poles in the neighborhood of the optimal Greenland-North America pole shows that when the best measure of misfit obtainable for a pole is greater than about 1.25 times the measure for the optimal set of rotations, the fit has degraded to the limit of acceptability. Such degradation is generally concentrated in the fit along one plate boundary (in this case the Greenland-North America plate boundary) and is usually due to poor fits of one or two sections of data.

Figure 6 displays the contour of the measure at the critical value about the preferred Greenland-North America pole. The region of confidence of this pole is a long, narrow area roughly joining the poles of Srivastava (1978) and Phillips and Tapscott (in preparation). This is not unexpected, as poles of rotation are usually well-constrained in a direction perpendicular to the general trend of the plate boundary, and poorly constrained along that trend. In this case, because the data are confined to a small area, one is unable to rule out absolutely any Greenland-North America finite poles along a 50° arc. If it is considered in combination with Greenland-Rockall and North America-Rockall rotations close to those of the optimal set, the Greenland-North America pole of Srivastava (1978) is not significantly different from that derived here.

FIGURE 6

Regions of confidence for the Greenland-North America finite rotation poles for Anomaly 24. The continuous contour denotes the region of confidence for the pole derived in this paper for the three plate system, and the dashed contour is that for the two plates alone. The Greenland-North America finite rotation poles for Anomaly 24 discussed in the text are also shown. Continental coastlines are shown for scale and orientation.

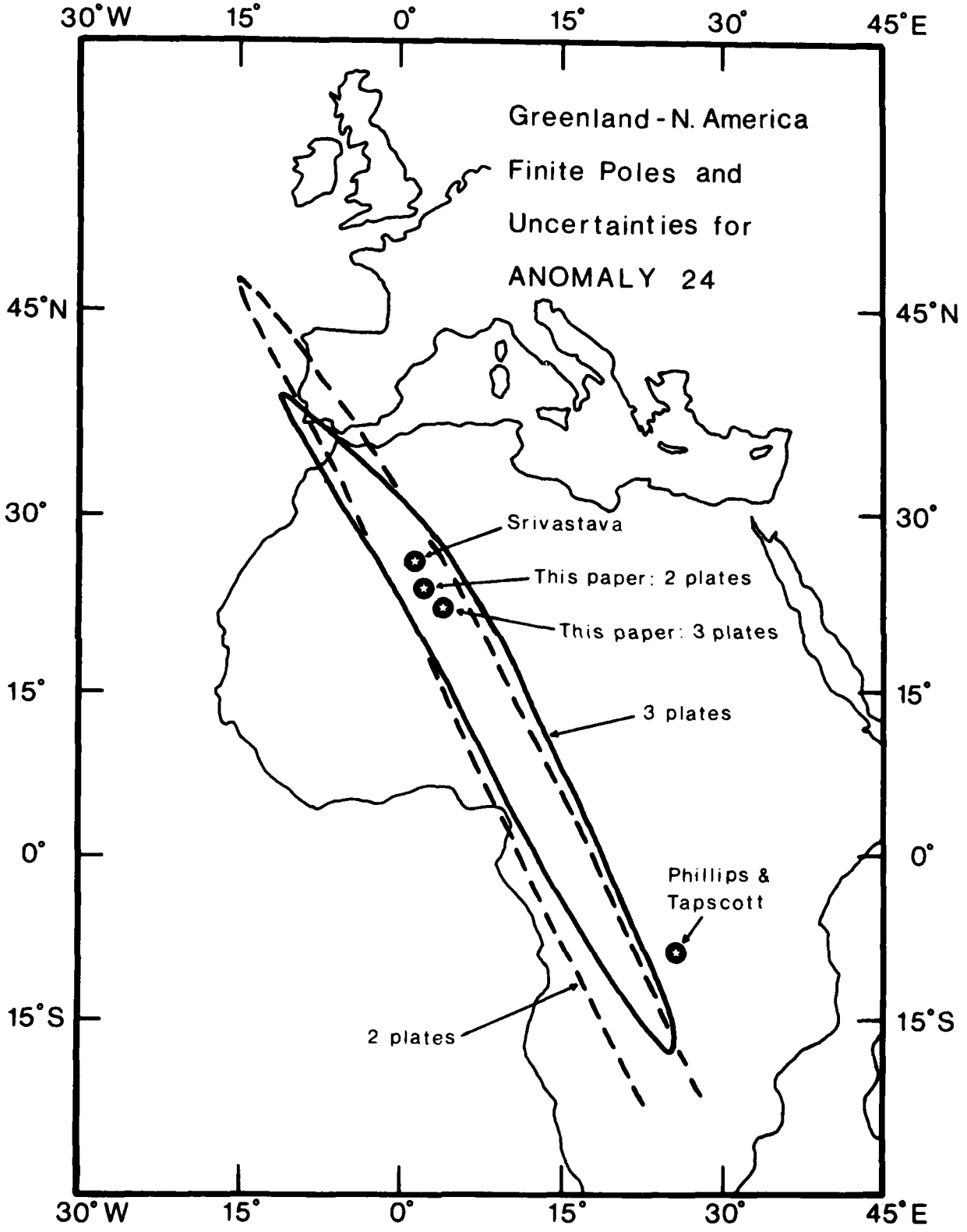
30°W
15°
0°
15°
30°
45°E
Greenland - N. America
Finite Poles and
Uncertainties for
ANOMALY 24
45°N
30°
15°
0°
15°S
Srivastava
This paper: 2 plates
This paper: 3 plates
3 plates
Phillips &
Tapscott
2 plates

It is of interest to compare these results to those following from the consideration of a system of only two plates. Application of Hellinger's method shows that a rotation of -2.69° about a pole at 23.5°N, 2.5°E best reconstructs the data along the Greenland-North American plate boundary without regard to the fit of the Rockall plate (Table 2). This pole lies between that of Srivastava (1978) and the pole derived in the present study of the three plate system. Contouring the region of confidence in a similar manner, one sees that it closely resembles that for the three plate system (Figure 6). The two regions trend somewhat differently, however, and the confidence region for the three plate system is more restricted in latitudinal extent. These differences result from the additional constraints imposed by the other two plate boundaries. In this example, these constraints are relatively weak, yet their effects are significant in limiting the uncertainty in the Greenland-North America pole of rotation.

THE LABRADOR SEA - ANOMALY 21

Locations of Anomaly 21 in the Labrador Sea and adjoining regions may be compiled from the same sources as above (Table 3, Figure 7). Testing Srivastava's (1978) reconstruction for Anomaly 21 time (Table 4), one finds that once again these rotations move Rockall Bank too far westward (Figure 8) and that a slight adjustment of the Greenland-Rockall rotation angle significantly improves the fit (Table 4). Simultaneous consideration of the three plate boundaries leads to an optimal set

TABLE 3. Anomaly 21 Locations Used in this Study.

Section	N. Lat.	W. Long.	N. Lat.	W. Long.	Section	N. Lat.	W. Long.	N. Lat.	W. Long.
	Greenland Plate		North American Plate			Greenland Plate		Rockall Plate	
1	57.43	42.50	56.65	44.08	1	58.07	41.28	57.00	24.80*
	57.50	43.63				58.46	40.65	57.45	24.00*
						59.33	39.54	58.70	22.00*
2	57.21	45.88	56.38	47.04		61.00	37.25*	59.30	21.00*
	57.28	46.87				61.80	36.10*	59.80	20.00*
3	57.75	48.51	56.79	48.93					
	57.80	48.87	56.95	49.54		North American Plate		Rockall Plate	
4	57.69	50.60	56.87	51.29	1	56.41	43.78	56.10	27.10*
	57.90	51.14	57.06	51.87		55.98	43.77	55.00	27.50*
	58.09	51.62	57.27	52.36					
	58.32	52.11	57.48	52.87	2	54.56	43.78	54.00	27.65*
						54.19	43.69	53.20	27.70*
5	58.77	52.95	57.94	53.67		53.74	43.60	52.40	27.75*
	59.05	53.25	58.17	53.98		53.20	43.46		
	59.32	53.53	58.46	54.34		52.79	43.33		
	59.59	53.79							
	59.85	54.02							

*From Phillips and Tapscott (in preparation). All other data are from Srivastava (1978).
All data are estimated to be accurate to within 10 km.

FIGURE 7

Locations of Anomaly 21 about the Labrador Sea triple junction. Symbols are as in Figure 2.

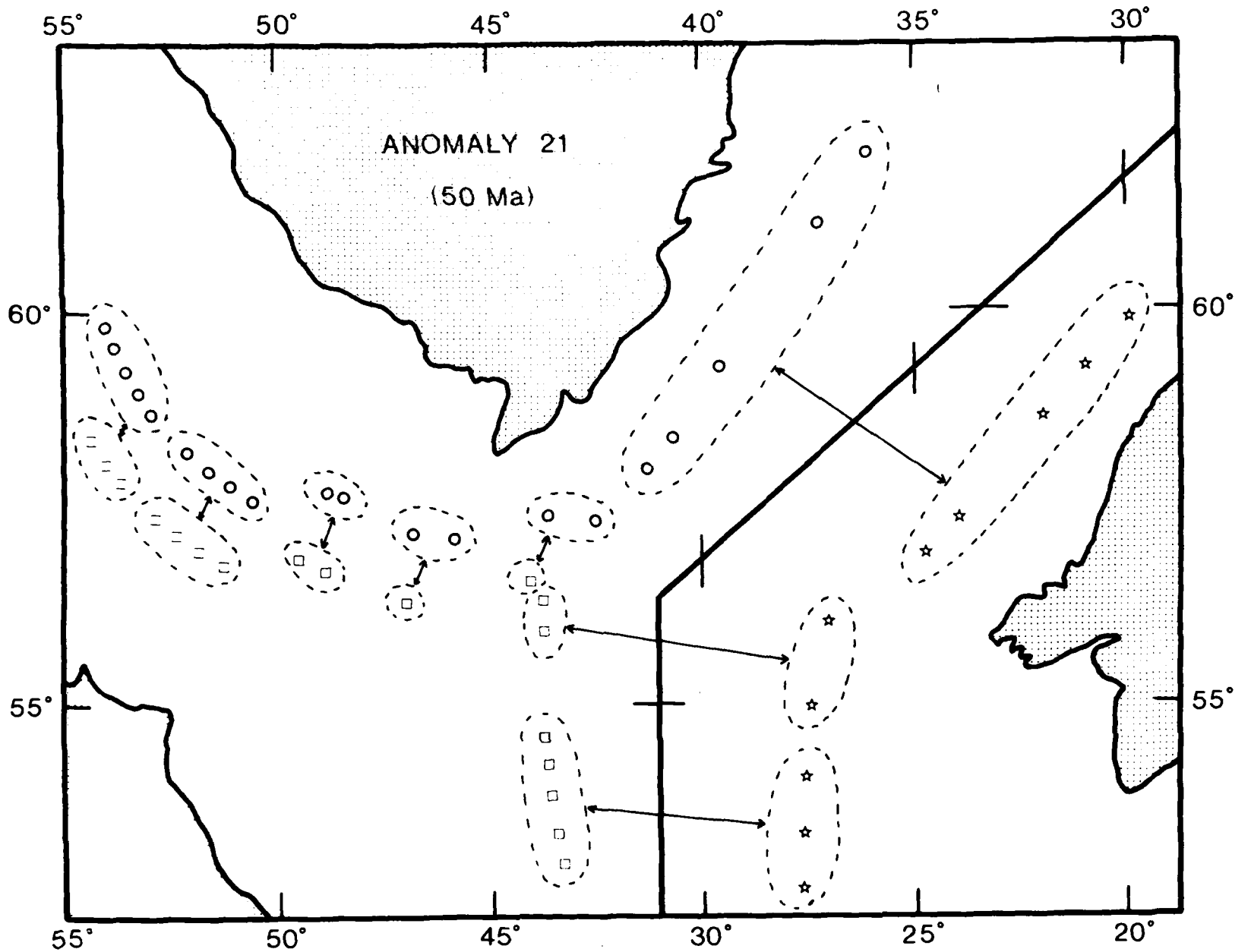
55°
50°
45°
40°
35°
30°
ANOMALY 21
(50 Ma)
60°
55°
55°
50°
45°
30°
25°
20°

TABLE 4. Comparison of the Quality of Reconstructions for Anomaly 21.

Source	Plate Pair*	Finite Rotation N. Lat.	E. Long.	Angle	Relative Measure	Total Relative Measure
Srivastava (1978)	N/G	13.0	2.0	-1.10	3.13	
	R/G	55.0	135.0	-9.59	15.2	35.5
	R/N	50.8	142.8	-9.87	17.1	
Revised after Srivastava (1978)	N/G	13.0	2.0	-1.10	3.13	
	R/G	55.0	135.0	-9.44	7.02	10.5
	R/N	50.7	142.9	-9.72	0.341	
This paper	N/G	16.8	1.3	-1.15	2.75	
	R/G	65.5	127.6	-10.41	2.10	5.42
	R/N	61.5	138.6	-10.44	0.574	
This paper (two plates)	N/G	-18.6	20.0	-0.95	2.24	—

* N/G signifies North America relative to Greenland;
R/G, Rockall relative to Greenland;
R/N, Rockall relative to North America.

FIGURE 8

A reconstruction of Anomaly 21 about the Labrador Sea triple junction using rotations of Srivastava (1978). Symbols are as in Figure 2.

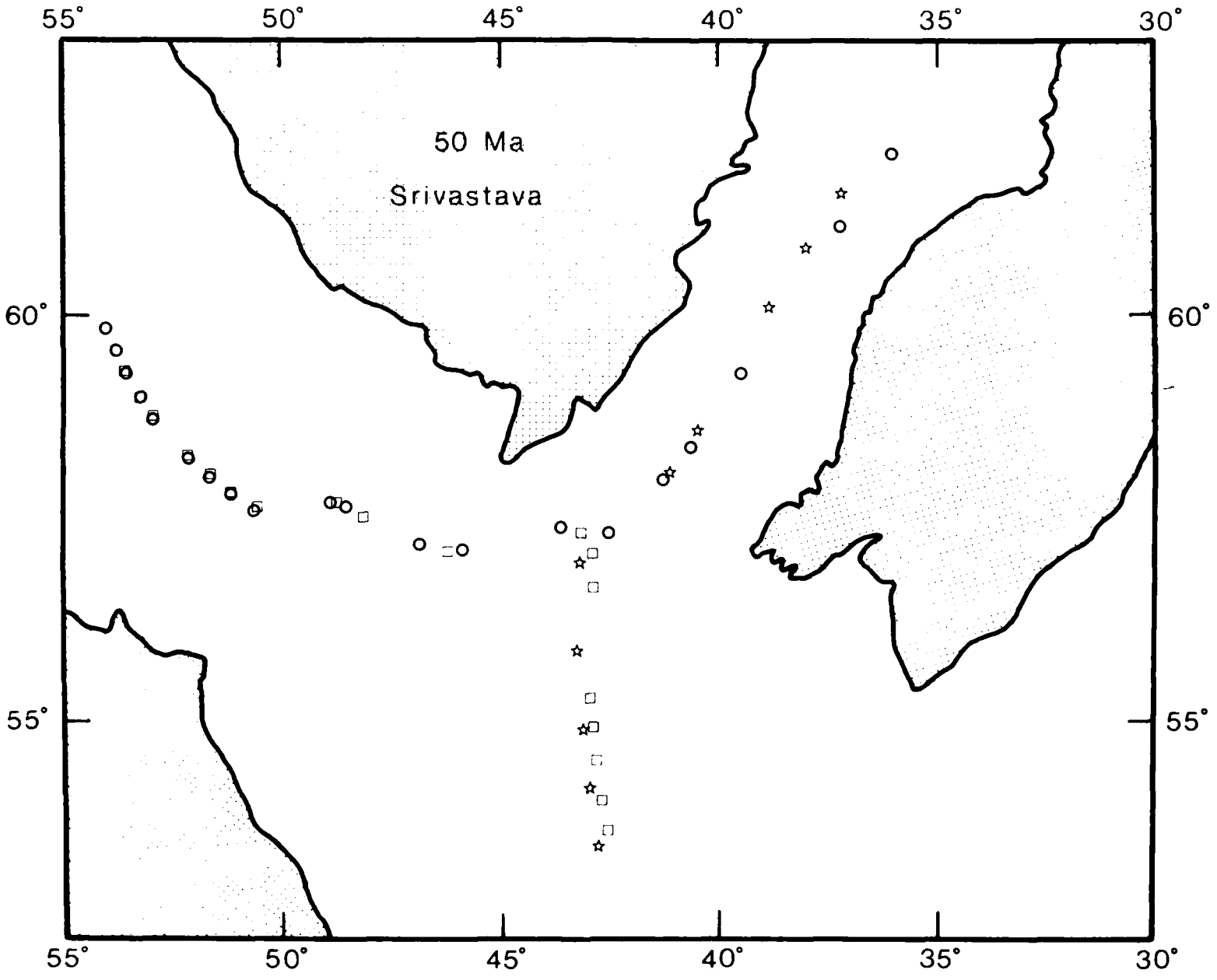
55°
50°
45°
40°
35°
30°
50 Ma
Srivastava
60°
55°

of finite rotations with a Greenland-North America pole close to that of Srivastava (Table 4). The other rotation poles have moved toward the northwest, as was the case for Anomaly 24. This yields a better reconstruction (Figure 9).

Figure 10 displays the uncertainty region of the Greenland-North America pole for the Anomaly 21 reconstruction. It is similar to that for Anomaly 24 (Figure 6), but shows two interesting facts. First, though the pole of Srivastava (1978) is within the acceptable region, it is close to its limits rather than along the axis of the ellipse. The difference between the two poles is more significant than is the case for the Anomaly 24 reconstructions. Second, and more striking, is the vast difference between the optimal rotations for the three plate system and the two plate system. The finite rotation which best fits Anomaly 21 in the Labrador Sea without regard to any data in the North Atlantic lies 40° away from the best pole for the three plate system (Table 4, Figure 10). Moreover, it is far more poorly constrained. This dramatically demonstrates the importance of using systems of several plates whenever possible to determine finite rotations.

DISCUSSION AND CAUTIONS

The examples discussed here demonstrate that the method presented in this paper provides a useful and powerful tool for determining the finite rotations necessary to best reconstruct multiple plate systems in plate tectonics. However, in using the computer program (Appendix), it is well to be wary of

FIGURE 9

A reconstruction of Anomaly 21 about the Labrador Sea triple junction using the rotations derived in this paper. Symbols are as in Figure 2.

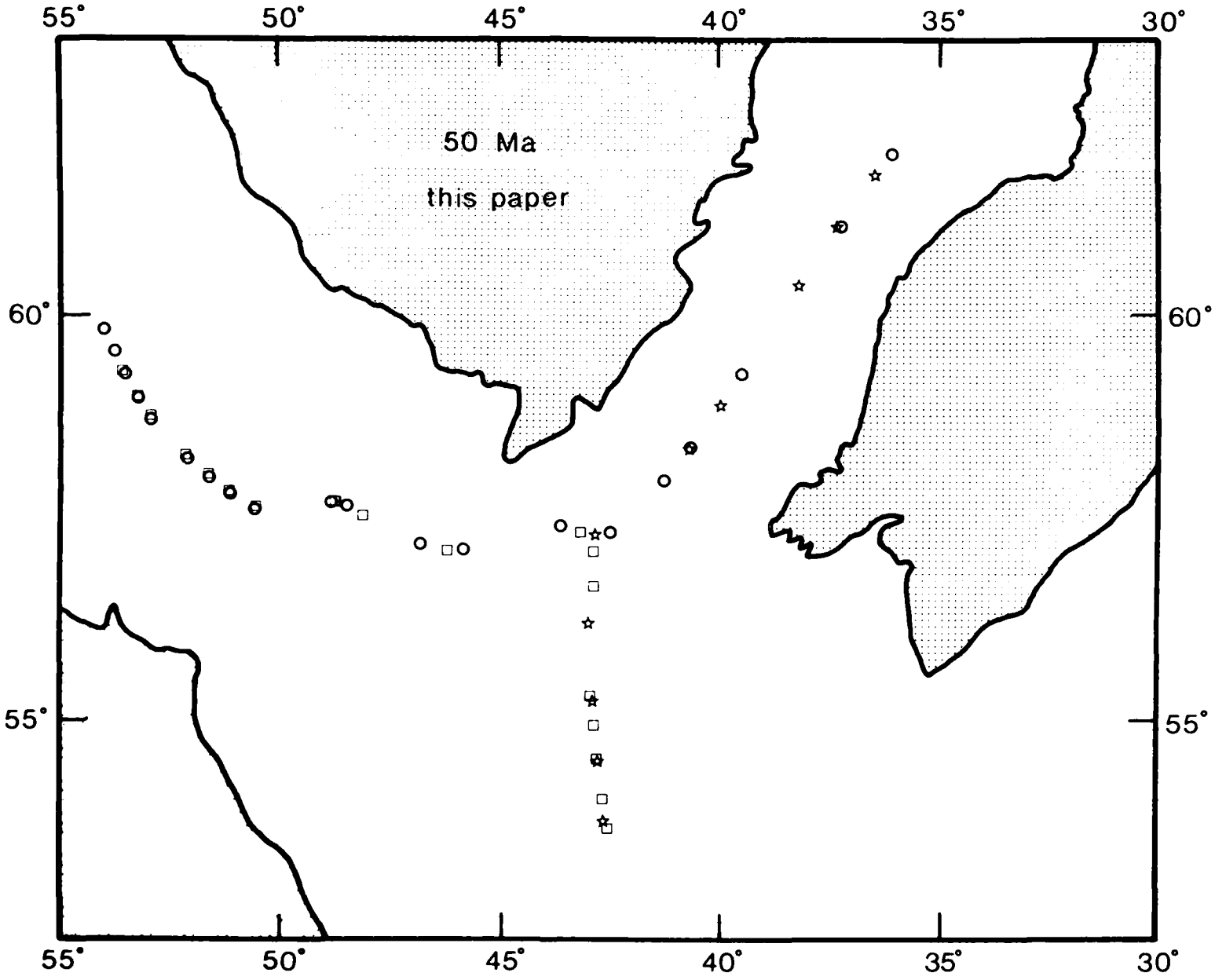
55°
50°
45°
40°
35°
30°
50 Ma
this paper
60°
55°

FIGURE 10

Regions of confidence for the Greenland-North America finite rotation poles for Anomaly 21. The continuous contour denotes the region of confidence for the pole derived in this paper for the three plate system, and the dashed contour is that for the two plates alone. The Greenland-North America finite rotation poles for Anomaly 21 discussed in the text are also shown. Continental coastlines are shown for scale and orientation.

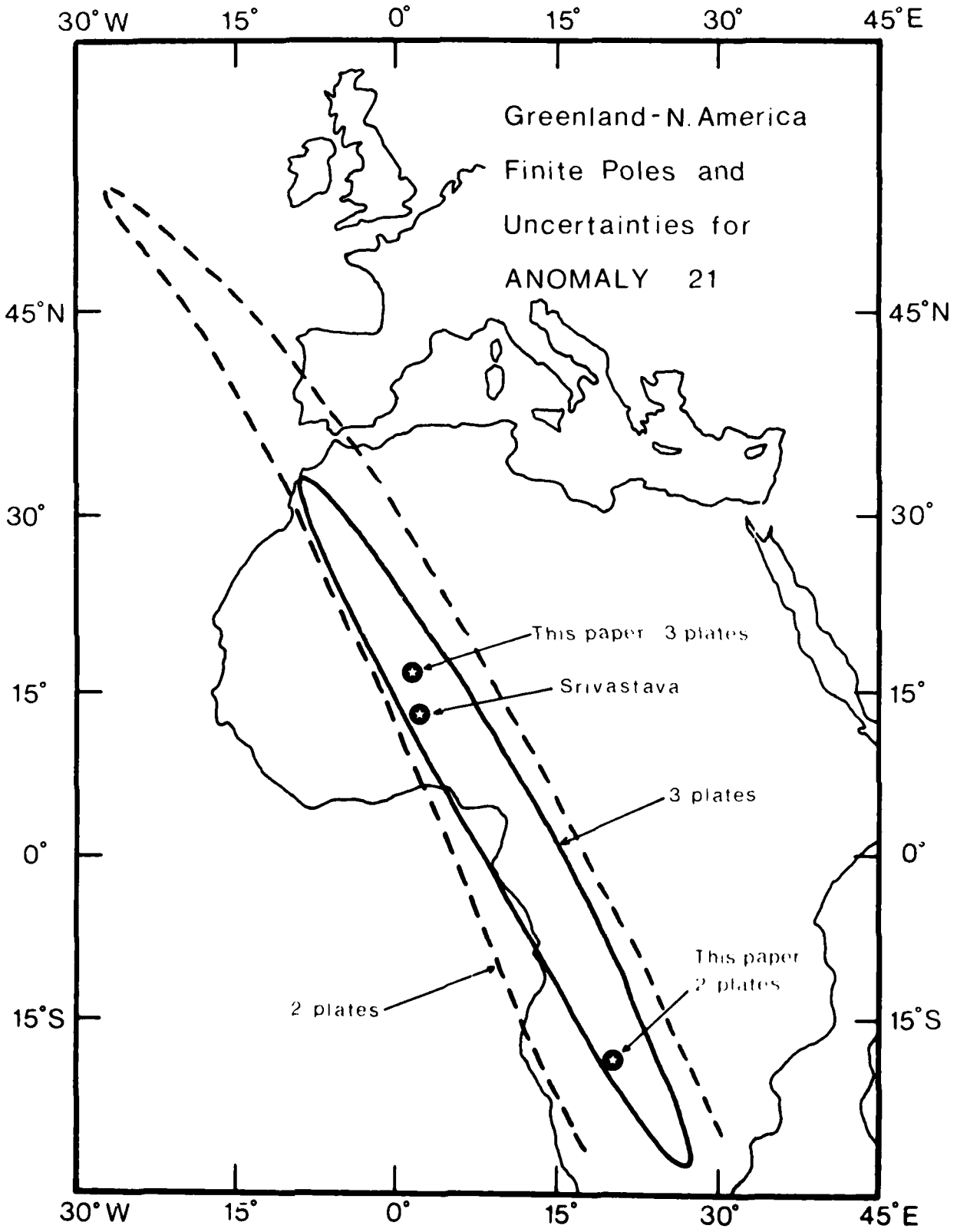
30°W
15°
0°
15°
30°
45°E
Greenland-N. America
Finite Poles and
Uncertainties for
ANOMALY 21
45°N
30°
15°
0°
15°S
This paper 3 plates
Srivastava
3 plates
This paper
2 plates
2 plates

several potential pitfalls.

In general, the measure of misfit varies smoothly when considered as a function of its six independent variables. Under some configurations of data, however, the measure may vary quite rapidly as a function of one or more of the variables, especially the rotation angles. When this is the case, the measure must be examined at suitably fine intervals of the variables. Moreover, the measure of misfit may have several local minima for some configurations of data. A survey of several poles can expose the problem if it exists. Finally, one must beware of a situation in which one of the finite rotations is small compared to the other two,in the sense that it is the difference between two rotations by nearly the same angle about nearly the same pole. As implied in the discussion of Hellinger (1979), this situation is unstable because a small perturbation in either of the two similar rotations can lead to a large change in the third rotation. Such a condition can also be an advantage, however, if the smaller rotation can be well-determined in its own right. This in turn can constrain the two larger rotations.

All the pitfalls may be safely avoided most easily if one first reconstructs each individual plate boundary and understands the problems associated with the fits of the separate plate pairs. The method presented in this paper, together with the two-plate finite rotation method of Hellinger (1979), enables one to discover reliable finite rotations to reconstruct the ancient positions of several plates, and to place limits on

their reliability. The method is applicable to a wide class of sea-floor spreading data and should prove generally useful in refining our knowledge of the tectonic history of the earth.

ACKNOWLEDGMENTS

I would like to thank J. G. Sclater for pointing me toward this problem and S. Hellinger for his invaluable help in many discussions. I also thank C. Denham, R. Detrick, P. Molnar, and H. Schouten for critically reviewing this manuscript. This work was supported by the Office of Naval Research contract N00014-75-C-0291 with the Massachusetts Institute of Technology.

REFERENCES

Bullard, E.C., J.E. Everett, and A.G. Smith, The fit of the continents around the Atlantic, Trans. Roy. Soc. London, Ser. A., 258, 41-51, 1965.

Johnson, G.L., and J. Egloff, Geophysical investigations of the west Reykjanes basin and southeast Greenland continental margin (abstract), Eos Trans. AGU, 54, 324, 1973.

Johnson, G.L., J. Egloff, J. Campsie, M. Rasmussen, F. Dittmer, and J. Freitag, Sediment distribution and crustal structure of the southern Labrador Sea, Bull. Geol. Soc. Denmark, 22, 7-24, 1972.

Hellinger, S., The statistics of finite rotations in plate tectonics, Ph.D. thesis, Mass. Inst. of Technol., 1979.

Kristoffersen, Y., and M. Talwani, The extinct triple junction south of Greenland and Tertiary motion of Greenland relative to North America, Bull. Geol. Soc. Amer., 88, 1037-1049, 1977.

Laughton, A.S., South Labrador Sea and the evolution of the North Atlantic, Nature, 232, 612, 1971.

McKenzie, D.P., and J.G. Sclater, The evolution of the Indian Ocean since the Late Cretaceous, Geophys. J. Roy. Astron. Soc., 25, 437-528, 1971.

Phillips, J.D., and C. Tapscott, The evolution of the Atlantic Ocean north of the Azores, in preparation.

Pilger, R.H., Jr., A method for finite plate reconstructions, with applications to Pacific-Nazca plate evolution, Geophys. Res. Lett., 5, 469-472, 1978.

Pitman, W.C., III, and M. Talwani, Sea-floor spreading in the North Atlantic, Bull. Geol. Soc. Amer., 83, 619-646, 1972.

Smith, A.G., and A. Hallam, The fit of the southern continents, Nature, 225, 139-144, 1970.

Srivastava, S.P., Evolution of the Labrador Sea and its bearing on the early evolution of the North Atlantic, Geophys. J. Roy. Astron. Soc., 52, 313-357, 1978.

Vogt, P.R., and O.E. Avery, Detailed magnetic surveys in the northeast Atlantic and Labrador Sea, J. Geophys. Res., 79, 363-389, 1974.

APPENDIX

```
C       PROGRAM PLATE3
C
C       ************************************************************************
C
C       PROGRAM PLATE3          JANUARY 1979          C.TAPSCOTT
C
C       THE PROGRAM ALLOWS ONE TO CALCULATE THE MEASURE OF FIT OF SEA-
C       FLOOR SPREADING DATA FOR A RECONSTRUCTION OF THREE PLATES AROUND A
C       TRIPLE JUNCTION, AND TO SEEK THE SET OF FINITE ROTATIONS DEFINING
C       THE BEST-FIT RECONSTRUCTION.
C
C       THE MEASURE OF FIT OF EACH PLATE PAIR IS CALCULATED ACCORDING TO
C       THE FITTING CRITERION PHI-0 OF HELLINGER (1979). THE TOTAL MEASURE
C       FOR THE RECONSTRUCTION IS THE SUM OF THE MEASURES OF THE PLATE
C       PAIRS.
C
C       ONE SPECIFIES TWO OF THE INITIAL FINITE RELATIVE ROTATIONS. THE
C       THIRD IS CALCULATED BY REQUIRING THE CYCLIC PRODUCT TO BE UNITY.
C
C       DATA ON EACH PLATE ALONG EACH PLATE BOUNDARY ARE SUBDIVIDED INTO
C       CORRESPONDING SECTIONS, EACH OF WHICH MAY BE WELL-APPROXIMATED BY
C       A GREAT CIRCLE (HELLINGER, 1979).
C
C       EACH DATUM HAS ASSOCIATED WITH IT AN UNCERTAINTY IN LOCATION,
C       DEFINED BY A STANDARD DEVIATION EXPRESSED IN KILOMETERS. IN THE
C       CALCULATION OF THE MEASURE, EACH DATUM IS WEIGHTED BY THE INVERSE
C       OF THE SQUARE OF ITS STANDARD DEVIATION OF ERROR.
C
C       REFERENCE:
C
C       HELLINGER, S., THE STATISTICS OF FINITE ROTATIONS IN PLATE
C            TECTONICS, PH. D. THESIS, MASS. INST. OF TECHNOL., 1979.
C
C       ************************************************************************
C
C       OPERATION:
C
C       ALL INPUT ON DEVICE 1.
C       ALL OUTPUT ON DEVICE 108 (LINE PRINTER).
C
C       ALL INPUT IS IN FREE-FIELD FORMAT (G FORMAT).
C
C
C       INPUT:
C
C       READ (NSECT(I),I=1,3),WFACTR,IPUT IN (5G) FORMAT.
C
C            NSECT(I)      THE NUMBER OF SECTIONS FOR PLATE BOUNDARY I.
C                          AT PRESENT, THE PROGRAM IS LIMITED TO NO MORE
C                          THAN TEN SECTIONS PER BOUNDARY.
```

```
C
C          WFACTR        ARBITRARY SCALING FACTOR TO KEEP THE MAGNITUDE
C                        OF THE VARIANCES NEAR 1.  DEFAULT VALUE = 100.
C
C          IPUT          IF IPUT = 0, INPUT DATA POINTS ARE LISTED.
C                        OTHERWISE, POINTS ARE NOT LISTED.  DEFAULT = 0.
C
C     READ DATA POINTS (ALAT(I),ALON(I),AERR(I),I=1,5) IN (15G) FORMAT.
C
C          LATITUDE AND LONGITUDE IN DECIMAL DEGREES (POSITIVE NORTH AND
C          EAST), AND ERROR IN KILOMETERS.
C
C          THE FIRST RECORD IS POINTS OF BOUNDARY 1, PLATE 1, SECTION 1.
C          THE SECOND IS POINTS OF       BOUNDARY 1, PLATE 1, SECTION 2.
C          ETC.
C          THEN                          BOUNDARY 1, PLATE 2, SECTION 1.
C                                        BOUNDARY 1, PLATE 2, SECTION 2.
C          ETC.
C          THEN THE SAME FOR BOUNDARY 2, AND THEN BOUNDARY 3.
C
C          AT PRESENT, THE PROGRAM IS LIMITED TO NO MORE THAN FIVE
C          POINTS PER SECTION FOR EACH PLATE (AND EACH BOUNDARY).
C
C          IF A GIVEN SECTION FOR A GIVEN PLATE AND BOUNDARY CONTAINS
C          FEWER THAN FIVE POINTS, THE STRING MUST BE TERMINATED BY A
C          DUMMY POINT WITH A LATITUDE GREATER THAN 90. OR A ZERO ERROR.
C
C     READ THE OPTION NUMBER IN (1G) FORMAT.
C
C          SEE BELOW FOR DESCRIPTIONS OF THE OPTIONS.
C
C     READ THE INITIAL ROTATIONS FOR BOUNDARIES 1 AND 2 IN (6G) FORMAT.
C
C          LATITUDE, LONGITUDE, ANGLE, LATITUDE, LONGITUDE, ANGLE.
C
C          THE PROGRAM WILL COMPUTE THE RESULTANT THIRD ROTATION.
C
C
C     OTHER INPUT FOLLOWS FOR SOME OF THE OPTIONS.
C
C
C     OPTION 1.
C
C     FOR THE GIVEN SET OF ROTATIONS, COMPUTE AND OUTPUT THE MEASURE FOR
C     EACH OF THE BOUNDARIES, AND THE TOTAL MEASURE.
C
C
C     OPTION -1.
C
C     THE SAME AS OPTION 1, EXCEPT THAT A DECOMPOSITION OF THE MEASURE
```

```
C     IS ALSO OUTPUT.
C
C     THE DECOMPOSITION CONSISTS OF THE EIGENVECTOR AND MEASURE OF EACH
C     SECTION, AND THE DEVIATION OF EACH POINT (RELATIVE TO ITS ERROR)
C     FROM THE BEST-FIT GREAT CIRCLE FOR ITS SECTION.
C
C
C     OPTION 2.
C
C     KEEPING THE FIRST ROTATION CONSTANT AND FIXING THE POLE OF THE
C     SECOND ROTATION, FIND THE ANGLE FOR THE SECOND ROTATION THAT
C     MINIMIZES THE MEASURE.
C
C          INPUT:
C
C               READ THE LARGER AND SMALLER INCREMENTS OF THE ANGLE
C               SEARCH AND THE HALF-RANGE OF THE ANGLE SEARCH IN (3G)
C               FORMAT.
C
C
C     OPTION -2.
C
C     THE SAME AS OPTION 2, EXCEPT THAT A DECOMPOSITION OF THE MEASURE
C     IS GIVEN FOR THE RESULT.
C
C
C     OPTION 3.
C
C     FIXING THE POLES OF THE FIRST AND SECOND ROTATIONS, SEARCH FOR THE
C     COMBINATION OF ROTATION ANGLES THAT MINIMIZES THE MEASURE.
C
C          INPUT:
C
C               AS IN OPTION 2.
C
C
C     OPTION -3.
C
C     THE SAME AS OPTION 3, EXCEPT THAT A DECOMPOSITION OF THE MEASURE
C     IS GIVEN FOR THE RESULT.
C
C
C     OPTION 4.
C
C     FIXING THE POLE OF THE FIRST ROTATION, SEARCH FOR THE COMBINATION
C     OF FIRST ROTATION ANGLE AND SECOND ROTATION POLE AND ANGLE THAT
C     MINIMIZES THE MEASURE.
C
C     THE PROGRAM SEARCHES A HEXAGONAL GRID OF SPECIFIED RADIUS ABOUT
C     THE STARTING POLE, RECENTERS THE GRID ON THE POLE GIVING THE BEST
```

```
C     MEASURE, AND REPEATS. IF THE BEST POLE IS IN THE CENTER OF THE
C     GRID, THE GRID IS REDUCED BY THE SPECIFIED FACTOR. THE SEARCH
C     PROCEEDS UNTIL THE GRID IS SMALLER THAN THE SPECIFIED LIMIT.
C
C     STEP NUMBER AND BEST RESULT ARE OUTPUT FOR EACH GRID.
C
C          INPUT:
C
C                GRID SEARCH PARAMETERS IN (3G) FORMAT.
C
C                     LARGEST AND SMALLEST GRID RADII IN DEGREES, AND
C                     GRID SIZE DECREASE FACTOR (DEFAULT VALUE = 0.5).
C
C                ANGLE SEARCH PARAMETERS IN (3G) FORMAT.
C
C                     AS IN OPTION 2.
C
C
C     OPTION -4.
C
C     THE SAME AS OPTION 4, EXCEPT THAT A DECOMPOSITION OF THE MEASURE
C     IS GIVEN FOR THE RESULT.
C
C
C     OPTION 5.
C
C     SIMILAR TO OPTION 4, BUT THE PROGRAM SEARCHES FOR THE BEST
C     COMBINATION OF POLES AND ANGLES FOR BOTH ROTATIONS.
C
C     THE RADII OF THE SEARCH GRIDS ARE REDUCED WHEN BOTH POLES OF THE
C     BEST-MEASURE COMBINATION LIE IN THE CENTERS OF THEIR RESPECTIVE
C     GRIDS.
C
C          INPUT:
C
C                AS IN OPTION 4.
C
C
C     OPTION -5.
C
C     THE SAME AS OPTION 5, EXCEPT THAT A DECOMPOSITION OF THE MEASURE
C     IS GIVEN FOR THE RESULT.
C
C
C     OPTION 6.
C
C     FIXING THE SECOND POLE, THE PROGRAM EXPLORES A LATITUDE-LONGITUDE
C     GRID FOR THE FIRST POLE, FINDING THE BEST COMBINATION OF ROTATION
C     ANGLES FOR EACH POLE OF THE GRID AND LISTING THE RESULT.
C
```

```
C           INPUT:
C
C                   READ THE GRID PARAMETERS IN (6G) FORMAT.
C
C                        LEAST LATITUDE, GREATEST LATITUDE, LATITUDE
C                        INCREMENT, LEAST LONGITUDE, GREATEST LONGITUDE,
C                        LONGITUDE INCREMENT.
C
C                   READ THE ANGLE SEARCH PARAMETERS IN (3G) FORMAT.
C
C                        AS IN OPTION 2.
C
C
C      OPTION -6.
C
C      SIMILAR TO OPTION 6, BUT FOR EACH POLE OF THE GRID, THE PROGRAM
C      SEARCHES FOR THE BEST SECOND ROTATION AS IN OPTION 4.
C
C           INPUT:
C
C                   LATITUDE-LONGITUDE GRID PARAMETERS IN (6G) FORMAT.
C
C                        AS IN OPTION 6.
C
C                   GRID SEARCH PARAMETERS IN (3G) FORMAT.
C
C                        AS IN OPTION 4.
C
C                   ANGLE SEARCH PARAMETERS IN (3G) FORMAT.
C
C                        AS IN OPTION 2.
C
C      ************************************************************
C
C
C      AFTER PERFORMING ITS TASK, THE PROGRAM IS READY TO READ ANOTHER
C      OPTION NUMBER AND CONTINUE.
C
C      AN OPTION GREATER THAN 90 WILL TERMINATE THE PROGRAM.
C
C      ************************************************************
C
C      MESSAGES:
C
C
C      * BEST ANGLE AT END OF RANGE *
C
C           IN THE COARSE SEARCH OF ROTATION ANGLES, THE BEST MEASURE WAS
C           ACHIEVED WITH AN ANGLE AT THE LIMIT OF THE HALF-RANGE.
C
```

AD-A089 103 WOODS HOLE OCEANOGRAPHIC INSTITUTION MASS F/G 8/7
THE EVOLUTION OF THE INDIAN OCEAN TRIPLE JUNCTION AND THE FINIT--ETC(U)
SEP 80 C R TAPSCOTT N00014-74-C-0262
UNCLASSIFIED WHOI-80-37 NL

3 of 3
AD A089103

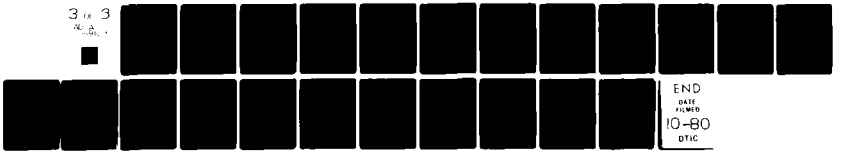

END
DATE FILMED
10-80
DTIC

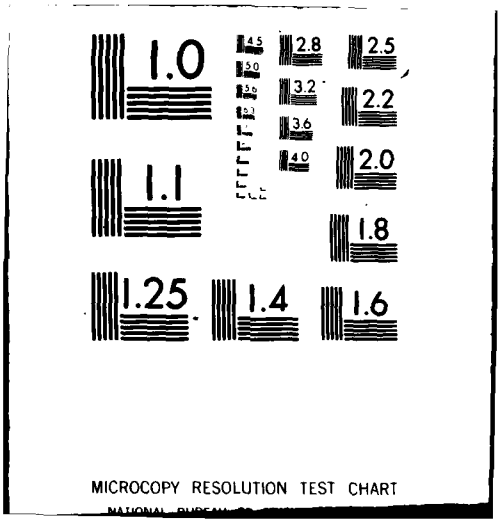
1.0
1.1
1.25
1.4
1.6
1.8
2.0
2.2
2.5
2.8
3.2
3.6
4.0
4.5
5.0
MICROCOPY RESOLUTION TEST CHART

```
C
C      * DOUBLY DEGENERATE MATRIX POSSIBLE *
C
C           THE BEST-FIT GREAT CIRCLE FOR A SECTION IS POORLY DETERMINED,
C           AND MAY BE IN ERROR.  BOUNDARY AND SECTION ARE GIVEN.
C
C
C      * NOT THREE UNEQUAL ROOTS *
C
C           THE ROTATION PRODUCES A COVARIANCE MATRIX FOR A SECTION THAT
C           DOES NOT HAVE THREE UNEQUAL REAL EIGENVALUES.  IT IS NOT
C           POSSIBLE TO COMPUTE THE BEST-FIT GREAT CIRCLE. BOUNDARY AND
C           SECTION ARE GIVEN.
C
C      ************************************************************************
C
C
C      PROGRAM PLATE3
C
C
C      ************************************************************************
C
      IMPLICIT DOUBLE PRECISION (A-H,O-Z)
C
      COMMON/XMAIN/ DATA(3,5,10,2,3),SIGMA(5,10,2,3),WT(5,10,2,3),
     Z NPTS(10,2,3),NSECT(3)
      COMMON/SUB1/ P(3,10,3)
      COMMON/SUB2/ EP(10,3)
      COMMON/SUB3/ DMESUR(10,3),SMESUR(3),XFACTR
      COMMON/SUB4/ RM(3,3,3)
      DIMENSION AROT(3,3),SROT(3)
      DATA RAD,RKM/1.7453292519943300-02,1.5695390-04/
      DATA IIN,IOUT/1,108/
C
      WRITE(IOUT,1)
    1 FORMAT(///1X,'PROGRAM PLATE3',10X,'JANUARY 1979',10X,
     Z 'C.TAPSCOTT',/)
C
C     READ NUMBER OF SECTIONS FOR THREE PLATE BOUNDARIES, AND READ
C     WFACTR.
C
      READ(IIN,2) (NSECT(I),I=1,3),WFACTR,IPUT
    2 FORMAT(5G)
      IF (WFACTR .LT. 0.1) WFACTR=100.
      XFACTR=RKM*RKM*WFACTR
C
C     READ THE DATA INTO THE DATA ARRAY.
C
      CALL GETEM(WFACTR,IPUT)
C
```

```
C     READ THE OPTION CODE AND READ THE STARTING ROTATIONS.
C
  999 READ(IIN,3) NOP
    3 FORMAT(1G)
      IF (NOP .GT. 90) GO TO 1000
      NCOMP=0
      IF (NOP .LT. 0) NCOMP=1
      WRITE(IOUT,4) NOP
    4 FORMAT(//1X,'OPTION = ',I3)
      NOP=IABS(NOP)
C
      READ(IIN,5) ((AROT(I,J),I=1,3),J=1,2)
    5 FORMAT(6G)
      IF ((DABS(AROT(1,1)) .GT. 90.) .OR. (DABS(AROT(1,2)) .GT. 90.))
     Z GO TO 1000
C
C     COMPUTE THE THIRD ROTATION AND THE MEASURE, AND WRITE THEM.
C
      CALL RSUM(0,AROT)
      CALL MEASUR(0,SUM)
      CALL PUTEM(0,AROT,SMESUR,SUM)
C
C     GO TO THE PROPER OPTION.
C
      GO TO (100,200,200,300,300,400), NOP
C
C     OPTION 1.  COMPUTE THE MEASURE FOR GIVEN ROTATIONS.
C
  100 IF (NCOMP .NE. 0) CALL DECOMP
      GO TO 999
C
C     OPTIONS 2 AND 3.  FIND THE BEST ANGLES FOR 1 OR 2 OF THE GIVEN
C     POLES.
C
C     READ THE ANGULAR SEARCH PARAMETERS.
C
  200 READ(IIN,20) ALARG,ASMAL,ARANG
   20 FORMAT(3G)
      ALARG=DABS(ALARG)
      ASMAL=DABS(ASMAL)
      ARANG=DABS(ARANG)
      IF (ALARG .LT. 1.0D-05) GO TO 1000
      IF (ASMAL .GE. ALARG) ASMAL=0.
      IF (ARANG .LT. ALARG) ARANG=ALARG
C
      GO TO (201,201,201,301,301,401), NOP
C
  201 WRITE(IOUT,21) ALARG,ASMAL,ARANG
   21 FORMAT(//1X,'ANGLE SEARCH: LARGER STEP    ',F8.3/15X,
     Z 'SMALLER STEP   ',F8.3/15X,'RANGE',10X,F8.3)
```

```
C
      CALL SANGL((3-NOP),AROT,ALARG,ASMAL,ARANG,SUM,1)
C
      K=NOP-2
      WRITE(IOUT,22) K
   22 FORMAT(//1X,'BEST ANGLES FOR BOUNDARIES ',I1,' 2 3')
      CALL PUTEM(0,AROT,SMESUR,SUM)
      IF (NCOMP .NE. 0) CALL DECOMP
      GO TO 999
C
C     OPTIONS 4 AND 5.  SEARCH ONE OR BOTH POLES.
C
  300 READ(IIN,20) XLARG,XSMAL,XMULT
      XLARG=DABS(XLARG)
      XSMAL=DABS(XSMAL)
      XMULT=DABS(XMULT)
      IF ((XLARG .GT. 90.) .OR. (XLARG .LT. 1.0D-05)) GO TO 1000
      IF ((XSMAL .GT. XLARG) .OR. (XSMAL .LT. 1.0D-05)) XSMAL=XLARG
      IF (XMULT .GE. 1.) XMULT=0.
      GO TO 200
C
  301 WRITE(IOUT,30) XLARG,ALARG,XSMAL,ASMAL,XMULT,ARANG
   30 FORMAT(//1X,'POLE SEARCH:',/3X,'LARGEST STEPS  ',2(2X,F8.3),/3X,
     Z 'SMALLEST STEPS ',2(2X,F8.3),/3X,'FACTOR AND RANGE ',2(F8.3,2X))
C
      CALL SPOL((5-NOP),AROT,XLARG,XSMAL,XMULT,ALARG,ASMAL,ARANG,SUM,1)
C
      IF (NCOMP .NE. 0) CALL DECOMP
      GO TO 999
C
C     OPTION 6.  EXPLORE A GRID FOR THE FIRST POLE.  EITHER FIX THE
C     LOCATION OF THE SECOND POLE, OR SEARCH FOR THE BEST FIT.
C
C     READ THE GRID PARAMETERS.
C
  400 READ(IIN,5) BOT,TOP,VSTEP,XLEFT,RIGHT,HSTEP
      WRITE(IOUT,40) BOT,TOP,VSTEP,XLEFT,RIGHT,HSTEP
   40 FORMAT(//1X,'GRID:',20X,'LIMITS',7X,'GRID SIZE',/6X,'LATITUDE',
     Z 4X,3(2X,F8.3),/6X,'LONGITUDE',3X,3(2X,F8.3))
C
C     READ THE POLE SEARCH PARAMETERS IF NECESSARY, AND READ THE ANGULAR
C     SEARCH PARAMETERS.
C
      IF (NCOMP .EQ. 0) GO TO 200
      GO TO 300
C
  401 IF (NCOMP .EQ. 0) WRITE(IOUT,21) ALARG,ASMAL,ARANG; GO TO 402
      WRITE(IOUT,30) XLARG,ALARG,XSMAL,ASMAL,XMULT,ARANG
C
  402 NV=(TOP-BOT)/VSTEP
```

```
      NH=(RIGHT-XLEFT)/HSTEP
C
      DO 600 IV=0,NV
      AROT(1,1)=BOT+VSTEP*FLOAT(IV)
C
      DO 500 IH=0,NH
      AROT(2,1)=XLEFT+HSTEP*FLOAT(IH)
      IF (NCOMP .NE. 0) GO TO 450
C
      CALL SANGL(0,AROT,ALARG,ASMAL,ARANG,SUM,0)
      CALL PUTEM(IH,AROT,SMESUR,SUM)
      GO TO 490
C
  450 CALL SPOL(1,AROT,XLARG,XSMAL,XMULT,ALARG,ASMAL,ARANG,SUM,0)
C
  490 IF (IH .NE. 0) GO TO 500
      SANG=AROT(3,1)
      DO 491 I=1,3
  491 SROT(I)=AROT(I,2)
C
  500 CONTINUE
C
      AROT(3,1)=SANG
      DO 501 I=1,3
  501 AROT(I,2)=SROT(I)
C
  600 CONTINUE
      GO TO 999
C
 1000 WRITE(IOUT,1001)
 1001 FORMAT(//)
      STOP
      END
C
C     ******************************************************************
C
      SUBROUTINE DECOMP
C
C     SUBROUTINE DECOMP          JANUARY 1979          C.TAPSCOTT
C
C     THE SUBROUTINE COMPUTES AND WRITES THE QUANTITIES INVOLVED IN
C     THE DECOMPOSITION OF THE MEASURE.
C
      IMPLICIT DOUBLE PRECISION (A-H,O-Z)
C
      COMMON/XMAIN/ DATA(3,5,10,2,3),SIGMA(5,10,2,3),WT(5,10,2,3),
     Z NPTS(10,2,3),NSECT(3)
      COMMON/SUB1/ P(3,10,3)
      COMMON/SUB3/ DMESUR(10,3),SMESUR(3),XFACTR
      COMMON/SUB4/ RM(3,3,3)
```

```
      DIMENSION DEV(5),T(3)
      DATA RAD,RKM,DKM/1.745329251994330D-02,1.569539D-04,1.112D+02/
      DATA IOUT/108/
C
      WRITE(IOUT,1)
    1 FORMAT(//1X,'DECOMPOSITION OF MEASURE',//5X,
     Z'MEASURE = SUM OF SQ. DEV. OF POINTS (REL. TO ST. DEV. OF ERROR)')
      WRITE(IOUT,2)
    2 FORMAT(/24X,'EIGENVECTOR',/1X,
     Z 'BOUNDARY SECTION   LATITUDE  LONGITUDE    MEASURE')
C
      DO 100 IB=1,3
      WRITE(IOUT,10)
   10 FORMAT(' ')
      DO 100 IS=1,NSECT(IB)
C
      PLAT=DASIN(P(3,IS,IB))/RAD
      PLON=DATAN2(P(2,IS,IB),P(1,IS,IB))/RAD
C
      D=DMESUR(IS,IB)/XFACTR
      WRITE(IOUT,11) IB,IS,PLAT,PLON,D
   11 FORMAT(4X,I1,7X,I2,6X,2(F8.3,2X),D12.6)
C
  100 CONTINUE
C
      WRITE(IOUT,3)
    3 FORMAT(/5X,'DEV. OF POINTS FROM GREAT CIRCLE (REL. TO ST. DEV. OF
     ZERROR)')
      WRITE(IOUT,4) (I,I=1,5)
    4 FORMAT(/1X,'BNDRY SECT PLATE',5(5X,'PT.',I1,1X))
C
      DO 400 IB=1,3
      WRITE(IOUT,10)
      DO 400 IS=1,NSECT(IB)
C
      NA=NPTS(IS,1,IB)
      DO 200 J=1,NA
      DEV(J)=DATA(1,J,IS,1,IB)*P(1,IS,IB)+DATA(2,J,IS,1,IB)*P(2,IS,IB)+
     Z DATA(3,J,IS,1,IB)*P(3,IS,IB)
      DEV(J)=DACOS(DEV(J))/RAD-90.
  200 DEV(J)=DEV(J)*DKM*RKM/SIGMA(J,IS,1,IB)
C
      K=1
      IF (IB .EQ. 3) K=2
      WRITE(IOUT,21) IB,IS,K,(DEV(J),J=1,NA)
   21 FORMAT(3X,I1,4X,I2,4X,I1,5X,5(F8.3,2X))
C
      NA=NPTS(IS,2,IB)
      DO 300 J=1,NA
      CALL ROTATE(RM(1,1,IB),DATA(1,J,IS,2,IB),T)
```

```
      DEV(J)=T(1)*P(1,IS,IB)+T(2)*P(2,IS,IB)+T(3)*P(3,IS,IB)
      DEV(J)=DACOS(DEV(J))/RAD-90.
  300 DEV(J)=DEV(J)*DKM*RKM/SIGMA(J,IS,2,IB)
C
      K=3
      IF (IB .EQ. 1) K=2
      WRITE(IOUT,21) IB,IS,K,(DEV(J),J=1,NA)
C
  400 CONTINUE
C
      RETURN
      END
C
C     ****************************************************************
C
      SUBROUTINE SPOL(N,AROT,XL,XS,XM,AL,AS,AR,FSUM,ISUM)
C
C     SUBROUTINE SPOL          JANUARY 1979          C.TAPSCOTT
C
C     THE SUBROUTINE SEARCHES FOR THE BEST PAIR OF POLES AND ANGLES IN
C     HEXAGONAL GRIDS DECREASING IN SIZE BY FACTOR XM FROM XL TO XS.
C     IF N .NE. 0 ONLY THE SECOND POLE IS VARIED.
C
      IMPLICIT DOUBLE PRECISION (A-H,O-Z)
C
      COMMON/SUB3/ DMESUR(10,3),SMESUR(3),XFACTR
      DIMENSION AROT(3,3),R(3,3),PLAT(7,2),PLON(7,2)
      DIMENSION IACODE(7),IBCODE(7)
      DATA IOUT/108/
C
      M=N
      IF (M .NE. 0) M=1
      M=M+1
      IF (ISUM .NE. 0) GO TO 1
      CALL RSUM(0,AROT)
      CALL MEASUR(0,FSUM)
C
    1 SIZE=XL
      NSTEP=0
      IA=1
      ITA=1
      ITB=1
      DO 100 I=1,3
      DO 100 J=1,2
  100 R(I,J)=AROT(I,J)
      WRITE(IOUT,10)
   10 FORMAT(/1X,'BOUNDARY LATITUDE  LONGITUDE   ANGLE',6X,
     Z 'MEASURE    TOTAL MEASURE')
      DO 101 I=1,7
      IACODE(I)=0
```

```
  101 IBCODE(I)=0
C
      GO TO (200,201), M
C
  200 CALL PSET(SIZE,AROT(1,1),AROT(2,1),PLAT(1,1),PLON(1,1))
  201 CALL PSET(SIZE,AROT(1,2),AROT(2,2),PLAT(1,2),PLON(1,2))
      GO TO (300,301), M
C
  300 DO 401 IA=1,7
      R(1,1)=PLAT(IA,1)
      R(2,1)=PLON(IA,1)
C
  301 DO 400 IB=1,7
      IF ((IACODE(IA) .NE. 0) .AND. (IBCODE(IB) .NE. 0)) GO TO 400
      R(1,2)=PLAT(IB,2)
      R(2,2)=PLON(IB,2)
C
      CALL SANGL(0,R,AL,AS,AR,SUM,0)
C
      IF (FSUM .LE. SUM) GO TO 400
      ITA=IA
      ITB=IB
      FSUM=SUM
      DO 302 I=1,3
      DO 302 J=1,2
  302 AROT(I,J)=R(I,J)
C
  400 CONTINUE
      GO TO (401,402), M
  401 CONTINUE
C
  402 NSTEP=NSTEP+1
      CALL RSUM(0,AROT)
      CALL MEASUR(0,FSUM)
C
      ITC=ITA*ITB
      IF (ITC .NE. 1) GO TO 500
      SIZE=SIZE*XM
      IF (SIZE .GE. XS) GO TO 500
      WRITE(IOUT,50)
   50 FORMAT(/1X,'SEARCH STOPPED')
  500 WRITE(IOUT,51) NSTEP
   51 FORMAT(/1X,'STEP',I5)
      CALL PUTEM(1,AROT,SMESUR,FSUM)
      IF (SIZE .LT. XS) GO TO 1000
C
      GO TO (600,601), M
C
  600 IF ((ITC .EQ. 1) .OR. (ITA .NE. 1)) CALL PSET(SIZE,AROT(1,1),
     Z AROT(2,1),PLAT(1,1),PLON(1,1))
```

```
  601 CALL ISET(ITC,ITA,IACODE)
C
      IF ((ITC .EQ. 1) .OR. (ITB .NE. 1)) CALL PSET(SIZE,AROT(1,2),
     Z AROT(2,2),PLAT(1,2),PLON(1,2))
      CALL ISET(ITC,ITB,IBCODE)
C
      ITA=1
      ITB=1
      GO TO (300,301), M
C
 1000 RETURN
      END
C
C     ***************************************************************
C
      SUBROUTINE SANGL(N,AROT,AL,AS,AR,FSUM,ISUM)
C
C     SUBROUTINE SANGL          JANUARY 1979          C.TAPSCOTT
C
C     THE SUBROUTINE SEARCHES FOR THE BEST COMBINATION AF ANGLES FOR THE
C     GIVEN POLES.  IF N .NE. 0 THEN ONLY THE ANGLE OF THE SECOND POLE
C     IS VARIED.
C
      IMPLICIT DOUBLE PRECISION (A-H,O-Z)
C
      DIMENSION AROT(3,3),R(3,3),C(2)
      DATA IOUT/108/
C
      M=N
      IF (M .NE. 0) M=1
      IF (ISUM .NE. 0) GO TO 1
      CALL RSUM(0,AROT)
      CALL MEASUR(0,FSUM)
C
    1 ITA=0
      ITB=0
      IA=0
      DIF=AL
      NL=AR/AL
      IF (NL .EQ. 0) NL=1
      IF (AS .LT. 1.0D-05) NS=0; GO TO 100
      NS=1.5*AL/AS
      IF (AS .GE. AL) NS=0
C
  100 LTIME=1
      DO 101 J=1,2
      DO 101 I=1,3
  101 R(I,J)=AROT(I,J)
C
  999 C(1)=AROT(3,1)
```

```
      C(2)=AROT(3,2)
      IF (M .NE. 0) GO TO 102
C
      DO 201 IA=-NL,NL
      R(3,1)=C(1)+FLOAT(IA)*DIF
C
  102 DO 200 IB=-NL,NL
      R(3,2)=C(2)+FLOAT(IB)*DIF
C
      MM=1
      IF ((M .EQ. 0) .AND. (IB .EQ. -NL)) MM=0
      CALL RSUM(MM,R)
      CALL MEASUR(MM,SUM)
      IF (FSUM .LE. SUM) GO TO 200
C
      AROT(3,2)=R(3,2)
      IF (M .EQ. 0) AROT(3,1)=R(3,1)
      DO 103 I=1,3
  103 AROT(I,3)=R(I,3)
      FSUM=SUM
      ITA=IABS(IA)
      ITB=IABS(IB)
C
  200 CONTINUE
      IF (M .NE. 0) GO TO 202
  201 CONTINUE
C
  202 GO TO (300,400) LTIME
C
  300 IF ((ITA .EQ. NL) .OR. (ITB .EQ. NL)) WRITE(IOUT,30)
   30 FORMAT(/1X,'* BEST ANGLE AT END OF RANGE *')
      IF (NS .EQ. 0) GO TO 400
      NL=NS
      DIF=AS
      LTIME=2
      GO TO 999
C
  400 CALL RSUM(M,AROT)
      CALL MEASUR(M,FSUM)
C
      RETURN
      END
C
C     ******************************************************************
C
      SUBROUTINE MEASUR(N,SUM)
C
C     SUBROUTINE MEASUR          JANUARY 1979          C.TAPSCOTT
C
C     THE SUBROUTINE CALCULATES THE MEASURE OF FIT FOR EACH BOUNDARY,
```

```
C     EXCEPTING BOUNDARY N, FOR THE ROTATION MATRICES RM.  THESE ARE
C     SUMMED TO OBTAIN THE OVERALL MEASURE, ACCORDING TO S.HELLINGER'S
C     CRITERION PHI-0.
C
      IMPLICIT DOUBLE PRECISION (A-H,O-Z)
C
      COMMON/XMAIN/ DATA(3,5,10,2,3),SIGMA(5,10,2,3),WT(5,10,2,3),
     Z NPTS(10,2,3),NSECT(3)
      COMMON/SUB1/ P(3,10,3)
      COMMON/SUB2/ EP(10,3)
      COMMON/SUB3/ DMESUR(10,3),SMESUR(3),XFACTR
      COMMON/SUB4/ RM(3,3,3)
      DIMENSION DMERGE(3,10),WMERGE(10)
      DATA IOUT/108/
C
      DO 300 IB=1,3
      IF (N .EQ. IB) GO TO 300
C
      SMESUR(IB)=0.
      DO 200 K=1,NSECT(IB)
C
      NA=NPTS(K,1,IB)
      DO 100 I=1,NA
      WMERGE(I)=WT(1,K,1,IB)
      DO 100 J=1,3
  100 DMERGE(J,I)=DATA(J,I,K,1,IB)
C
      NB=NPTS(K,2,IB)
      DO 101 I=1,NB
      WMERGE(I+NA)=WT(I,K,2,IB)
  101 CALL ROTATE(RM(1,1,IB),DATA(1,I,K,2,IB),DMERGE(1,I+NA))
C
      NAB=NA+NB
      CALL EIGEN(DMERGE,WMERGE,NAB,P(1,K,IB),EP(K,IB),NFLAG)
      GO TO (104,103,102), NFLAG
C
  102 WRITE(IOUT,10) IB,K
   10 FORMAT(1X,'* NOT THREE UNEQUAL RCOTS *',12X,'BOUNDARY, SECTION = '
     Z ,I1,1X,I2)
      GO TO 104
  103 WRITE(IOUT,11) IB,K
   11 FORMAT(1X,'* DOUBLY DEGENERATE MATRIX POSSIBLE *  BOUNDARY, SECTIO
     ZN = ',I1,1X,I2)
C
  104 DMESUR(K,IB)=EP(K,IB)
C
  200 SMESUR(IB)=SMESUR(IB)+DMESUR(K,IB)
C
  300 CONTINUE
C
```

```
      SUM=SMESUR(1)+SMESUR(2)+SMESUR(3)
C
      RETURN
      END
C
C     ***************************************************************************
C
      SUBROUTINE EIGEN(X,WT,N,P,EP,NFLAG)
C
C     SUBROUTINE EIGEN          NOVEMBER 1978          S.HELLINGER
C
C     P,Q,R ARE EIGENVECTORS ASSOCIATED WITH EIGENVALUES EP,EQ,ER
C     X=LINEAR ARRAY CONTAINING DATA POINTS IN CARTESIAN COORDINATES
C     WT= LINEAR ARRAY WHICH CONTAINS WEIGHTS FOR DATA POINTS. WT(K) IS
C     PROPORTIONAL TO SQUARE OF STANDARD DEVIATION OF ERROR FOR K TH
C     POINT, IWT= INTEGER VARAIABLE TO INDICATE WHETHER DATA IS TO BE
C     WEIGHTED ACCORDING TO WT ARRAY. IWT=0 INDICATES WEIGHTING TO BE
C     USED. IF IWT.NE.0 THEN NO WEIGHTING IN FINDING EIGENVECTORS
C     AND EIGENVALUES.
C     N=NUMBER OF DATA POINTS
C     VEC=3X3 ARRAY CONTAINING EIGENVECTORS, STORED COLUMN-WISE
C     D=LINEAR ARRAY CONTAINING EIGENVALUES. ELEMENT L CONTAINS
C     EIGENVALUE FOR EIGENVECTOR IN COLUMN OF ARRAY VEC.
C     A=3X3 COVARIANCE MATRIX. SIX INDEPENDENT ELEMENTS STORED IN
C     LINEAR ARRAY S(6).
C     S(1)=A(1,1)
C     S(2)=A(1,2)=A(2,1)
C     S(3)=A(2,2)
C     S(4)=A(1,3)=A(3,1)
C     S(5)=A(2,3)=A(3,2)
C     S(6)=A(3,3)
      IMPLICIT REAL*8 (A-E,P-Z)
      DIMENSION VEC(3,3),A(3,3),P(3),Q(3),R(3),S(6),D(3),CD(3)
      DIMENSION WT(10),X(1)
      DATA C/0.74074074074074D-01/,C120/0.209439510239319D+01/
      DATA C240/0.418879020478639D+01/,XZERO/1.0D-05/
      NFLAG=1
C     CREATE SYMMETRIC COVARIANCE MATRIX FROM DATA.
C     **NO WEIGHTING FOR N=2**
      DO 5 I=1,6
5     S(I)=0.
      IF(N.EQ.2) GO TO 8
C     WEIGHTED SOLUTION
      DO 6 M=1,N
      MM=3*M
      S(1)=S(1)+X(MM-2)*X(MM-2)/WT(M)
      S(2)=S(2)+X(MM-2)*X(MM-1)/WT(M)
      S(3)=S(3)+X(MM-1)*X(MM-1)/WT(M)
      S(4)=S(4)+X(MM-2)*X(MM)/WT(M)
      S(5)=S(5)+X(MM-1)*X(MM)/WT(M)
```

```
6       S(6)=S(6)+X(MM)*X(MM)/WT(M)
        GO TO 9
C       UNWEIGHTED SOLUTION
8       DO 10 M=1,N
        MM=3*M
        S(1)=S(1)+X(MM-2)*X(MM-2)
        S(2)=S(2)+X(MM-2)*X(MM-1)
        S(3)=S(3)+X(MM-1)*X(MM-1)
        S(4)=S(4)+X(MM-2)*X(MM)
        S(5)=S(5)+X(MM-1)*X(MM)
10      S(6)=S(6)+X(MM)*X(MM)
9       CONTINUE
C       SOLVE CUBIC DETERMINANTAL EQUATION FOR EIGENVALUES
        PP=-(S(1)+S(3)+S(6))
        QQ=S(1)*S(6)+S(1)*S(3)+S(3)*S(6)-S(5)*S(5)-S(2)*S(2)-S(4)*S(4)
        RR=S(1)*S(5)*S(5)+S(2)*S(2)*S(6)+S(4)*S(4)*S(3)-S(1)*S(3)*S(6)
       Z   -2.*S(2)*S(4)*S(5)
C       SOLVE REDUCED EQUATION
        AA=QQ-PP*PP/3.
        BB=C*PP*PP*PP-PP*QQ/3. + RR
        AA=AA/3.
        BB=BB/2.
C       CHECK FOR THREE REAL UNEQUAL ROOTS
        AAA=AA*AA*AA
        SP=BB*BB+AAA
        IF(SP.GE.0.) GO TO 50
C       HAVE THREE REAL UNEQUAL ROOTS. FIND THEM
        PHI=DARCOS( -BB/DSQRT(-AAA) )
        PHI=PHI/3.
        AAA=2.*DSQRT(-AA)
        D(1)=AAA*DCOS(PHI)
        D(2)=AAA*DCOS(PHI+C120)
        D(3)=AAA*DCOS(PHI+C240)
C       D(1),D(2),D(3) ARE ROOTS OF REDUCED EQUATION. FIND ROOTS
C       OF ORIGINAL EQUATION.
        PP=PP/3.
        D(1)=D(1)-PP
        D(2)=D(2)-PP
        D(3)=D(3)-PP
C       FIND MINIMUM EIGENVALUE AND PLACE IT IN D(1)
        IF( (D(1).LE.D(2)).AND.(D(1).LE.D(3)) ) GO TO 30
        MIN=3
        IF( D(2).LE.D(3) ) MIN=2
C       EXCHANGE EIGENVALUES
        CD(1)=D(1)
        D(1)=D(MIN)
        D(MIN)=CD(1)
C       COMPUTE EIGENVECTORS
C        HAVE ROOTS OF ORIGINAL EQUATION=EIGENVALUES OF COVARIANCE MATRIX
C       FIND EIGENVECTORS ASSOCIATED WIOH EIGENVALUES. DONE BY FINDING
```

```
C       LINEARLY INDEPENDENT ROWS OF MATRIX  A-D(J)*I,  J=1,3 , I=IDENTITY
C       MATRIX. EIGENVECTOR IS THEN IN DIRECTION OF CROSS-PRODUCT OF
C       LINEARLY INDEPENDENT ROW-VECTORS.
30      A(1,2)=S(2)
        A(2,1)=S(2)
        A(1,3)=S(4)
        A(3,1)=S(4)
        A(2,3)=S(5)
        A(3,2)=S(5)
        J=1
        A(1,1)=S(1)-D(J)
        A(2,2)=S(3)-D(J)
        A(3,3)=S(6)-D(J)
C       TEST FOR LINEAR INDEPENDENCE OF ROW-VECTORS (=COLUMN-VECTORS)
        DO 440 M=2,3
        DO 44 L=1,3
44      R(L)=A(1,L)/A(M,L)
        MROW=M
        IF( DABS( R(1)-R(2) ).GT.XZERO ) GO TO 441
        IF( DABS( R(1)-R(3) ).GT.XZERO ) GO TO 441
440     CONTINUE
C       MAY HAVE DOUBLY DEGENERATE MATRIX. PRINT WARNING MESSAGE. COMPUTE
C       VECTOR PRODUCT OF PAIRS OF ROWS. CHOOSE VECTOR WITH GREATEST
C       MAGNITUDE TO BE DIRECTION OF EIGENVECTOR. NORMALIZE LENGTH TO 1.
        NFLAG=2
        CALL CROSS( A(1,1),A(1,2),P )
        CALL CROSS( A(1,1),A(1,3),Q )
        CALL CROSS( A(1,2),A(1,3),R )
        CD(1)=P(1)*P(1)+P(2)*P(2)+P(3)*P(3)
        CD(2)=Q(1)*Q(1)+Q(2)*Q(2)+Q(3)*Q(3)
        CD(3)=R(1)*R(1)+R(2)*R(2)+R(3)*R(3)
        MM=1
        IF( CD(2).GT.CD(1) ) MM=2
        IF( CD(MM).LT.CD(3) ) MM=3
        SP=DSQRT( CD(MM) )
        GO TO (4402,4403,4404), MM
4402    DO 44021 I=1,3
44021   VEC(I,J)=P(I)/SP
        GO TO 40
4403    DO 44031 I=1,3
44031   VEC(I,J)=Q(I)/SP
        GO TO 40
4404    DO 44041 I=1,3
44041   VEC(I,J)=R(I)/SP
        GO TO 40
C       ROW (MROW) IS LINEARLY INDEPENDENT OF ROW 1. COMPUTE EIGENVECTOR.
441     CALL CROSS( A(1,1),A(1,MROW),VEC(1,J) )
C       VEC(1,J) NOW CONTAINS FIRST ELEMENT OF UN-NORMALIZED EIGENVECTOR.
C       MAKE LENGTH =1.
        AAA=VEC(1,J)*VEC(1,J)+VEC(2,J)*VEC(2,J)+VEC(3,J)*VEC(3,J)
```

```
      AAA=DSQRT(AAA)
      DO 4415 I=1,3
4415  VEC(I,J)=VEC(I,J)/AAA
C
40    DO 41 L=1,3
41    P(L)=VEC(L,1)
      EP=D(1)
      RETURN
C     TEST FOR THREE UNEQUAL ROOTS FAILED. PRINT MESSAGE.
50    NFLAG=3
      RETURN
      END
C
C     ******************************************************************
C
      SUBROUTINE PSET(S,XLAT,XLON,PLAT,PLON)
C
C     SUBROUTINE PSET          JANUARY 1979          C.TAPSCOTT
C
C     THE SUBROUTINE RETURNS A HEXAGONAL GRID OF LATITUDE-LONGITUDE
C     COORDINATES OF RADIUS S CENTERED AT XLAT, XLON.
C
      IMPLICIT DOUBLE PRECISION (A-H,O-Z)
C
      DIMENSION PLAT(7),PLON(7),R(3,3),P(3),Q(3)
      DATA RAD/1.7453292519943300-02/
C
      PLAT(1)=XLAT
      PLON(1)=XLON
C
      P(1)=0.
      P(2)=XLON+90.
      P(3)=90.-XLAT
      CALL RMAT(P,R)
C
      T=0.
      DT=60.*RAD
      P(3)=DCOS(S*RAD)
      DP=DSIN(S*RAD)
C
      DO 100 I=2,7
      P(1)=DP*DCOS(T)
      P(2)=DP*DSIN(T)
      CALL ROTATE(R,P,Q)
      PLAT(I)=90.-(DACOS(Q(3))/RAD)
      PLON(I)=DATAN2(Q(2),Q(1))/RAD
  100 T=T+DT
C
      RETURN
      END
```

```
C
C     ***********************************************************************
C
      SUBROUTINE RSUM(N,AROT)
C
C     SUBROUTINE RSUM          JANUARY 1979          C.TAPSCOTT
C
C     THE SUBROUTINE RETURNS THE RESULTANT POLE AND ANGLE AND ROTATION
C     MATRICES FOR ROTATIONS 1 AND 2, LEAVING THE ROTATION MATRIX FOR
C     ROTATION N=0,1,2 UNCHANGED.
C
      IMPLICIT DOUBLE PRECISION (A-H,O-Z)
C
      COMMON/SUB4/ RM(3,3,3)
      DIMENSION AROT(3,3),Q(3,3)
C
      IF (N .EQ. 1) GO TO 100
      CALL RMAT(AROT(1,1),RM(1,1,1))
C
  100 IF (N .EQ. 2) GO TO 200
      CALL RMAT(AROT(1,2),RM(1,1,2))
C
  200 DO 201 I=1,3
      DO 201 J=1,3
  201 Q(I,J)=RM(J,I,1)
C
      CALL MM33(Q,RM(1,1,2),RM(1,1,3))
      CALL RINVERT(RM(1,1,3),AROT(1,3))
C
      RETURN
      END
C
C     ***********************************************************************
C
      SUBROUTINE ISET(L,M,N)
C
C     SUBROUTINE ISET          JANUARY 1979          C.TAPSCOTT
C
C     THE SUBROUTINE SETS THE ELEMENTS OF THE ARRAY N AS CODES TO AVOID
C     UNECESSARY RECALCULATION IN SUBRCUTINE SPOL.
C
      DIMENSION N(7)
C
      N(1)=1
      DO 100 I=2,7
  100 N(I)=0
      IF (L .EQ. 1) RETURN
C
      IF (M .GT. 1) GO TO 102
      DO 101 I=2,7
```

```
  101 N(I)=1
      RETURN
C
  102 DO 103 I=M+2,M+4
      J=I
      IF (J .GE. 8) J=J-6
  103 N(J)=1
C
      RETURN
      END
C
C     ******************************************************************
C
      SUBROUTINE GETEM(W,IPUT)
C
C     SUBROUTINE GETEM          JANUARY 1979          C.TAPSCOTT
C
C     THE SUBROUTINE READS THE DATA SECTIONS, CONVERTS THE POINTS TO
C     CARTESIAN COORDINATES, AND PLACES THEM IN THE DATA ARRAY.
C
      IMPLICIT DOUBLE PRECISION (A-H,O-Z)
C
      COMMON/XMAIN/DATA(3,5,10,2,3),SIGMA(5,10,2,3),WT(5,10,2,3),
     Z NPTS(10,2,3),NSECT(3)
      DIMENSION ALAT(5),ALON(5),AERR(5)
      DATA RAD,RKM/1.7453292519943300-02,1.569539D-04/
      DATA IIN,IOUT/1,108/
C
      WRITE(IOUT,1)
    1 FORMAT(/,'BOUNDARY PLATE SECTION POINTS',/)
C
      DO 200 IB=1,3
      DO 200 IP=1,2
      K=IP
      IF ((IB .EQ. 2) .AND. (IP .EQ. 2)) K=3
      IF (IB .EQ. 3) K=IP+1
      DO 200 IS=1,NSECT(IB)
C
      READ(IIN,10) (ALAT(J),ALON(J),AERR(J),J=1,5)
   10 FORMAT(15G)
      IF (IPUT .NE. 0) GO TO 99
      WRITE(IOUT,11) IB,K,IS,(ALAT(J),ALON(J),AERR(J),J=1,5)
   11 FORMAT(1X,I1,1X,I1,1X,I2,3X,5(F6.2,1X,F7.2,1X,F4.1,5X))
C
   99 DO 100 J=1,5
      IF ((ALAT(J) .GT. 90.) .OR. (AERR(J) .LT. 0.01)) GO TO 101
C
      CLAT=DCOS(RAD*ALAT(J))
      SLAT=DSIN(RAD*ALAT(J))
      CLON=DCOS(RAD*ALON(J))
```

```
      SLON=DSIN(RAD*ALON(J))
C
      DATA(1,J,IS,IP,IB)=CLAT*CLON
      DATA(2,J,IS,IP,IB)=CLAT*SLON
      DATA(3,J,IS,IP,IB)=SLAT
      SIGMA(J,IS,IP,IB)=AERR(J)*RKM
  100 WT(J,IS,IP,IB)=AERR(J)*AERR(J)/W
C
  101 NPTS(IS,IP,IB)=J-1
C
  200 CONTINUE
C
      RETURN
      END
C
C     ***************************************************************
C
      SUBROUTINE PUTEM(IT,A,S,T)
C
C     SUBROUTINE PUTEM          JANUARY 1979          C.TAPSCOTT
C
C     THE SUBROUTINE WRITES THE ROTATION POLES AND ASSOCIATED MEASURES.
C
      DOUBLE PRECISION A(3,3),S(3),T
C
      DATA IOUT/108/
C
      IF (IT .NE. 0) GO TO 100
C
      WRITE(IOUT,1)
    1 FORMAT(//1X,'BOUNDARY LATITUDE  LONGITUDE   ANGLE',6X,
     Z 'MEASURE     TOTAL MEASURE')
C
  100 WRITE(IOUT,10) (J,(A(I,J),I=1,3),S(J),J=1,3),T
   10 FORMAT(3(/4X,I1,5X,3(F8.3,2X),D12.6),/54X,D12.6)
C
      RETURN
      END
C
C     ***************************************************************
C
      SUBROUTINE CROSS(A,B,C)
C
C     SUBROUTINE CROSS          NOVEMBER 1978          S.HELLINGER
C
C     THE SUBROUTINE COMPUTES THE CROSS PRODUCT OF TWO VECTORS AS AXB=C.
C
      DOUBLE PRECISION A(3),B(3),C(3)
C
      C(1)=A(2)*B(3)-A(3)*B(2)
```

```
      C(2)=A(3)*B(1)-A(1)*B(3)
      C(3)=A(1)*B(2)-A(2)*B(1)
C
      RETURN
      END
C
C     ***************************************************************
C
      SUBROUTINE MM33(A,B,C)
C
C     SUBROUTINE MM33          JANUARY 1979          C.TAPSCOTT
C
C     THE SUBROUTINE MULTIPLIES 3*3 MATRICES AS A*B=C.
C
      DOUBLE PRECISION A(3,3),B(3,3),C(3,3)
C
      DO 100 I=1,3
      DO 100 J=1,3
      C(I,J)=0.
      DO 100 K=1,3
  100 C(I,J)=C(I,J)+A(I,K)*B(K,J)
C
      RETURN
      END
C
C     ***************************************************************
C
      SUBROUTINE RINVERT(R,P)
C
C     SUBROUTINE RINVERT          JANUARY 1979          C.TAPSCOTT
C
C
C     THE SUBROUTINE CALCULATES THE ROTATION AXIS AND ANGLE OF THE
C     ROTATION MATRIX R.
C
      IMPLICIT DOUBLE PRECISION (A-H,O-Z)
C
      DIMENSION R(3,3),P(3)
C
      R90=DASIN(1.)
C
      CA=(R(1,1)+R(2,2)+R(3,3)-1.)/2.
      IF (DABS(CA) .GT. 1.) CA=DSIGN(1.,CA)
      IF ((1.-CA) .GT. (1.5D-10)) GO TO 100
C
      THETA=R90
      PHI=0.
      ALPHA=0.
      GO TO 1000
C
```

```
  100 CT=(R(3,3)-CA)/(1.-CA)
      IF (CT .LT. 0.) CT=0.
      IF (CT .GT. 1.) CT=1.
      CT=DSQRT(CT)
      THETA=DACOS(CT)
C
      IF (THETA .GT. 1.75D-05) GO TO 200
      PHI=0.
      SA=(R(2,1)-R(1,2))/(2.*CT)
      GO TO 900
C
  200 IF (CT .GT. 1.75D-05) GO TO 300
      IF ((CA+1.) .LT. 1.5D-10) GO TO 250
C
      SP=R(1,3)-R(3,1)
      CP=R(3,2)-R(2,3)
      IF (SP .EQ. 0.) PHI=R90-DSIGN(R90,CP); GO TO 201
      IF (CP .EQ. 0.) PHI=DSIGN(R90,SP); GO TO 202
      PHI=DATAN2(SP,CP)
      IF (DABS(CP) .LT. DABS(SP)) GO TO 202
  201 SA=CP/(2.*DSIN(PHI)*DSIN(THETA))
      GO TO 900
  202 SA=SP/(2.*DCOS(PHI)*DSIN(THETA))
      GO TO 900
C
  250 THETA=R90
      ALPHA=2.*R90
      CP=(R(1,1)+1.)/2.
      IF (CP .LT. 0.) CP=0.
      IF (CP .GT. 1.) CP=1.
      CP=DSQRT(CP)
      PHI=DSIGN(DACOS(CP),(R(1,2)+R(2,1)))
      GO TO 1000
C
  300 CP=(R(1,3)+R(3,1))/(2.*(1.-CA))
      SP=(R(2,3)+R(3,2))/(2.*(1.-CA))
      IF (SP .EQ. 0.) PHI=R90-DSIGN(R90,CP); GO TO 301
      IF (CP .EQ. 0.) PHI=DSIGN(R90,SP); GO TO 301
      PHI=DATAN2(SP,CP)
C
  301 A=R(2,1)-R(1,2)
      B=R(1,3)-R(3,1)
      C=R(3,2)-R(2,3)
      IF (DABS(A) .LT. DABS(B)) GO TO 302
      IF (DABS(A) .LT. DABS(C)) GO TO 303
      SA=A/(2.*CT)
      GO TO 900
  302 IF (DABS(B) .LT. DABS(C)) GO TO 303
      SA=B/(2.*DSIN(PHI)*DSIN(THETA))
      GO TO 900
```

```
  303 SA=C/(2.*DCOS(PHI)*DSIN(THETA))
C
  900 IF (SA .EQ. 0.) ALPHA=R90-DSIGN(R90,CA); GO TO 1000
      IF (CA .EQ. 0.) ALPHA=DSIGN(R90,SA); GO TO 1000
      ALPHA=DATAN2(SA,CA)
C
 1000 P(1)=90.-(THETA*90./R90)
      P(2)=PHI*90./R90
      P(3)=ALPHA*90./R90
C
      RETURN
      END
C
C     ******************************************************************
C
      SUBROUTINE RMAT(Q,R)
C
C     SUBROUTINE RMAT          JANUARY 1979          C.TAPSCOTT
C
C     THE SUBROUTINE COMPUTES THE ROTATION MATRIX R ASSOCIATED WITH THE
C     ROTATION Q = (LAT. LONG. ANGLE).
C
      IMPLICIT DOUBLE PRECISION (A-H,O-Z)
C
      DIMENSION Q(3),R(3,3)
      DATA RAD/1.7453292519943D-02/
C
      T=(90.-Q(1))*RAD
      P=Q(2)*RAD
      A=Q(3)*RAD
C
      CT=DCOS(T)
      ST=DSIN(T)
      CP=DCOS(P)
      SP=DSIN(P)
      CA=DCOS(A)
      SA=DSIN(A)
      WA=1.-CA
C
      R(1,1)=CA+(WA*CP*CP*ST*ST)
      R(2,2)=CA+(WA*SP*SP*ST*ST)
      R(3,3)=CA+(WA*CT*CT)
C
      U=WA*CP*SP*ST*ST
      V=CT*SA
      R(1,2)=U-V
      R(2,1)=U+V
C
      U=WA*CP*CT*ST
      V=SP*ST*SA
```

```
      R(1,3)=U+V
      R(3,1)=U-V
C
      U=WA*SP*CT*ST
      V=CP*ST*SA
      R(2,3)=U-V
      R(3,2)=U+V
C
      RETURN
      END
C
C     ***************************************************************
C
      SUBROUTINE ROTATE(R,V,VR)
C
C     SUBROUTINE ROTATE          JANUARY 1979          C.TAPSCOTT
C
C     THE SUBROUTINE RATATES THE VECTOR V TO VR BY THE MATRIX R.
C
      DOUBLE PRECISION R(3,3),V(3),VR(3)
C
      DO 100 I=1,3
      VR(I)=0.
      DO 100 J=1,3
  100 VR(I)=VR(I)+R(I,J)*V(J)
C
      RETURN
      END
```

MANDATORY DISTRIBUTION LIST

FOR UNCLASSIFIED TECHNICAL REPORTS, REPRINTS, AND FINAL REPORTS
PUBLISHED BY OCEANOGRAPHIC CONTRACTORS
OF THE OCEAN SCIENCE AND TECHNOLOGY DIVISION
OF THE OFFICE OF NAVAL RESEARCH

(REVISED NOVEMBER 1978)

1 Deputy Under Secretary of Defense
(Research and Advanced Technology)
Military Assistant for Environmental Science
Room 3D129
Washington, D.C. 20301

Office of Naval Research
800 North Quincy Street
Arlington, VA 22217
3 ATTN: Code 483
1 ATTN: Code 460
2 ATTN: 102B

1 CDR J. C. Harlett, (USN)
ONR Representative
Woods Hole Oceanographic Inst.
Woods Hole, MA 02543

Commanding Officer
Naval Research Laboratory
Washington, D.C. 20375
6 ATTN: Library, Code 2627

12 Defense Documentation Center
Cameron Station
Alexandria, VA 22314
ATTN: DCA

Commander
Naval Oceanographic Office
NSTL Station
Bay St. Louis, MS 39522
1 ATTN: Code 8100
1 ATTN: Code 6000
1 ATTN: Code 3300

1 NODC/NOAA
Code D781
Wisconsin Avenue, N.W.
Washington, D.C. 20235

Woods Hole Oceanographic Institution
WHOI-80-37

THE EVOLUTION OF THE INDIAN OCEAN TRIPLE JUNCTION AND THE FINITE ROTATION PROBLEM by Christopher R. Tapscott. 210 pages. September 1980. Prepared for the Office of Naval Research under Contracts N00014-74-C-0262; NR 083-004 and N00014-75-C-0291 (MIT).

Refer to page 12 of thesis for abstract.

1. Plate tectonics
2. Earth's lithosphere
I. Tapscott, Christopher R.
II. N00014-74-C-0262; NR 083-004
III. N00014-75-C-0291

This card is UNCLASSIFIED

Woods Hole Oceanographic Institution
WHOI-80-37

THE EVOLUTION OF THE INDIAN OCEAN TRIPLE JUNCTION AND THE FINITE ROTATION PROBLEM by Christopher R. Tapscott. 210 pages. September 1980. Prepared for the Office of Naval Research under Contracts N00014-74-C-0262; NR 083-004 and N00014-75-C-0291 (MIT).

Refer to page 12 of thesis for abstract.

1. Plate tectonics
2. Earth's lithosphere
I. Tapscott, Christopher R.
II. N00014-74-C-0262; NR 083-004
III. N00014-75-C-0291

This card is UNCLASSIFIED

Woods Hole Oceanographic Institution
WHOI-80-37

THE EVOLUTION OF THE INDIAN OCEAN TRIPLE JUNCTION AND THE FINITE ROTATION PROBLEM by Christopher R. Tapscott. 210 pages. September 1980. Prepared for the Office of Naval Research under Contracts N00014-74-C-0262; NR 083-004 and N00014-75-C-0291 (MIT).

Refer to page 12 of thesis for abstract.

1. Plate tectonics
2. Earth's lithosphere
I. Tapscott, Christopher R.
II. N00014-74-C-0262; NR 083-004
III. N00014-75-C-0291

This card is UNCLASSIFIED

Woods Hole Oceanographic Institution
WHOI-80-37

THE EVOLUTION OF THE INDIAN OCEAN TRIPLE JUNCTION AND THE FINITE ROTATION PROBLEM by Christopher R. Tapscott. 210 pages. September 1980. Prepared for the Office of Naval Research under Contracts N00014-74-C-0262; NR 083-004 and N00014-75-C-0291 (MIT).

Refer to page 12 of thesis for abstract.

1. Plate tectonics
2. Earth's lithosphere
I. Tapscott, Christopher R.
II. N00014-74-C-0262; NR 083-004
III. N00014-75-C-0291

This card is UNCLASSIFIED